

The Role of NFATc1 in Burkitt Lymphoma and in *Eμ-Myc*-induced B Cell Lymphoma

Die Rolle des NFATc1 Transkriptionsfaktors im Burkitt Lymphom
und im *Eμ-Myc*-induzierten B-Zell Lymphom



Doctoral thesis for a doctoral degree
at the Graduate School of Life Sciences,
Julius-Maximilians-Universität Würzburg,
Section:

Infection and Immunology

Submitted by

Krisna Murti

Born in

Palembang, South Sumatera, Indonesia

Wuerzburg 2014

Submitted on:
Office stamp

Members of the *Promotionskomitees*:

Chairperson : Prof. Dr. Thomas Hünig

Primary Supervisor : Prof. Dr. Edgar Serfling

Supervisor (Second) : Priv.-Doz. Dr. Heike Hermann

Supervisor (Third) : Dr. Andris Avots

Date of Public Defense:.....

Date of Receipt of Certificate:.....

Acknowledgement

With great respect, I would very much like to sincerely thank all people who helped and supported me during my stay at University of Wuerzburg:

I would like to express my special thanks to Prof. Dr. Edgar Serfling for allowing me to join his group, and for his care and supervisions. His wealth of knowledge and enthusiasm for research was amazing. I would have to express my heartfelt thanks to Dr. Andris Avots. Throughout the years, I was extremely fortunate to have his supervision, care, interest, knowledge and ideas related to my project. Special thanks for the generosity of his time during invaluable discussions and in the formulation of my doctoral dissertation. I would have to express my sincere thanks to Priv.-Doz. Dr. Heike Hermann for her valuable time.

I was very honoured to acknowledge Prof. Dr. Andreas Rosenwald, the Head of Institute of Pathology, University of Wuerzburg, for giving me his permission to use patient blocks, some materials and equipment from his laboratory.

My special appreciation to Prof. Dr. med. German Ott, *Chefarzt*, Department of Pathology, Robert-Bosch-Krankenhaus, Stuttgart, for his information about BCL6.

I would express my gratitudes to Dr. Friederike Berberich-Siebelt, for translation of thesis summary, Dr. Stefan Klein-Heßling for some technical explanations. The laboratory will not be the same without scientific discussions with Dr. Khalid Muhammad, Dr. Amiya K. Patra, Dr. Martin Väth and Dr. Ronald Rudolf. I also owe thanks to them. Further I would like to be grateful to Dr. Rhoda Busch and to Hendrik Fender for helping me in some experiments. Thanks also go to Hani Alrefai, Lena Dietz, Tobias Pusch, Duong Pham Anh Thuy, Nadine Winter, Janina Findeis and also to Dr. Jolly Deb and Dr. Sankar Bhattacharyya for their friendship and enjoyable time throughout the year. Special thanks should be delivered to Doris Michel, Ilona Pietrowski and Angelika Skiadas for their helps and supports.

I greatly appreciated Prof. Dr. Thomas Hünig from Institute for Virology and Immunobiology, University of Wuerzburg, for the opportunity to join his outstanding Immunomodulation Program.

My huge thanks for sweet-hearted collaborations belonged to other Pathology, Histochemical and Immunohistology, and also Hematology laboratories' group members. You all gave me great support and help with sharing knowledge, methods and materials.

I wish to thank German Academic Exchange Services (DAAD) for providing me funding through DAAD Scholarship to study in Germany.

Many thanks go to Prof. Dr. Badia Perizade (Rector of Sriwijaya University), Dr. Muhammad Zulkarnain (Dean of Faculty of Medicine, Sriwijaya University), and Heni Maulani, M.D. (Head of Department of Anatomical Pathology, Faculty of Medicine, Sriwijaya University) and their staff, for giving me help when I needed.

Huge thanks to my parents, my sisters and my brother for their moral supports, understandings and prayers, to hope my success. Finally, I am very grateful, indebted and want to heartily thank my husband (Dr.-phil. Arinafril) and my three kids (Nabila Khairunisah Arinafril, Naufal Arinafril and Nafila Taufik Arinafril), for allowing me to spend years to study in Germany. For their loves, endless supports and prayers, encouragement and especially for their extremely patience, more sadness than happiness during my hard life in Germany, a country which is more than 10.000 km away from them. Without their understandings, I could not make them proud of me.

Table of Contents

1. Erklärung an Eidesstattliche Erklärung (Affidavit)	1
2. Summary/Abstract	2
3. Zusammenfassung	3
4. Introduction	5
4.1 Lymphoma	5
4.2 Burkitt lymphoma	5
4.2.1 Epidemiology and risk factors of BL	6
4.2.2 Clinical presentation of BL	6
4.2.3 Morphology of BL	7
4.2.4 Pathogenesis and molecular signature of BL	8
4.2.4.1 MYC	9
4.2.4.2 BCL6	10
4.3 B cell development	11
4.3.1 The early B cell development	11
4.3.2 Germinal center reaction	13
4.4 Burkitt lymphoma models	15
4.5 Survival factors for BL cells	15
4.6 Nuclear Factor of Activated T-Cell (NFAT)	16
4.6.1 Regulation of NFAT activity	17
4.6.2 NFATc1	19
4.6.3 NFATc1 and carcinogenesis	20
4.7 Objectives of the thesis	21
5. Materials and Methods	22
5.1 Materials	22
5.1.1 Chemicals	22
5.1.2 Buffers	22
5.1.3 Antibiotics and inhibitors	25
5.1.4 Antibodies and reagents	25
5.1.5 Oligonucleotides	26
5.1.5.1 Primers for genotyping of mouse tail	26
5.1.5.2 Primers for Reverse Transcriptase (RT) and Real-Time PCR	26
5.1.6 Enzymes	27
5.1.7 Kits and systems	27
5.1.8 Stimulators	27
5.1.9 Size standards	27
5.1.10 Cell lines	28
5.1.11 Experimental animals	28
5.1.12 Consumable	28
5.1.13 Instruments and accessories	29
5.1.14 Electronical data processing	29
5.2 Methods	30
5.2.1 Cellular technics	30
5.2.1.1 Culture of cells	30
5.2.1.2 Centrifugation of cells	30
5.2.1.3 Counting of cells	30
5.2.1.4 Freezing and thawing of cells	30
5.2.1.5 Cell isolation and culture	31

5.2.1.5.1	Positive selection of human CD19 ⁺ B Lymphocytes	31
5.2.1.5.2	Isolation of mouse B lymphocytes	31
5.2.1.5.3	Culture of <i>Eμ-Myc</i> tumor cells	31
5.2.2	Flow cytometry (FACS)	31
5.2.2.1	Surface marker staining	31
5.2.2.2	Intracellular staining for Ki67	31
5.2.2.3	Annexin V/PI-staining	32
5.2.3	<i>In vivo</i> experiments and mouse models	32
5.2.3.1	Generation of secondary tumors	32
5.2.4	Working with proteins	32
5.2.4.1	Preparation of protein extracts	32
5.2.4.2	Protein concentration measurement (Bradford assay)	33
5.2.4.3	Sample preparation and separation on the SDS-PAGE	33
5.2.4.4	Immunological detection of proteins (Western Blotting)	33
5.2.4.5	Stripping of membranes	34
5.2.5	Working with nucleic acids	34
5.2.5.1	Isolation of genomic DNA from cells or mouse tail biopsies	34
5.2.5.2	Isolation of total RNA from cells with trizol	34
5.2.5.3	Isolation of total RNA from frozen section tissues	35
5.2.5.4	Measurement of RNA	35
5.2.5.5	Reverse transcription	35
5.2.5.6	Polymerase chain reaction (PCR)	35
5.2.5.7	RT-PCR	36
5.2.5.8	Real-Time PCR	36
5.2.5.9	Gel electrophoresis	37
5.2.6	Imaging	37
5.2.6.1	Confocal fluorescence microscopy	37
5.2.6.2	Preparation of histological and immunohistochemical samples	37
5.2.6.3	Immunocytochemistry	38
5.2.6.4	Staining of the immunohistological sections (confocal microscope)	38
5.2.6.5	Staining of the immunohistological sections (peroxidase based)	38
5.3	Statistical Analysis	39
6.	Results	40
6.1	NFATc1 and tumorigenesis	40
6.2	NFATc1 expression in Burkitt lymphoma	40
6.3	Development of B cell lymphomas in <i>Eμ-Myc</i> mouse models	42
6.4	Immunophenotype of <i>Eμ-Myc</i> induced tumors	43
6.5	NFATc1 expression in <i>Eμ-Myc</i> mouse tumors	44
6.6	Nuclear residence of NFATc1 in BL and <i>Eμ-Myc</i> tumor cell lines is only partially dependent on calcineurin	46
6.7	Nuclear residence of NFATc1 in BL cell lines depends on intracellular Ca ²⁺ level	49
6.8	Prolonged NFATc1 protein half-life mediated by MYC	51
6.9	NFATc1 expression is regulated at the post-transcriptional level in BL and <i>Eμ-Myc</i> BCLs	53
6.10	Expression of NFATc1 isoforms BL, BL cell lines and in <i>Eμ-Myc</i> induced tumor	54
6.11	Tumorigenesis in <i>Eμ-Myc/Nfatc1^{flx/flx}/mb1-cre</i> mice	56
6.12	NFATc1 expression is not abolished in BCL cells of <i>Eμ-Myc/Nfatc1^{flx/flx}/mb1-cre</i> mice	58
6.13	Development of secondary <i>Eμ-Myc/Nfatc1^{flx/flx}/mb1-cre</i> tumors	59
6.14	NFATc1 is required for survival of <i>Eμ-Myc</i> -induced BCL cells	60

6.15 Caspase-3 and -7 are activated in <i>Eμ-Myc/Nfatc1^{flx/flx}/mb1-cre</i> tumor cells	62
6.16 Interaction of CD40-CD40L induced apoptosis of <i>Eμ-Myc</i> induced BCL cells	63
6.17 Interaction between NFATc1 and BCL6 in maintenance of BL	63
7. Discussion	67
7.1 NFATc1 expression in Burkitt lymphoma	67
7.2 B cell lymphomas in <i>Eμ-Myc</i> mice	67
7.3 NFATc1 expression in <i>Eμ-Myc</i> mouse tumors	68
7.4 Comparative analysis of NFATc1 isoform expression in BL, BL cell lines and <i>Eμ-Myc</i> induced tumor	68
7.5 Stability NFATc1 protein in <i>MYC</i> induced tumors	69
7.6 Nuclear residence of NFATc1 in <i>MYC</i> induced tumors is largely insensitive to calcineurine inhibitors	69
7.7 Tumorigenesis in <i>Eμ-myc/Nfatc1^{flx/flx}/mb1-cre</i> mice	70
7.8 Interaction of NFATc1 and BCL6 in maintenance of BL survival	71
8. References	73
9. Appendix	85
9.1 Attended conferences	85
9.2 Poster and oral presentations at conferences and symposia	85
9.3 Attended workshops	86
10. List of publications	87
11. Abbreviation	88
12. Curriculum vitae	89

Affidavit

I hereby declare that my thesis entitled “The Role of NFATc1 in Burkitt Lymphoma and in *Eμ-Myc*-induced B Cell Lymphoma” is the results of my own work. I did not receive any help or support from commercial consultant. All sources and / or materials applied are listed and specified in the thesis.

Furthermore, I verify that this thesis has not yet been submitted as part of another examination process neither in identical nor in similar form.

Eidesstattliche Erklärung

Hiermit erkläre ich an Eides statt, die Dissertation ”Die Rolle des NFATc1 Transkriptionsfaktors im Burkitt Lymphom und im *Eμ-Myc*-induzierten B-Zell Lymphom“ eigenständig, d.h. insbesondere selbstständig und ohne Hilfe eines kommerziellen Promotionsberaters, angefertigt und keine anderen als die von mir angegebenen Quellen und Hilfsmittel verwendet zu haben.

Ich erkläre außerdem, dass die Dissertation weder in gleicher noch in ähnlicher Form bereits in einem anderen Prüfungsverfahren vorgelegen hat.

Würzburg, June 17th, 2014

Summary

Burkitt lymphoma (BL) is a highly aggressive B cell malignancy. Rituximab, a humanized antibody against CD20, in a combination with chemotherapy is a current treatment of choice for B-cell lymphomas including BL. However, certain group of BL patients are resistant to Rituximab therapy. Therefore, alternative treatments targeting survival pathways of BL are needed.

In BL deregulation of MYC expression, together with additional mutations, inhibits differentiation of germinal centre (GC) B cells and drives proliferation of tumor cells. Pro-apoptotic properties of MYC are counteracted through the B-cell receptor (BCR) and phosphoinositide-3-kinase (PI3K) pathway to ensure survival of BL cells. In normal B-cells BCR triggering activates both NF- κ B and NFAT-dependent survival signals. Since BL cells do not exhibit constitutive NF- κ B activity, we hypothesized that anti-apoptotic NFATc1A isoform might provide a major survival signal for BL cells.

We show that NFATc1 is constitutively expressed in nuclei of BL, in BL cell lines and in *E μ -Myc*-induced B cell lymphoma (BCL) cells. Nuclear residence of NFATc1 in these entities depends on intracellular Ca²⁺ levels but is largely insensitive to cyclosporine A (CsA) treatment and therefore independent from calcineurine (CN) activity. The protein/protein interaction between the regulatory domain of NFATc1 and DNA binding domain of BCL6 likely contributes to sustained nuclear residence of NFATc1 and to the regulation of proposed NFATc1-MYC-BCL6-PRDM1 network in B-cell lymphomas.

Our data revealed lack of strict correlation between the expression of six NFATc1 isoforms in different BL-related entities suggesting that both NFATc1/ α A and - β A isoforms provide survival functions and that NFATc1/ α / β B and - α / β C isoforms either do not possess pro-apoptotic properties in BL cells or these properties are counterbalanced. In addition, we show that in BL entities expression of NFATc1 protein is largely regulated at post-transcriptional level, including MYC dependent increase of protein stability.

Functionally we show that conditional inactivation of *Nfatc1* gene in *E μ -Myc* mice prevents development of BCL tumors with mature B cell immunophenotype (IgD⁺). Loss of NFATc1 expression in BCL cells *ex vivo* results in apoptosis of tumor cells.

Together our results identify NFATc1 as an important survival factor in BL cells and, hence, as a promising target for alternative therapeutic strategies for BL.

Zusammenfassung

Das Burkitt Lymphom (BL) ist eine hoch aggressive B-Zellentartung. Rituximab, ein humanisierter Antikörper gegen CD20, in Kombination mit Chemotherapie ist die augenblickliche Behandlung der Wahl für B-Zelllymphome inklusive dem BL. Allerdings sind bestimmte Gruppen der BL-Patienten resistent gegenüber einer Rituximabtherapie. Deshalb werden alternative Behandlungsmöglichkeiten, die das Überleben der BL gezielt beeinflussen, gesucht.

Die Deregulation der MYC-Expression, zusammen mit weiteren Mutationen, inhibiert die Differenzierung der Keimzentrums- (GC-) B-Zellen im BL und treibt die Proliferation der Tumorzellen. Die pro-apoptotischen Eigenschaften von MYC sind durch den B-Zellrezeptor (BCR) und *Phosphoinositid-3-Kinase* (PI3K)-Signalwege gegenreguliert, was zum Überleben der BL-Zellen führt. Da BL-Zellen keine konstitutive NF- κ B-Aktivität aufweisen, stellten wir die Hypothese auf, dass die anti-apoptotischen Isoformen von NFATc1A ein Hauptüberlebenssignal für BL-Zellen bereitstellen könnten.

Wir zeigen, dass NFATc1 konstitutiv in den Kernen primärer BL-Zellen, der BL-Zelllinien und in den Zellen eines *E μ -MYC*-induzierten B-Zelllymphoms (BCL) vorliegt. Nukleäre NFATc1-Präsenz in diesen Entitäten hängt von intrazellulären Ca²⁺-Mengen ab, ist aber weitestgehend unempfindlich gegenüber Cyclosporine A (CsA)-Behandlung und unabhängig von Calcineurin (CN)-Aktivität. Stattdessen trägt wahrscheinlich die Protein/Proteininteraktion zwischen der regulatorischen Domäne von NFATc1 und der DNA-Bindungsdomäne von BCL6 zur anhaltenden nukleären Präsenz von NFATc1 und dem vorgeschlagenen NFATc1-MYC-BCL6-PRDM1-Netzwerk in B-Zelllymphomen bei.

Unsere Daten ergaben keine strenge Korrelation zwischen der Expression der sechs NFATc1-Isoformen in verschiedenen BL-verwandten Entitäten. Dies suggeriert, dass sowohl NFATc1/ α A wie $-\beta$ A Überlebenssignale vermitteln und dass NFATc1 α / β B und $-\alpha$ / β C-Isoformen in BL-Zellen keine pro-apoptotischen Eigenschaften besitzen oder diese Funktionen gegenreguliert werden. Des Weiteren zeigen wir, dass in BL-Entitäten die Expression der NFATc1-Proteine auf posttranskriptioneller Ebene reguliert werden. Dies schließt einen MYC-abhängigen Anstieg der Proteinstabilität ein.

In Bezug auf die Funktion von NFATc1 zeigen wir, dass seine konditionelle Inaktivierung in *E μ -MYC*-Mäusen die Entwicklung von BCL-Tumoren mit reifem T-Zellimmunphänotyp (IgD⁺) verhindert. Dementsprechend resultiert der Verlust der NFATc1-Expression in BCL-Zellen *ex vivo* in einer Apoptose der Tumorzellen.

Zusammengefasst brandmarken unsere Resultate NFATc1 als einen entscheidenden Überlebensfaktor in BL-Zellen bzw. identifizieren es als vielversprechendes Ziel alternativer therapeutischer Strategien in BL.

4. Introduction

4.1 Lymphomas

Lymphomas are defined as neoplastic transformations of the lymphoid system. The majority of lymphomas (90%) are non-Hodgkin lymphomas (NHLs), and the rest are considered as Hodgkin lymphomas (HLs) (Shankland et al., 2012). NHLs show morphologic heterogeneity and close to 90-95% of them are of B cell origin (Küppers, 2005; Shankland et al., 2012). The most common subtype of NHLs is diffuse large B cell lymphoma (DLBCL, around 30.6%), followed by follicular lymphoma (FL, around 22.1%) while Burkitt lymphoma (BL) constitutes less than 1% among NHLs cases (The Non-Hodgkin's Lymphoma Classification Project, 1997).

In the World Health organization (WHO) Classification, DLBCL and BL are considered as mature B-cell neoplasms (Swerdlow et al., 2008). BL and LBCL (DLBCL) are categorized as high-growth fraction lymphomas because they have high proliferation index, the tumor sizes are larger and they are clinically more aggressive (Sanchez-Beato et al., 2003).

4.2 Burkitt Lymphoma

In 1958 Dennis Burkitt first described a malignancy associated with jaw sarcomas among African children (Burkitt, 1958). The sarcoma was identified as a form of lymphoma and later identified as BL (O'Connor, 1961; Burkitt, 1983). BL is included in highly aggressive B cell malignancies (Hecht and Aster, 2000) and is the first B cell malignancy identified related to HIV (Ferry, 2006). It is one of lymphoid tumors specified with chromosomal translocation (Zech et al., 1976). *MYC* translocation is the hallmark of BL (Jaffe and Pitaluga, 2011). In addition, BL cells are the fastest growing tumor cells (Burkitt, 1983; Kalungi et al., 2012).

Several studies (Tamaru et al., 1995; Klein et al., 1995) found eBLs and sBLs are most likely derived from germinal center (GC) B cells, while another study suggest that sBL might develop from memory B cells (Isobe et al., 2002).

BL cells have a rapid doubling time, *i.e.* the tumor cells proliferate extremely fast (Burkitt, 1983; Blum et al., 2004; Kalungi et al., 2012). Therefore, considered treatment for BL is intensive and short-cycle chemotherapy, but toxic and side effects emerge (Blum et al., 2004). Rituximab, a humanized anti-CD20 monoclonal antibody, either single or in combination therapy contributes to the improved survival of NHL including BL patients (Jazirehi et al., 2007; Dunleavy et al., 2013). Rituximab is considered as an additional agent because cross-linking of CD20 kills tumor cells (Bonavida and Vega, 2005). So far, various modified protocol of combination therapy are existing (Blum et al., 2004; Dunleavy et al., 2013; Castillo et al., 2013). A study group applied a low intensity-

combination chemotherapy protocol consisted of infused etoposide, prednisone, vincristine, cyclophosphamide, doxorubicin and Rituximab (EPOCH-R) with better result in patients of adults sBL and immunodeficiency-associated BL (Dunleavy et al., 2013). Although improve survival in many treated patients, resistant to Rituximab in certain patients is developed (Bonavida and Vega, 2005; Jazirehi et al., 2007).

In developed countries where the best medical and infrastructure cares are accessible, 90% of survival rate can be achieved (Molyneux et al., 2012). In developing countries, cure rate is lower because of limited access to medical care. Early detection and treatment are important for better survival of BL (Shankland et al., 2012). Untreated patients typically die within months (Hummel et al., 2006). Optimal therapy for BL is still unsatisfied, therefore, attempts to improve and develop alternative treatments targeting survival pathways of BL are important.

4.2.1 Epidemiology and risk factors of BL

Based on epidemiology WHO classifies three clinical variants of BL with different clinical presentation, morphology and biology (Leoncini et al., 2008). Endemic variants (eBL) mostly found in Africa specifically in “the lymphoma belt” of Africa and Papua New Guinea. In these regions, eBL prevails among children (Burkitt, 1958; 1983; van den Bosch, 2004). Sporadic BL type (sBL) is distributed all over the world and occurs predominantly in children and adults (Shapira and Peylan-Ramu, 1998; Ferry, 2006). Immunodeficiency-associated BL is a subtype with main relation to the infection of human immunodeficiency virus (HIV), also other immunosuppression conditions such as inherited immunodeficiency (Ferry, 2006) and post-transplant recipients (Gong, 2006). BL occurs more frequently in AIDS population, than in immunosuppressed transplant recipients (Beral et al., 1991), indicating that immunosuppression alone is not responsible for BL development (Schulz et al., 1996). Epstein Barr Virus (EBV) and malaria infections are considered as co-factors of BL (Burkitt, 1983; van den Bosch, 2004). In Africa BL is usually related to EBV, however, in the USA, EBV is identified in less than 20% of sBL cases and in around 50% of AIDS related BL cases (Beral et al., 1991).

4.2.2 Clinical presentation of BL

Different geographic locations show a diverse clinical presentation of BL. In Africa, where eBL cases are mostly found, the involvement of head and neck encompassing jaw, facial bones, and other extra nodal sites occur in majority cases, followed by abdominal involvement. Tumors at these locations affect predominantly males (Burkitt, 1958; 1983; Walusansa et al., 2012). The most common sites of sBL are abdominal organs, while jaw tumors occur at lower percentage (Shapira and Peylan-Ramu,

1998). Similarly, abdominal regions are most common sites in immunodeficiency-related BLs in adults (Blum et al., 2004).

4.2.3 Morphology of BL

Histologically, BL consists of uniformly monomorphic, medium sized cells with round nuclei, multiple nucleoli, and moderately abundant basophilic cytoplasm. The tumor cells proliferate fast (proliferation index of Ki67 is nearly 100%, Bellan et al., 2003; Blum et al., 2004).

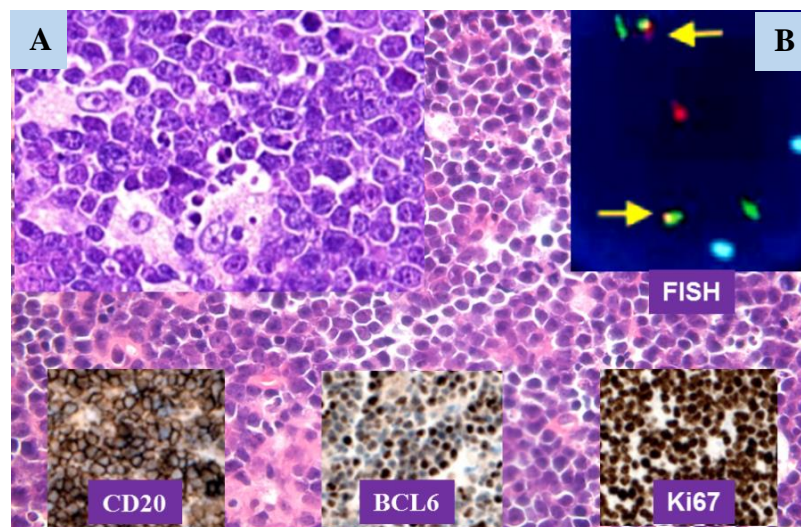


Fig. 1 The characteristic morphology of BL. **A.** Histologic features of BL comprising monomorphic, medium sized cells with round nuclei, multiple nucleoli, and relatively abundant basophilic cytoplasm. The characteristic “starry sky” pattern is formed because of numerous scattered macrophages, which have ingested apoptotic tumor cells. Immunohistochemistry reveals typical BL immunophenotype CD20⁺, BCL6⁺ and Ki67⁺ in almost 100% tumor cells, including CD10⁺ and BCL2⁻ (not shown). **B.** The translocation of *MYC* to *immunoglobulin Heavy (IgH)* chain genes is specified by FISH analysis with probes for 14q32/*IgH* (green), 8q24/*MYC* (red) and a chromosome 8 centromere probe (aqua blue). The fusion products t(8;14)(q24;q32) are in yellow (arrows). Modified from Blum et al., 2004; Molyneux et al., 2012 and our own data (A).

Due to the high rate of apoptosis numerous macrophages which have ingested apoptotic tumor cells were found in tumors resulting in a characteristic “starry sky” pattern (Fig. 1). BL cells express IgM, CD19, CD20, CD22, CD79a, CD10, and BCL6. BL are negative for BCL2, CD5, CD23, CD34 and TdT (Blum et al., 2004; Ferry, 2006). Molecular cytogenetics, *i.e.* fluorescence *in situ* hybridization (FISH) and staining with monoclonal antibodies specific to MYC and BCL6 are widely used as molecular tools in study of aggressive lymphomas including BL diagnosis (Jaffe and Pittaluga, 2011; Molyneux et al., 2012; Ott et al., 2013; G. Ott, Pers. Comm.).

4.2.4 Pathogenesis and molecular signature of BL

BCLs, including BL, originated from different stages of B cell differentiation. Therefore, most BCLs represent common stages of B cell differentiation (Fig. 2, Evans and Hancock, 2003; Jaffe et al., 2008). GC B cells undergo clonal expansion through modifications of their DNA involving somatic hypermutation (SHM), class switch recombination (CSR), and receptor editing. If these processes unsuccessful resulting in chromosomal translocations thereby lymphomagenesis (Küppers et al., 1999).

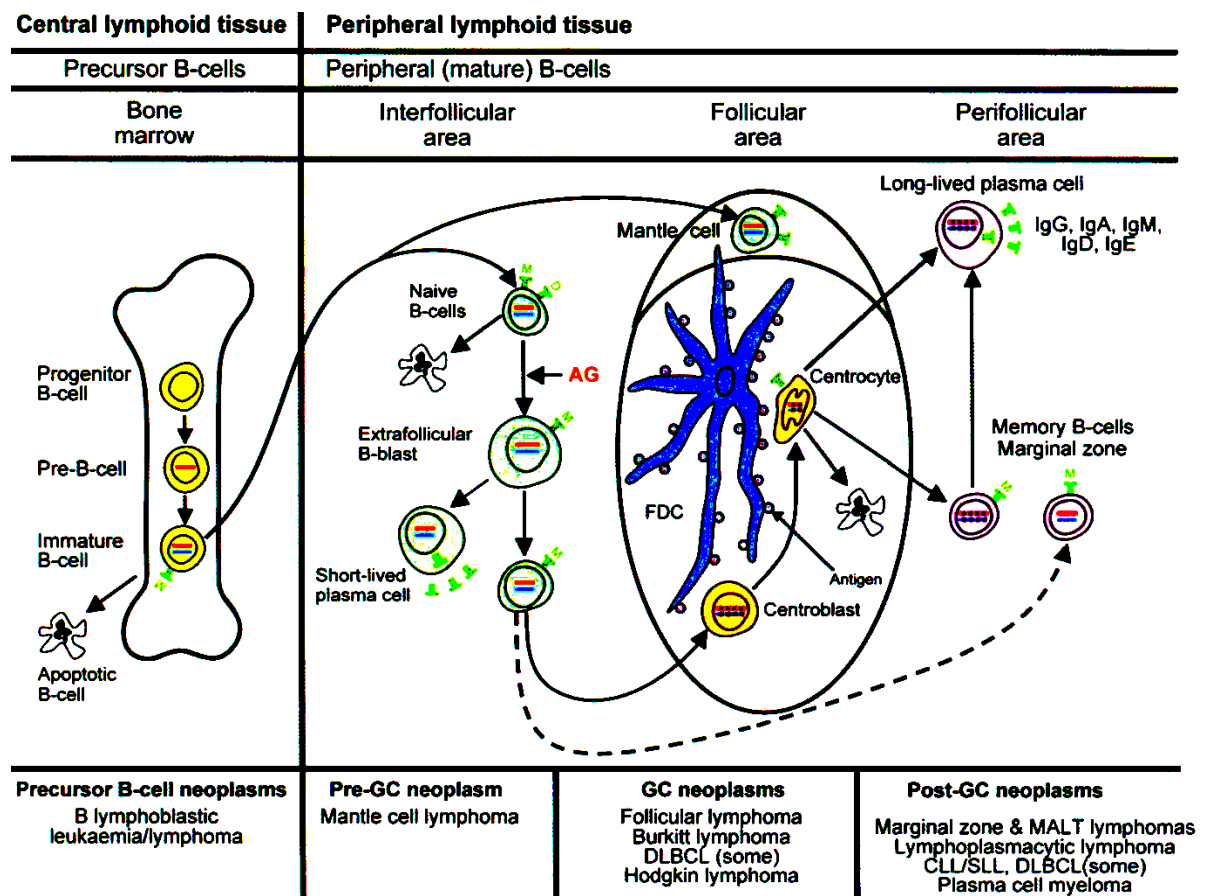


Fig. 2 Aberrant B cell development results in malignant transformation of B cells. During development, B cells undergo several processes, including SHM and CSR. These processes possess the risk of malignant transformation. Most leukemias and B cell lymphomas have immunophenotypes resembling the developmental stage of the B cell prior aberrant transformations. Based on Jaffe et al., 2008.

In BCLs, chromosomal translocations are the major mechanism of activation and deregulation of proto-oncogenes (Evans and Hancock, 2003). Chromosomal translocations in BCLs mostly involve the MYC and Ig loci (Küppers, 2005; Nussenzweig and Nussenzweig, 2010). In GCs, activation-induced cytidine deaminase (AID) mediates the process of chromosomal breaks in the

MYC locus during SHM and CSR (Calado et al., 2012). Since AID and c-Myc proteins are co-expressed in subsets of c-Myc⁺ GC B cells, activation of atypical AID during MYC transcription could lead to chromosomal translocation in GC B cells (Nussenzweig and Nussenzweig, 2010; Dominguez-Sola et al., 2012). Both MYC and transcriptional repressor BCL6 are crucial for the formation and maintenance of GC cells (Calado et al., 2012). The translocations lead to juxtaposition of transcriptional control elements in the Ig locus to the MYC promoter. Thereby the BCL6 binding sites in the MYC 5' region may be eliminated in some cases (Dominguez-Sola et al., 2012). The strong enhancer activity of Ig genes dominates BCL6-mediated repression, thus preventing the suppression of MYC transcription by BCL6 in the DZ (Dominguez-Sola et al., 2012).

MYC overexpression is a common genetic feature of BL because of translocation of MYC to Ig H genes (Sánchez-Beato et al., 2003). However, the presence of B cells with MYC translocation in the people without lymphomas suggests that MYC alone is not sufficient to generate BL (Janzt et al., 2003). Additional mutations, such as TP53, MYC itself, TCF3, ID3 (an inhibitor of TCF3, Schmitz et al., 2012), and CCND3 (Sander et al., 2012) were also identified in BL. Increased tonic B cell receptor (BCR) signaling via activated TCF3 leads to activation of phosphatidylinositol3-OH kinase (PI3K) pathway, thereby maintaining BL survival. TCF3 mutation also activates CCND3 (Schmitz et al., 2014). Cyclin D3, a cell cycle regulator is more stable due to CCND3 mutations in human BL and a mouse model causes progression of cell cycle. Thus, cyclin D3 mutant may contribute to BL pathogenesis. Accordingly, the collaboration of MYC and PI3K, is one important point for BL pathogenesis (Schmitz et al., 2012; Sander et al., 2012).

Gene expression profiling studies by Dave et al. (2006) have characterized a specific BL signature such as the expression of MYC target genes. GC-B associated genes are identified as highly expressed, while the expression of NF-κB target genes and MHC complex class I genes are downregulated (Dave et al., 2006; Hummel et al., 2006). Expression of *Nfkb1* is blocked in human BL and is declined in most *Eμ-Myc* tumor cells (Keller et al., 2005). By using microRNA profiles, Lenze and colleagues demonstrated that BL and DLBCL are discrete lymphoma types (Lenze et al., 2011).

4.2.4.1 MYC

The MYC (*c-Myc*) gene situated on chromosome 8q24 is a member of the proto-oncogenic *Myc* family, consisting of *c-Myc*, *N-Myc*, *L-Myc*, *S-Myc*, and *B-Myc*. Each of MYC proteins has specific function (Ryan and Birnie, 1996). Basically, *c-Myc* regulates cell-cycle progression and apoptosis and is involved in cellular transformation. *N-Myc* and *L-Myc* control cell-cycle progression and

cellular transformation. *S-Myc* and *B-Myc* have opposite functions *i.e.* they act as growth suppressor inhibit neoplastic transformation (Ryan and Birnie, 1996).

MYC has an N-terminal transactivation domain and a C terminal basic helix-loop-helix-leucine zipper (bHLH-LZ) that dimerizes with the MAX protein (Slack et al., 2011). MYC is a nuclear phosphoprotein and forms a complex with MAX to bind E-Box DNA motifs, in this manner regulating a huge number of target genes (Grandori et al., 1985; Arvanitis and Felsher, 2006). The stability and degradation of MYC are regulated by two N-terminal phosphorylation sites, Thr 58 and Ser 62, under control of the Ras effector pathways, Raf/ERK and PI-3K/AKT (Sears et al., 2000).

MYC is a critical regulator of a many physiological cell functions, such as cell growth, metabolism, apoptosis, proliferation, angiogenesis, migration, invasion, and preservation of telomerase (Evan et al., 2005; Vita and Henriksson, 2006; Wierstra and Alves, 2008; Levens, 2008). Therefore, expression of *MYC* gene is under stringent control mechanism (Wierstra and Alves, 2008; Mognol et al., 2012).

Deregulation of MYC expression alone is not sufficient to generate lymphomas, since the t(8;14) translocation has been detected at very low levels in blood of healthy individuals (Janz et al., 2003). MYC overexpression has been found in close to 70% of all human cancers (Klapproth and Wirth, 2010). Basically, high MYC overexpression specifies clinically more aggressive tumors with a worse prognosis than tumors with low/not detectable MYC expression (Smith et al., 2010; Ott et al., 2013). The majority of BL have *MYC* translocated to the heavy chain region t(8;14)(q24;q32) (Zech et al., 1976) or less commonly to the lambda t(2;8)(p12;q24) or kappa (t(8;22)(q24;q11) light chain (Bernheim et al., 1981). After *MYC* translocation, the silencing of the *MYC* gene is prevented by positive regulatory elements of *Ig* genes *i.e.* enhancers (Wierstra and Alves, 2008).

4.2.4.2 BCL6

Together with deregulated *MYC* gene, dysfunctional proto-oncogene *BCL6* plays a major role in the pathogenesis of GC origin lymphomas including BL (Basso et al., 2010). Most GC-derived malignancies highly express *BCL6* (Bunting and Melnick, 2013). B cell lymphoma 6 (*BCL6*) is a transcriptional repressor and member of the BTB/POZ (bric-a-brac, tram track, broad complex/pox virus zinc finger) family of transcription factors consisting of a N terminal-POZ domain and six C-terminal C₂H₂ Krüppel-like zinc fingers (Lemercier et al., 2002; Mascle et al., 2003, Basso et al., 2010). *BCL6* represses numerous genes involved in activation and differentiation of lymphoid cells, in cell cycle regulation and in immune responses (Sánchez-Beato et al., 2003). These functions are performed via binding to promoter sequences thereby affecting their transcriptional activities (Pasqualucci et al., 2003) or through recruitment of class I and II histone deacetylase complexes

(HDAC, Basso and Dalla-Favera, 2012). BCL6 is degraded by the ubiquitin/proteasome pathway following its phosphorylation via mitogen-activated protein kinases (MAPKs, Niu et al., 1998) or via p300 mediated acetylation (Bereshchenko et al., 2002)

BCL6 is an important modulator of differentiation and function of B cell lineage. During rearrangement of *Ig-L* chain genes of pre-B cell in bone marrow (BM), BCL6 protects pre-B cells from DNA damage (Duy et al., 2010). BCL6 mediates pre-BCR signaling for exit from cell cycle by down-regulation of MYC expression levels (Nahar et al., 2013).

During GC formation, both in the DZ and LZ, BCL6 is a crucial factor together with MYC (Dominguez-Sola et al., 2012; Calado et al., 2012). The expression of BCL6 was identified in almost all lymphomas derived from GC B cells including BL (Sánchez-Beato et al., 2003). Mutations of BCL6 were found in around 30% to 50% of BLs (Hecht and Aster, 2000). Many studies have analyzed the mechanisms of BCL6 overexpression mostly in DLBCLs, which occur via translocations or hypermutations of its promoter (Duan et al., 2012). Although BCL6 overexpression and nuclear localization is observed in near all BL cases (G. Ott, personal communication; Sánchez-Beato et al., 2003), involved molecular mechanisms are less clear.

4.3 B cell development

As a part of the adaptive immune system, B lymphocytes protect against a large number of pathogens. The production of antibodies by B cells is an essential component of humoral immunity. Malignancy and other abnormalities may arise from alteration of certain pathways during B-cell development (Pieper et al., 2013).

Human and mouse B cells generated from the fetal liver and BM from hematopoietic stem cells (HSC). After serial stages of differentiation through B cell pathways, immature B cells leave the BM to peripheral lymphoid organs and complete their differentiation at these sites (Kondo et al., 2003; Cobaledo et al., 2007; Pieper et al., 2013).

4.3.1 The early B cell development

The earliest progenitors of B-lineage, pre-pro-B cells do not synthesize Ig since their *Ig* genes are in unrearranged germ line configuration (Hardy et al., 1991; Hardy and Hayakawa, 2001). The expression of the recombination activating genes, *Rag 1 and 2* is not detected on these cells (Oettinger et al., 1990). The formation of pro-B cells is initiated by D_H to J_H rearrangement followed by V_H to D_HJ_H rearrangement at IgH locus (Kitamura et al., 1992). The surface expression of B220 and CD19 together with $Ig\alpha/Ig\beta$ identified the pro-B cell stage identity (Fig. 3, Nagasawa, 2006; Kurosaki et al., 2010).

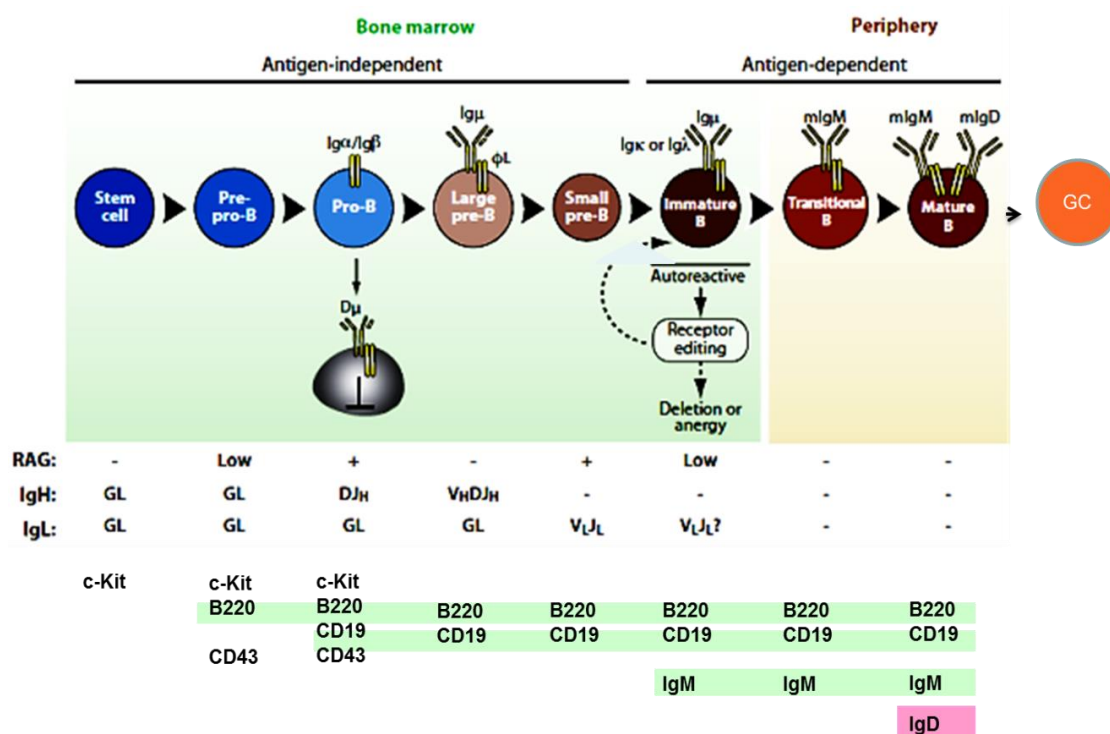


Fig. 3 B cell development. B cell sub-populations are defined by the expression of surface markers and referred as pre-pro-B cells, pro-B cells, large pre-B cells and small pre-B cells. Immature B cells leave the BM and move to the peripheral lymphoid organs. In these sites they complete their maturation by forming GC and subsequently generate memory- and plasma B cells. Modified from Nagasawa, 2006; Kurosaki et al., 2010.

Upon completion of V_HD_HJ_H recombination, pre-B cells transiently express an Ig μH chain (Fig. 3), surrogate light chains (SLC); VpreB and λ5 polypeptides and Igα-Igβ (Zhang et al., 2004). Following several rounds of cell division, pre-B cells become small pre-B cells. Accordingly, increased Rag1 and Rag2 expression is needed to initiate IgL chain rearrangements (Cain et al., 2009). This results in expression of IgM (Fig. 3 and 4) on the surface of immature B cells (Nagasawa, 2006; Pieper et al., 2013). At this stage, external antigens can be identified by these B cells (Hardy et al., 1991; Hardy and Hayakawa, 2001). Immature B cells migrate to peripheral sites through blood stream and develop into mature B cells (Nagasawa, 2006).

Transitional B cells (referred as T1 and T2), are temporary stages before B cells becoming mature (Cain et al., 2009). During T1 and T2 maturation, tolerance processes continue, as evidenced from decreased number of auto-reactive clones (Cain et al., 2009). After receptor-mediated negative selection to remove autoreactive clones remaining B cells finally become mature and co-express IgM and IgD on their surface (Cain et al., 2009; Kurosaki et al., 2010).

Mature B cells consists of three populations *i.e.* B-1B, follicular (FO) and marginal zone (MZ) B cells (Carey et al., 2008). B-1B cells are derived from fetal liver stem cells, most of them express CD5 and they are located in serous body cavity including peritoneum (Hardy and Hayakawa, 2001; Casola, 2007). FO-B cells or so called B2-B cells develop from BM precursor cells are located in the follicles of lymphoid organs and form majority of peripheral B cell (Hardy and Hayakawa, 2001; Casola, 2007). As MZ-B cells are situated adjacent to marginal sinus of spleen, they can easily detect pathogens from blood stream (Thomas et al., 2006; Carey et al., 2008).

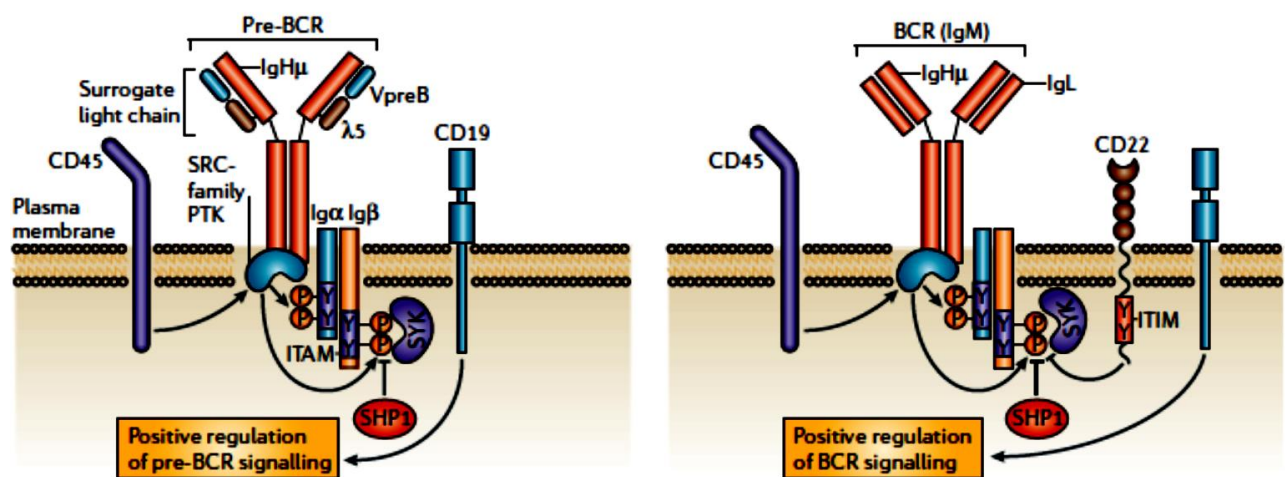


Fig. 4 Composition of the pre-BCR and BCR. The pre-BCR and BCR consist of transmembrane of *IgH* that is related to *Igα* and *Igβ*, and the surrogate light chain ($\lambda 5$ and *VpreB*) or *IgL*, respectively. Sarcoma (SRC)-family protein tyrosine kinase (PTK) phosphorylates tyrosine residues (Y) in the immunoreceptor tyrosine-based activation motifs (ITAMs) of the *Igα* and *Igβ* heterodimers. This results in the activation of spleen tyrosine kinase (SYK) which phosphorylate numerous downstream targets. Based on Monroe, 2006.

4.3.2 Germinal center reaction

GC development initiates when B cells migrate into the T-cell area of the peripheral lymphoid tissues (spleen, lymph nodes and Peyer's patches), where they are activated by the interaction with T cells (MacLennan, 1994; Klein and Dalla-Favera, 2008). Activated B cells have two fates: they either differentiate into short-living plasma cells or form GCs (Tarlinton, 2006). Formation of GCs is specified with the progressive up regulation of *BCL6* and the concomitant down regulation of *c-Myc* expression (Dominguez-Sola et al., 2012; Calado et al., 2012). The transcriptional co-activator *BOB.1/OBF.1* (B cell octamer binding protein 1/Octamer binding factor 1 (a lymphocyte specific transcriptional coactivator)) seems has an important role in GC formation, as inactivation of this gene in a mouse model suppressed GC development (Hess et al., 2001). Interaction of *BOB.1/OBF.1* protein with *Oct1* and *Oct2* leads to transcriptional activity of octamer motifs (Greiner et al., 2000).

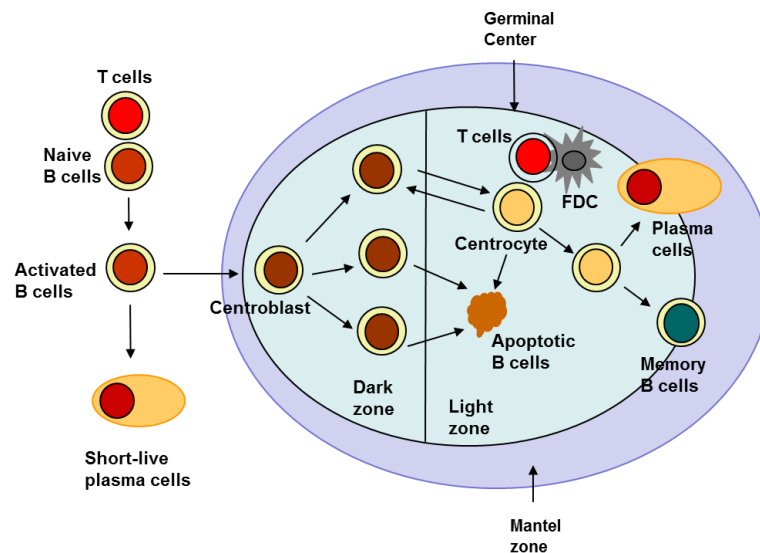


Fig. 5 Germinal center reaction. Naïve B cells migrate to the T-cell zone and are activated by T cells. Activated B cells may differentiate into short-living plasma cells or enter the DZ, proliferate and become centroblasts. Centroblasts undergo SHM which introduces high rate mutations and most mutations lead to reduced antigen affinity of their BCR, if this occurs they undergo apoptosis. Centroblasts enter the LZ and differentiate into centrocytes. Upon activation by T cells and follicular dendritic cells (FDCs), centrocytes differentiate into memory B or plasma cells or re-enter the DZ. Centrocytes which fail to bind antigens undergo apoptosis. Modified from Küppers, 2005; Tarlinton, 2006; Victora and Nussenzweig, 2012.

GC development is usually completed but it is still immature within 4 days after immunization, becomes mature about 10 days (Calado et al., 2012) and reached maximum size around 2 weeks (Klein and Dalla-Favera, 2008). GC is divided into discrete anatomic structure so called DZ and LZ (Nieuwenhuis and Opstelten, 1984; MacLennan, 1994). The DZ contains centroblasts - cycling B cells, where SHM is initiated. Conversely, the LZ besides follicular dendritic cells (FDCs) and follicular T helper cells comprises of centrocytes - non-proliferating B cells, which undergo CSR and clonal selection (Fig. 5, MacLennan, 1994; Klein and Dalla-Favera, 2008). In the LZ, c-Myc is re-expressed since its expression is required by centrocytes to re-enter the DZ, thereby maintaining the GC cells nature (Dominguez-Sola et al., 2012; Calado et al., 2012). In addition, NF- κ B activity and IRF4 expression is upregulated, but BCL6 is down regulated (Calado et al., 2012). Centrocytes differentiate into plasma cells and memory B cells or undergo apoptosis if they fail to bind antigens (Fig. 5, Tarlinton, 2006).

Genetic alterations in the GCs are introduced through SHM and CSR of *Ig* genes. Both processes need AID (Muramatsu et al., 2000). SHM modifies the variable region of rearranged *Ig* genes (Bross et al., 2000). CSR facilitates isotype switching of the IgH of activated B cells from IgM and IgD to either IgG, IgA or IgE (Klein and Dalla-Favera, 2008).

4.4 Burkitt lymphoma models

Many *in vitro* and *in vivo* tumor models were developed to study the pathogenesis of BL. Numerous cell lines were derived from BL patients such as Ramos, Namalwa, Raji, Daudi cells etc. One limitation of these cell lines is constant MYC expression level. Therefore Tet-system and estrogen receptor fusion systems (Felsher and Bishop, 1999; Arvanitis and Felsher, 2006) were used to create conditional overexpression of c-Myc to induce tumorigenesis *in vivo* and to manipulate MYC expression in tumors.

Deregulation of *MYC* expression has a significant effect on the development of lymphomas. In the majority of BL, the *MYC* gene has been activated by translocation to the *IgH*-chain locus. It is coupled to the lymphoid-specific enhancer (*E μ*) of the *IgH*-chain locus (Willis and Dyer, 2000). Based on this concept *in vivo* models were generated. Adam and colleagues (Adam et al., 1985) created transgenic *E μ -Myc* mice using transgenic construct which is equivalent to a rearranged *MYC* allele in plasmacytoma ABPC17 (Corcoran et al., 1985). In this model the transcription of the transgene is driven by the control elements from the *IgH-chain* gene. Hence, the *MYC* transgene is transcribed only in the B cell lineage. After several weeks of latency these mice develop clonal pre-B, mature B cell lymphomas (BCLs), and mixed pre-B/B lymphomas (Adam et al., 1985; Harris et al., 1988). This suggests that progression to malignancy in *E μ -Myc* mice, like in human BL, depends on additional oncogenic events (Harris et al., 1988). In respect to tumor origin, transgenic *E μ -Myc* mice do not reflect human BL. Therefore, further mouse models were created. The role of BCR signalling in MYC-induced lymphomas was also investigated through the generation of transgenic model based on *E μ -Myc* mice. In this model, B cells express the BCR with the specificity for simultaneously expressed transgenic protein antigen. However, instead of clonal development at clonal tumors authors observed polyclonal proliferation of all B cells (Refaeli et al., 2008). Finally, Sander and colleagues successfully generated a transgenic mouse model which shows close similarities to human BL in respect to histology, surface and internal markers and gene expression profile (Sander et al., 2012). In this model, the cooperation of MYC and the PI3K pathways in BL pathogenesis was established (Sander et al., 2012), similar to conclusion from gene expression profiling of human BL (Schmitz et al., 2012).

4.5 Survival factors for BL cells

Activation of oncogenes and inactivation of tumor suppressor genes in malignant tumors result in an uncontrolled cell growth, which destroy the architecture of surrounding tissues and lead to spread of tumor cells to other sites (Hanahan and Weinberg, 2000). The rapid growth of BL cells suggests low apoptotic but high proliferation rate indicating deregulation of apoptotic pathways (Kalungi et al.,

2012). However, BLs show a low activity of the pro-survival NF- κ B signaling (Dave et al., 2006). BL cells are also often negative for Bcl-2 (Molyneux et al., 2012). Recent evidence from a mouse model indicated the cooperation between the MYC and phosphoinositide 3-kinase (PI3K) cascade during progression of BL-like tumor cells (Sander et al., 2012). Akt (protein kinase B/PKB) is a serine/threonine kinase and activated via phosphorylation by PI3K (Qiao et al., 2013). Mutation and amplification of Akt/PKB isoforms are identified in human cancers (Brugge et al., 2007). BL almost always shows an activity of the PI3K-dependent mTORC1 complex (Schmitz et al., 2012).

Besides NF- κ B pathway, NFAT family proteins are major regulators of activation-induced cell death (AICD) in T- and B-cells. Immunoreceptor triggering results in a massive synthesis of anti-apoptotic NFATc1/ α A isoform in T- (Chuvpilo et al., 2002) and B-cells (Bhattacharyya et al., 2011). Therefore we hypothesized that NFATc1 might be important survival factor for BL cells and might represent specific therapeutic target.

4.6 Nuclear Factor of Activated T-Cell (NFAT)

The Nuclear Factor of Activated T Cell (NFAT) proteins were initially discovered as T cell receptor induced factors regulating the interleukin-2 (IL-2) promoter (Shaw et al., 1988; Serfling et al., 1989) and other lymphokine genes in T cells (Serfling et al., 2006a). Nowadays, the members of NFAT family are identified as important regulators that play roles in heart, cardiac valves and septum (de la Pompa et al., 1998), in blood vessels, the muscular and nervous systems (Graef et al., 2001), in myeloid cells (Fric et al., 2012), in osteoclasts and osteoblast (Winslow et al., 2006), in astrocytes (Furman et al., 2012), the skin (Al-Daraji et al., 2009), and control hair growth (Horsley et al., 2008).

The NFAT family consists of four closely related proteins, the genuine NFATc1 (=NFAT2, NFATc), NFATc2 (=NFAT1, NFATp), NFATc3 (NFAT4, NFATx), NFATc4 (=NFAT3) factors and a more distant relative, NFAT5 (TonEBP, OREBP, NFATz). NFATc1-c4 are calcium (Ca^{2+})/calcineurin (CN)-dependent, whereas NFAT5 is a distinct family member, which reacts to osmotic stress (Fig. 6 and 7, Lopez-Rodriguez et al., 1999; Macian, 2005). All NFATs contain a highly conserved DNA binding domain (RSD), which binds to the core DNA motif A/TGGAAA, cooperate with other factors, such as AP1 except NFAT5 (Serfling et al., 2004).

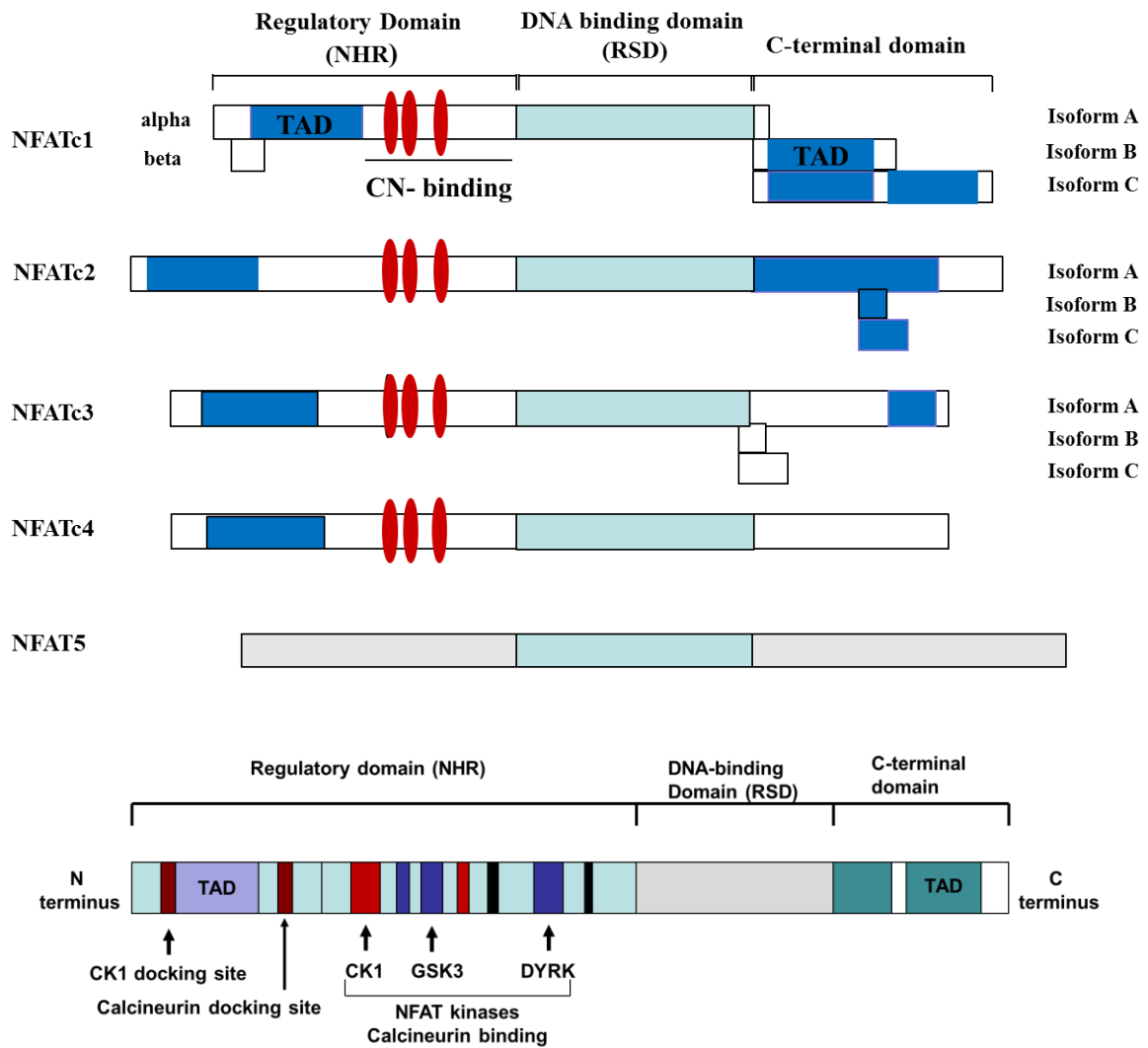


Fig. 6 Structure of the NFAT family members. NFATc1-c4 are closely related. They contain Ca^{2+} /CN dependent regulatory domain, NFAT homology region (NHR), highly conserved DNA binding domain (RSD) and a carboxy-terminal domain. The C-terminal domain contains TADs and regulatory elements, *i.e.* sumoylation sites. The NHR consists of transactivating domain, docking sites for casein kinase 1 (CK1) and CN and multiple phosphorylation sites targeted by CN. Based on Serfling et al., 2006a; Müller and Rao, 2010.

4.6.1 Regulation of NFAT activity

The activity of NFATc1-c4 proteins is tightly controlled by the Ca^{2+} /calmodulin serine/threonine dependent phosphatase CN (Loh et al., 1996a). In resting cells, NFAT transcription factors are heavily phosphorylated and localized in cytosol (Rao et al., 1997). Activation of NFAT proteins involves three steps: dephosphorylation, nuclear translocation, and increase in DNA binding affinity (Rao et al., 1997). This activation is regulated through the stimulation of cell surface receptors coupled to Ca^{2+} mobilization, such as the antigen receptors on T and B cells, the $\text{Fc}\gamma$ receptors on macrophages and NK cells, and receptors coupled to certain heterotrimeric G proteins. As a

consequence, inositol (1,4,5) trisphosphate (InsP₃) and diacylglycerol (DAG) are generated. DAG activates the RAS/PKC pathway. InsP₃ mediates the release of Ca²⁺ from internal stores, followed by the opening of specific store-operated calcium channels (CRAC), resulting in the influx of extracellular Ca²⁺ and the Ca²⁺/calmodulin-dependent activation of CN (Rao et al., 1997; Gwack et al., 2007). Activated CN dephosphorylates multiple phosphoserine residues on cytosolic NFAT proteins and, thereby, enables their nuclear translocation (Luo et al., 1996; Shibasaki et al., 1996; Hogan et al., 2003).

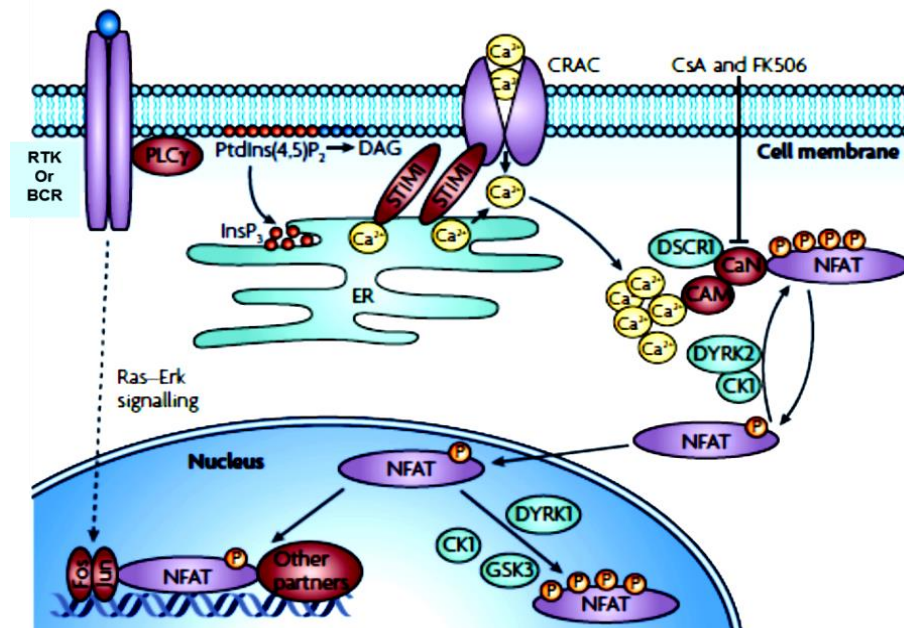


Fig. 7 Calcium signaling and NFAT activation. Receptor tyrosine kinases (RTKs) and immune receptors, such as the BCR, activate the phospholipase C_γ (PLC_γ) which in turn hydrolyses phosphatidylinositol-4,5-bisphosphate (PtdIns (4,5)P₂). This releases inositol-1,4,5-trisphosphate (InsP₃) and diacylglycerol (DAG) and results in loss of Ca²⁺ binding to stromal interaction molecule 1 (STIM1), due to Ca²⁺ release from endoplasmic reticulum (ER). The Ca²⁺ release then activates Ca²⁺ channels (CRAC), leads to opening of CRAC channels and allows sustained extracellular Ca²⁺ influx. Calmodulin binds to Ca²⁺ and the phosphatase CN resulting in a binding of Ca²⁺ to the CN regulatory B subunit, thus exposing the CAM-binding site on the catalytic A subunit and releasing an autoinhibitory sequence in CN from the catalytic pocket. The phosphatase CN dephosphorylates NFAT and promotes its nuclear translocation. Based on Mancini and Toker, 2009.

In the nucleus, NFAT proteins bind to specific *cis*- and *trans*-elements to control the transcription of their target genes either alone or in cooperation with other factors (Loh et al., 1996; Chen et al., 1998; Garcia-Cozar et al., 1998). As a major upstream regulator of NFAT proteins, the Ca²⁺/calmodulin-dependent activation of CN is the main target for inhibition by the well-characterized CN inhibitors cyclosporin A (CsA) and tacrolimus (FK506) (Loh et al., 1996a). The nuclear export of NFAT is regulated through the phosphorylation of its serine residues by certain kinases, such as by glycogen synthase kinase-3 (GSK), protein kinase A (PKA), casein kinase 1

(CK1), p38 MAPK and c-Jun N-terminal kinase 1 (JNK1). The activity of these kinases leads to the termination of CN signal (Beals et al., 1997; Sheridan et al., 2002; Okamura et al., 2004; Gomez del arco et al., 2000; Liang et al., 2003).

Based on the close interaction between the phosphatase CN and NFAT, a peptide, namely VIVIT was carefully chosen. This peptide inhibits that interaction, thus, preventing activation of NFAT (Aramburu et al., 1999).

4.6.2 NFATc1

Among the NFAT members, NFATc1 is special, since its short isoform, NFATc1/ α A is highly induced in activated lymphocytes and is able to autoregulate transcription of *Nfatc1* gene via binding to the inducible P1 promoter leading to predominant expression of anti-apoptotic NFATc1/ α A isoform (Serfling et al., 2006, Serfling et al., 2012). Correspondingly, NFATc1 deficiency results in reduced proliferation of B-cells and reduction of B1a cell population (Bhattacharyya et al., 2011), as well as decreased IL4 and IL6 expression (Ranger et al., 1998; Yoshida et al., 1998).

The highly conserved murine and human *NFATc1* genes span ~110kb and 140kb DNA, respectively and comprises of 11 exons (Serfling et al., 2006). In lymphocytes, *Nfatc1* transcription is regulated by two promoters, the inducible promoter P1 located upstream of exon 1 and the constitutive promoter P2 situated upstream of exon 2 (Chuvpilo et al., 1999). Due to two polyA sites, pA1 and pA2, and alternative splicing events six prominent isoforms are generated which differ in the length of their C terminal peptide (Fig. 8, Serfling et al., 2006). Depending on the promoter usage, the *Nfatc1* gene is transcribed into either the α or β isoforms (Park et al., 1996; Chuvpilo et al., 1999; Chuvpilo et al., 2002).

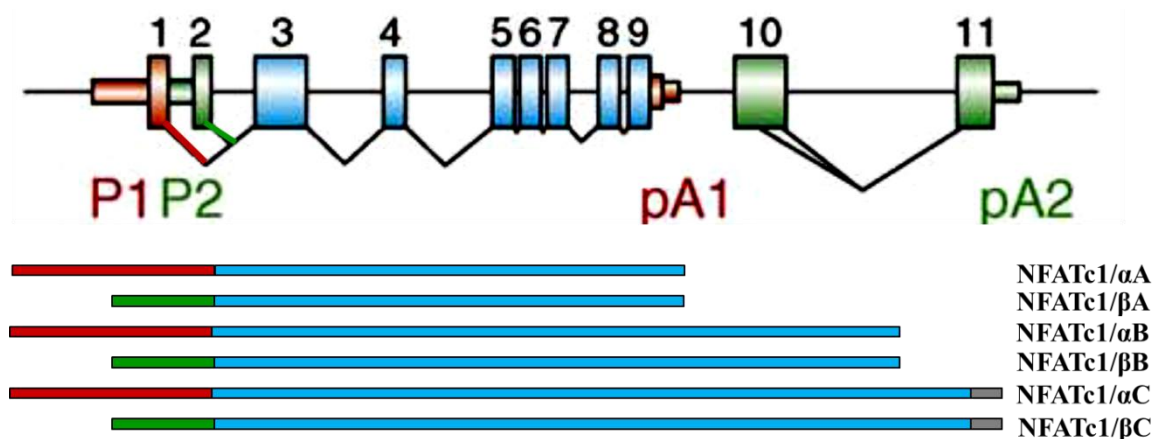


Fig. 8 Structure of the *Nfatc1* gene and the generation of six NFATc1 isoforms. P1, P2 promoters and two poly A addition sites, pA1 and pA2 are indicated. N-terminal α - and β -peptides are indicated as red and green, respectively. Based on Serfling et al., 2006.

In resting lymphocytes the transcription of the *Nfatc1* gene is controlled by the P2 promoter and distal polyA2 site (Chuvpilo et al., 2002). Switching to the P1 promoter and the use of proximal polyA site pA1 as a consequence of stimulation of lymphocytes through their immune receptors leads to the synthesis of NFATc1/ α A mRNA encoding the inducible short NFATc1 isoform (NFATc1/ α A). This isoform lacks the C-terminal peptide (~ 250 aa) and hence lacks a second TAD characteristic for most of longer NFATc1 isoforms proteins (Avots et al., 1999; Chuvpilo et al., 2002). NFATc1/ α A, the shortest of six isoforms contains a specific N-terminal peptide, designated as α -peptide, which differs from NFATc1/ β isoforms (Serfling et al., 2006). The longer isoforms NFATc1/B and NFATc1/C contain an extra C-terminal peptide of 128 and 246 aa, respectively, and are expressed constitutively from the P2 promoter (Serfling et al., 2006). In addition, the expression of the *NFATc1* gene is also regulated by remote enhancer elements (Hock et al., 2013).

The P1 promoter sequences are highly conserved between mouse and human. The P1 and P2 promoters form DNase I–hypersensitive chromatin sites and encompass a CpG islands. P1 harbors multiple DNA motifs for the binding of inducible transcription factors, such as for CREB, Fos, ATF, and palindromic NFAT sites (Serfling et al., 2012).

4.6.3 NFATc1 and carcinogenesis

In addition to their central role in the immune response, NFATc1 proteins regulate the proliferation and apoptosis of other normal and tumor cells. Both NFATc1 and NFATc2 proteins were identified as regulators of COX-2 expression in colon carcinoma cells (Duque et al., 2005). Nuclear localization of NFATc1 was detected in DLBCLs (Pham et al., 2010), in pancreatic cancer cells (Buchholz et al., 2006), in BL (Marafioti et al., 2005), and in certain T cell lymphomas/leukemias (Medyouf et al., 2007; Abbott et al., 1998). Activation of NFATc1 induces formation of ovarian and skin tumors *in vivo* (Tripathi et al., 2013). In addition, expression of constitutively active NFATc1 version promotes cancer cell invasion via down regulation of E-cadherin expression (Oikawa et al., 2013).

NFATc1 is one of transcriptional activators of the *MYC* promoter (Wierstra and Alves, 2008; Willis and Dyer, 2000). In pancreatic cancer cells and preadipocyte, NFATc1 stimulated *MYC* mRNA and protein expression (Buchholz et al., 2006; Neal and Clipstone, 2003). In several tumors such as in leukemias, lymphomas, pancreatic, colon and breast cancers, both NFAT and *MYC* are over-expressed (Marafioti et al., 2004; Jauliac et al., 2002; Buchholz et al., 2006; Medyouf et al., 2007; Pham et al., 2010). Together these findings suggest that NFATc1 might contribute to high levels of *MYC* expression in human malignancies.

4.7 Objectives of the thesis

Burkitt lymphoma (BL) is a highly aggressive B cell malignancy driven by high expression levels of MYC. Pro-apoptotic properties of MYC in lymphoma cells are counteracted by survival pathways. In normal B-cells BCR triggering activates both NF κ B- and NFAT-dependent survival signals. Since BL cells do not exhibit constitutive NF κ B activity, we hypothesized that anti-apoptotic component of NFATc1 signaling might provide a major survival signal for BL cells.

The aim of the current thesis was to investigate the role of anti- and pro-apoptotic NFATc1 isoforms in BL and in BCL, with a final goal to evaluate their potential as therapeutic targets.

We show that CN-independent anti-apoptotic NFATc1A isoforms are constitutively expressed and nuclear in all BL-related entities analysed. In the absence of NFATc1 expansion of experimental BCL tumors is strictly compromised. Activities of pro-apoptotic NFATc1B/C isoforms are counteracted in BL cell lines. Therefore, our results implicate the whole NFATc1 gene and NFATc1 α A/ β A isoforms as novel therapeutic targets to treat BL and other B cell malignancies

5. Materials and Methods

5.1 Materials

5.1.1 Chemicals

Acetic acid	Liquid Nitrogen
Acrylamide/Bisacrylamide	Magnesium chloride
Ammonium peroxodisulfate (APS)	Methanol
Agar	Midori green (Nippon genetic Europe GmbH)
Agarose	Natrium azide
Boric acid	Natrium chloride (NaCl)
Bovine Serum Albumin (BSA)	Natrium hydrogenphosphate
Bradford reagent	Natrium hydroxyde
Bromophenol blue	Natrium pyruvate
β -Mercapthoethanol	Natrium carbonate
Chlorofom (Trichlormethane)	Paraformaldehyde
DAPI (4',6-diamidino-2-phenylindole)	Phosphate acid
Disodium hydrogen phosphate	Phenylmethylsulphonylfluoride (PMSF)
Dimethyl-sulfoxide (DMSO)	Ponceau S
Dithiothreitol (DTT)	Power SYBR Green PCR Master Mix
Distilled water (dH ₂ O)	Propidium iodide
Ethidium bromide (EtBr)	Sodium dodecyl sulfate (SDS)
Ethylendiamintetraacetate acid (EDTA)	Sulfuric acid
Ethylene glycol tetraacetate acid (EGTA)	TEMED (Tetramethylenediamine)
Ethanol	Tissue Tec
Fetal calf serum (FCS)	Tris
Fluoroshield (+DAPI)	Triton-X-100
Glycerin	Trypan Blue Solution
Glycin	Trypsin/EDTA
Hydrogen chloride (HCL)	Tween 20
Isopropanol (2-propanol)	2x PCR Mix
Kalium chloride	6x DNA loading dye

Unless otherwise indicated, all materials were from Amersham Biosciences, AppliChem, BioRad, Calbiochem, Fermentas, Fluka, Gibco, Merck, PeqLab, Roche Diagnostics and Roche Molecular Biochemicals, Roth, Serva and Sigma-Aldrich.

5.1.2 Buffers

All buffers and solutions were diluted with distilled water (dH₂O).

Annexin-Binding Buffer (1X)	HEPES (pH 7.4)	10 mM
	NaCl ₂	149 mM
	CaCl ₂	2.5 mM

Buffer-A	HEPES (pH 7.9)	10 mM
	KCl	10mM
	EDTA	0.1 mM
	EGTA	0.1 mM
Buffer-B	HEPES (pH 7.9)	20 mM
	NaCl	0.4 M
	EDTA	1 mM
	EGTA	1 mM
FACS-buffer	Na ₂ HPO ₄ (pH 7.4)	10 mM
	NaCl	137 mM
	KCl	2.6 mM
	KH ₂ PO ₄	1.8 mM
	BSA	0.1% (w/v)
	(NaN ₃)	0.1% (w/v)
Genomic lysis buffer	Tris (pH 8.0)	50 mM
	NaCl	300 mM
	SDS	0.2% (w/v)
	EDTA	25 mM
	Proteinase K	1000 U/ml
Laemmli-buffer (1x)	Tris-HCl (pH 6.8)	125 mM
	SDS	4% (w/v)
	Glycerin	20% (w/v)
	β-Mercaptoethanol	10% (w/v)
	Bromphenol Blue	0.004% (w/v)
HBS-Puffer (2x)	HEPES (pH 7.05)	50 mM
	NaCl	280 mM
	KCl	10 mM
	Dextrose	12 mM
	Na ₂ HPO ₄	1.5 mM
MACS-buffer	NaCl (pH 7.4)	137 mM
	Na ₂ HPO ₄	10 mM
	KCl	2.6 mM
	KH ₂ PO ₄	1.8 mM
	BSA	0.1% (w/v)
	EDTA	2 mM
PBS (1x)	NaCl (pH 7.4)	137 mM
	Na ₂ HPO ₄	10 mM
	KCl	2.6 mM
	KH ₂ PO ₄	1.8 mM

Red blood cell lysis buffer:

<u>Solution A</u>	<u>Solution B</u>	<u>Solution C</u>	<u>Ready-to-use buffer</u>
14g NH ₄ Cl	0.42g MgCl ₂ x6H ₂ O	2.25g NaHCO ₃	10ml solution A
0.74g KCl	0.14g MgSO ₄ x7H ₂ O		2.5ml solution B
0.6g Na ₂ HPO ₄	0.341gCaCl ₂		2.5ml solution C
0.048g KH ₂ PO ₄			
RIPA-buffer (1x)	Tris-HCl 1M (pH 7.5)	50 mM	
	NaCl 5M	150 mM	
	TritonX-100	1 %	
	Na-deoxycholat	1 %	
	SDS 20%	0.1 %	
	EDTA 0.5M pH 8	1 mM	
SDS-running buffer	Tris-HCl (pH 8.4)	25 mM	
	Glycin	192 mM	
	SDS	0.1% (w/v)	
Stripping-buffer	Tris-HCl (pH 6.8)	65 mM	
	SDS	2% (w/v)	
	β-Mercaptoethanol	100 mM	
TAE buffer (50x)	Tris acetate (pH 8.2-8.4)	2 M	
	EDTA	0.5 M	
TBS (1x)	Tris-HCl (pH 7.5)	25 mM	
	Glycin	150 mM	
	(NaN ₃)	0.1% (w/v)	
TBS-Tween	Tris-HCl (pH 7.5)	25 mM	
	Glycin	150 mM	
	Tween 20	0.2% (v/v)	
Transfer-buffer	Tris-HCl (pH 8.4)	48 mM	
	Glycin	40 mM	
	SDS	14 mM	
	Methanol	20% (v/v)	
10% Resolving gel (10 ml)	H ₂ O	4.0 ml	
	30% Polyacrylamide	3.3 ml	
	1.5 M Tris (pH 8.8)	2.5 ml	
	10% APS	0.1 ml	
	10% SDS	0.1 ml	
	TEMED	0.004 ml	

Stacking gel (3 ml)	H ₂ O	2.1ml
	30% Polyacrylamide	0.5 ml
	1.5 M Tris (pH 6.8)	0.25 ml
	10% APS	0.3 ml
	10% SDS	0.3 ml
	TEMED	0.003 ml

5.1.3 Antibiotics and inhibitors

Ampicillin	Sigma-Aldrich
BAPTA AM [1,2-Bis(2-aminophenoxy)ethane -N,N,N',N'-tetraacetic acid tetrakis (acetoxymethyl ester)]	Santa Cruz Biotechnology
Cyclosporine A (CsA)	Calbiochem
HALT Protease inhibitor cocktail	Thermo scientific
Penicillin/Streptomycin	Gibco
Jak3 inhibitor	Calbiochem

5.1.4 Antibodies and Reagents

Fluorescence-conjugated antibodies and reagents for FACS analysis (anti-mouse)

Annexin V APC	BD Pharmingen
Antibody Diluent	Dako
B220 Biotin (RA3-6B2)	BD Pharmingen
CD19 PE (1D3)	BD Pharmingen
CD16/32/Fc block (93)	BD Pharmingen
IgD PE (IA6-2)	Jackson Laboratory
IgM APC (1/41)	eBiosciences
IgM FITC (B121-15F9)	eBiosciences
Ki-67 Alexa Fluor 647 (Sol A 15)	eBiosciences
Streptavidin APC	eBiosciences
Streptavidin eFluor 450	eBiosciences
Streptavidin PerCP.Cy5.5	BD Pharmingen

Primary antibodies for Western Blot, immunohistochemistry and immunofluorescence analysis

Mouse anti NFATc1 (7A6)	BD Pharmingen
Mouse anti-β Actin (C4)	Santa Cruz Biotechnology
Goat anti CD20 (M-20, polyclonal)	Santa Cruz Biotechnology
Mouse anti dsRed (polyclonal)	Santa Cruz Biotechnology
Mouse anti-c-Myc (9E10)	Santa Cruz Biotechnology
Rabbit anti BCL6 (D65C10)	Cell Signaling
Mouse anti-CD68 (KP1)	Dako

HRP conjugated secondary antibodies for Western Blot and immunohistochemistry analysis

Goat anti Mouse HRP	Sigma-Aldrich
Goat anti Rabbit HRP	Sigma-Aldrich

Secondary antibodies for immunofluorescence

Goat- anti-Mouse Alexa Fluor 555	eBiosciences
Goat- anti-Mouse Alexa Fluor 488	eBiosciences
Goat- anti-Rabbit Alexa Fluor 555	eBiosciences
Goat- anti-Rabbit Alexa Fluor 488	eBiosciences
Streptavidin Alexa Fluor 488	eBiosciences
Goat-anti-Mouse Alexa Fluor 647	Dianova
Donkey anti-Goat Alexa Fluor 488	Invitrogen

5.1.5 Oligonucleotides

All oligonucleotides were synthesized by Eurofins/MWG/operon or Sigma-Aldrich and dissolved in dH₂O at a final concentration of 100pmol/μl.

5.1.5.1 Primers for genotyping of mouse tails

Primers	Target	Sequences	Product size (bp)
<i>Eμ-myc for</i> <i>Eμ-myc rev</i>	<i>Eμ-myc</i> transgene	cagctggcgtaatagcgaagag ctgtgactggtgagtactcaacc	850
<i>Nfatc1flox for</i> <i>Nfatc1flox rev</i>	5' <i>NFATc1</i> flx site	cctatttaaacacctccctcg ccatctctctgaccaacagaagccag	425 (flx) 320 (wt)
<i>mb1-cre for</i> <i>mb1-cre rev</i>	<i>mb-1 cre</i> knock-in	acctctgatgaagtcaggaagaac ggagatgtcctcactctgattct	500
<i>mb1-wt for</i> <i>mb1-wt rev</i>	<i>mb-1 wt</i> allele	ctgctggtagaagggggt cctgctgaggtcagggagcc	400
M16 dsRed_seq-L	<i>NFATc1-dsRed</i> knock-in allele	cctgcctctctcagccttga cctcgaagttcatggagcgc	893

5.1.5.2 Primers for Reverse Transcriptase (RT) and Real-Time PCR

RT- PCR

Primers	Target	Sequences
qRT mL32 F qRT mL32 R (Buxade et al., 2012)	mouse <i>L-32</i>	accagtcagaccgatatgtg attgtggaccaggaacttcg
m <i>NFATc1</i> -Ex3 m <i>NFATc1</i> -Ex7	mouse <i>Nfatc1</i>	catgcccctctgtggccc ggagccttccacgaaaatg
m <i>NFATc1</i> P1-U #867 m <i>NFATc1</i> P1/P2-L #868 m <i>NFATc1</i> P2-U #869	mouse <i>Nfatc1</i> -P1 and-P2 promoters	gggagcggagaaactttgc gatctcgattctcgactctcc cgacttcgattcctcttcgag
h <i>L-32</i> -U1 h <i>L-32</i> -L1	human <i>L-32</i>	ttgtgaagcccaagatcgtc agcactccagctccttgac
h <i>NFATc1</i> -1U h <i>NFATc1</i> -1L	human <i>NFATc1</i>	agctgcatggctacttggag ctctgcttctccaccagagg
h <i>NFATc1</i> P1-U #867 h <i>NFATc1</i> P1/P2-L #868 h <i>NFATc1</i> P2-U #869	human <i>NFATc1</i> -P1 and P2 promoters	cttcgggagaggagaaactttg gaggttatctcgatgcgaggac tcgacttcgagttcctcttcg

Real-Time PCR

Primers	Target	Sequences
<i>mActin</i> -F <i>mActin</i> -R	mouse β - <i>actin</i>	gacggccagggtcatcactattg aggaaggctggaaaagagcc
qRT <i>HPRT</i> for qRT <i>HPRT</i> rev	mouse <i>Hprt</i>	agcctaagatgagcgcaagt ttactaggcagatggccaca
qRT <i>mL32</i> F (Buxade) qRT <i>mL32</i> R (Buxade et al., 2012)	mouse <i>L-32</i>	accagtcagaccgatattgtg attgtggaccaggaacttgc
qRT <i>NFATc1</i> fwd qRT <i>NFATc1</i> rev	mouse <i>Nfatc1</i>	gatccgaagctcgatggac agtctctttccccgacatca
P1 promoter Dir P1 promoter rev	mouse <i>Nfatc1</i> -P1 promoter	gggagcggagaaactttgc cagggtcgaggtgacactagg
P2 (Ex2/3-Ex3) Dir P2 (Ex2/3-Ex3) rev	mouse <i>Nfatc1</i> -P2 promoter	aggacccggagttcgacttc gcagggctcgaggtgacactag
qRT-h <i>NFATc2</i> -U qRT-h <i>NFATc2</i> -L	human <i>NFATc2</i>	gggccactatgagacagaa aagatctgaagtcccagaggc

5.1.6 Enzymes

ADVANCE HRP enzyme	Dako
Peroxidase	Dako
Proteinase K (822U/ml)	Fermentas

5.1.7 Kits and systems

anti-mouse B cell-isolation kits	Miltenyi Biotec
iScript cDNA synthesis kits	BioRad
PCR Master Mix (2x)	Fermentas
SuperSignal West Pico ECL Substrate	Pierce/Thermo Scientific
Trizol reagent	Invitrogen
First Strand cDNA Synthesis Kit	Fermentas
ADVANCE HRP LINK	Dako
Diaminobenzidine (DAB)	Dako

5.1.8 Stimulators

Ionomyacin	Sigma-Aldrich
TPA (PMA)	Merck
anti-IgM	Dianova
anti-CD40	R&D

5.1.9 Size Standard

DNA-Marker Gene Ruler 1 kb	Thermo Scientific
DNA-Marker Gene Ruler 100 bp	Thermo Scientific
PageRuler™ Prestained Protein Ladder	Thermo Scientific

5.1.10 Cell lines

Cell lines	Characteristics	Growth Medium
Ramos	Human BL cell line	RPMI, 10%FCS, 0.1% β mercapthoethanol
Namalwa	Human BL cell line	RPMI, 10%FCS, 0.1% β mercapthoethanol
P-493-6	Human B cell line immortalized with EBV	RPMI, 15%FCS, 0.1% β mercapthoethanol

5.1.11 Experimental animals

All mice used in a current study were kept and bred in a twelve hour circadian rhythm at 22°C and suitable humidity in the animal houses of the Institute of Pathology, the Institute of Microbiology and Hygiene and at the Center for Experimental Molecular Medicine (ZEMM) of the University of Wuerzburg. The animals were feed with a special animal pelleted diet and water *ad libitum*. All offspring were genotyped at the age of about 4 weeks.

The experimental animals were 8-20 weeks old gender-matched littermates. For some experiments with *E μ -Myc* mice age-and gender-matched wild type mice were used as controls. All mouse lines were maintained on C57BL/6 background.

Mouse strains

C57BL/6
 B6.*E μ -myc*
 B6.*NFATc1^{flx/flx}*
 B6.*mb1-cre*
 B6.*NFATc1-dsRed*

Origin/Reference

Jackson Laboratory/Charles River
 Adam et al. (1985)
 A. Rao, Harvard University
 Hobeika et al. (2006)
 Rhoda Busch, Institute of Pathology,
 University of Würzburg

5.1.12 Consumables

Cell culture plates (96 well)
 Cell culture plates (6, 12, 24, 48 well)
 Cell culture plates (6cm, 10cm)
 Cell culture flasks (75cm flask)
 Cell separation columns (LS)
 Cell strainer (70 μ m)
 Cover slips
 Cryo tube (2ml)
 Cuvette (quartz)
 Cuvette (plastic)
 Erlenmeyer flasks (1000ml, 500ml, 100ml)
 FACS tubes
 Falcon tubes 15ml and 50ml
 Forceps for animal preparation
 Freezing container

Greiner, Nunc
 Greiner, Nunc
 Greiner, Nunc
 Greiner
 Milteny Biotech
 BD Bioscience
 Paul Marienfeld GmbH
 Greiner
 Hellma
 Braun
 Schott
 Greiner
 Greiner
 Hartenstein
 Nalgene

Microcentrifuge tubes (1.5ml, 2ml)	Eppendorf
Mini surgery kit (animal preparation)	Hartenstein
Object glass slides	Hartenstein
Pasteur-pipettes	Hartenstein
PCR plates, white (96 well)	Thermo Fisher
Pipette tips (1000µl, 100µl, 10)	Sarstedt
Serological pipette (25ml, 10ml, 5ml, 2ml)	Greiner
Sterile filters (0.2µm, 0.45µm)	Sartorius stedim
Syringe (2ml, 5ml, 10ml)	Braun
Syringe Needle (23GA, 20GA)	Hartenstein
Tuberculin syringe (26 GA 3/8")	Braun
Protran BA 85 Nitrocellulose	GE Healthcare
Wathman 3MM filter paper	Hartenstein
X-ray cassette	Hartenstein

5.1.13 Instruments and accessories

Autoclave	Systec Dx45
Balance	Hartenstein
Camera (mounting in light microscope)	Olympus Colorview
Centrifuge	Eppendorf
Cold centrifuge	Heraeus
Confocal microscope TCS SP5 II	Leica Microsystems
Cuvettes Brand	Hellma
Gel Doc™ XR+	BioRad
Heating blocks	Hartenstein
Light microscope (dual head)	Olympus
Microcentrifuge	Eppendorf
Microwave	Privileg
Neubauer counting chamber	Brand
PCR machine	Primus 96
pH meter	WTW
Real-Time RCR machine	ABI Prism 7000
SDS-PAGE apparatus	Hofer
Spectrophotometer GeneQuant Pro	Amersham Bioscience
Spectrophotometer	Pharmacia
Spectrophotometer Nanodrop	PeqLab
Vortexer	Eppendorf
Waterbath	Heidolph
Western blot apparatus	Hofer
FACS Canto II	BD Bioscience
CO ₂ Incubator	Heraeus Instruments

5.1.14 Electronical data processing

Collection, extraction, analysis and presentation of the data and pictures were performed using Lenovo lap top. In addition the following programs were used:

BD FACS Diva 5.0; FlowJo Software (Tree Star); FusionCapt Advance of Fusion Vilber Lourmat program; GraphPad Prism 5; Image Lab Software; Leica Software ImagePro Plus; Microsoft Office

Excel 2010; Microsoft Office PowerPoint 2010; Microsoft Office Word 2010; Thomson EndNote X7 0.2.

5.2 Methods

5.2.1 Cellular Technics

5.2.1.1 Culture of cells

The cells were maintained in a humidified incubator at 37°C and 5% CO₂.

Depending of cell types the following media from Gibco were used:

DMEM, supplemented with 10% FCS (v/v); 2mM L-Glutamin; 1mM Natrium-Pyruvat; 100 U/ml Penicillin/Streptomycin

RPMI supplemented with 10% FCS (v/v); 2 mM L-Glutamin; 1 mM Natrium-Pyruvat 100 U/ml Penicillin/Streptomycin and 50 µM β-Mercaptoethanol

X-Vivo 15, supplemented with 10% FCS (v/v); 2 mM L-Glutamin; 100 µM NEAA; 1mM Natrium-Pyruvat; 100 U/ml Penicillin/Streptomycin and 50 µM β-Mercaptoethanol

5.2.1.2 Centrifugation of cells

The centrifugation of the cells was performed, unless otherwise stated, in a Rotina 420R (Hettich) for 5 min at 1400 rpm in 4° C.

5.2.1.3 Counting of cells

A Neubauer chamber was used to determine the number of cells. The cell suspension was mixed with trypan blue solution to stain the dead cells (Viability test). The cells were loaded into the counting compartment of the chamber. Four fields were counted and the cell density per ml calculated according the chamber dilution factor (1×10^4) and the used dilution of cell suspension

5.2.1.4 Freezing and thawing of cells

The cells (approximately $1-4 \times 10^7$) were resuspended in cold freezing medium (FCS 90% (v/v), DMSO 10% (v/v)), transferred into the cryo tubes, stored for 24 hrs at -70° C in isopropanol freezing container and finally transferred under liquid nitrogen for long-term storage.

The cells were thawed in a 37°C water bath and transferred into the 50 ml centrifuge tube with 10 ml of corresponding growth medium. After centrifugation, the cells were resuspended in fresh growth medium and placed in incubator.

5.2.1.5 Cell isolation and culture

5.2.1.5.1 Positive selection of human CD19⁺ B lymphocytes

PBMCs were labeled with CD19 Microbeads conjugated to monoclonal anti-human CD19 antibody. The magnetically labeled cells were retained on the column and eluted as CD19⁺ B cells (positively selected cell fraction).

5.2.1.5.2 Isolation of mouse B lymphocytes

Naive B cell isolation was performed with Miltenyi's B cell isolation kit according to manufacturer's instructions and typically yielded 95-98% purity B cell population. The cells were seeded in X-vivo medium at a density of 5×10^6 /ml.

5.2.1.5.3 Culture of *E μ -Myc* tumor cells

The B cells were cultivated in the concentration of $5-10 \times 10^6$ per ml. The medium was refreshed daily by replacing 50% of old medium with the fresh one.

5.2.2 Flow cytometry (FACS)

Principally, FACS analysis is based on sorting of living cells according to the size, structure, surface molecules properties, and intracellular protein composition. This application requires markers with fluorescent dye-coupled antibodies to stain cells. During measurement in a FACS machine, cells pass through laser and are sorted based on the size (forward scatter), granularity (side scatter) and fluorescence emission to determine specific cellular parameters.

5.2.2.1 Surface marker staining

Approximately 1×10^6 cells used for each FACS staining were washed with cold FACS buffer. The cell pellet was resuspended in 100 μ l of master mix containing the Fc block (1:300) and corresponding antibodies (1:300). After 20 min incubation at RT in the dark the cells were washed twice with 1 ml of FACS buffer. Biotinylated antibodies were visualized after further incubation for 20 min with fluorescence-labeled Streptavidin (1:300), followed by two washes with FACS buffer. The cells were transferred into the FACS tubes, analysed immediately on FACS Canto II or fixed with formaldehyde (2% final concentration).

5.2.2.2 Intracellular staining for Ki67

Intracellular staining was performed using the Foxp3 staining kit (eBioscience). After staining of the surface markers, cells were washed with FACS buffer, fixed with fixation solution (eBioscience Fixation/Permeabilization) and permeabilized (eBioscience Permeabilization Buffer). Cells were

incubated with 1:400 dilution of Ki67 in 1X permeabilization buffer at RT for 20 minutes in dark, washed for three times with 1X permeabilization buffer, resuspended in 200 μ l of 1X permeabilization buffer, transferred into FACS tubes and analysed on FACS Canto II.

5.2.2.3 Annexin V/PI-staining

The cells were washed with FACS-buffer followed with 1x Annexin binding buffer (ABB) before resuspended in 100 μ l of 1x ABB in addition of 1 μ l of Annexin V. The cells were incubated for 15 minutes at RT in dark. Additional 100 μ l of 1x ABB was added to stop the binding reaction. The samples were measured within one hour after staining and 1 μ l of PI (1mg/ml) was added just before the measurement.

5.2.3 *In vivo* experiments

5.2.3.1 Generation of secondary tumors

Primary tumor cells (10×10^6) were subcutaneously injected into the left or right buttock of wt C57BL/6 mice. The subcutaneous tumor can be detected within one week post injection. The mice were sacrificed 3 days – 2 weeks later and the tumors were analysed.

5.2.4 Working with proteins

5.2.4.1. Preparation of protein extracts

The cells were washed with 1 ml of ice-cold PBS, transferred into the 1.5 ml reaction tube and centrifuged (5.000 rpm for 4 min), the supernatant was removed. The whole protein extract was prepared by dissolving the cell pellet in three packed-cell-volumes of RIPA buffer supplemented with protease inhibitor cocktail. Followed by incubation for 15 min on ice, frozen in liquid nitrogen and stored at -70° C. Final lysis of the cells was carried out by multiply freeze-thaw in liquid nitrogen followed by vigorous vortex for 30 min at 4° . Extracts were cleared by 15 min centrifugation at 13.200 rpm.

To prepare nuclear and cytosolic protein extracts the cells were incubated on ice for 15 min in 120 μ l of hypotonic buffer A with protease inhibitor. The 10% of NP40 was added (25 μ l) followed by short vortexing (10 sec). The cytosolic extract was attained after centrifugation of cell suspension at 9000 rpm for 5 min. Nuclei were extracted with buffer B. After vigorous vortexing for 30 min the nuclear extracts were cleared by 15 min centrifugation at 13.000 rpm. The extracts were snap-frozen in liquid nitrogen and stored at -70° C.

5.2.4.2 Protein concentration measurement (Bradford assay)

The concentration of protein of the samples was determined using the Bradford assay. The assessment is a colorimetric protein assay, based on an absorbance shift of the dye Coomassie Brilliant Blue G-250 in Bradford reagent. Under acidic conditions, the red form of the dye is converted into its bluer form to bind to the measured protein. A ready-made protein assay reagent (BioRad) was used with dilution 1:4. The diluted Bradford reagent (1000 μ l) was mixed with 1 μ l protein sample and transferred in a plastic cuvette. The measurement was carried out at absorption 595 nm.

5.2.4.3 Sample preparation and separation on the SDS-PAGE

Protein extracts (between 20 and 50 μ g of protein per sample) were mixed with 5x Laemmli buffer and heated for 10 min at 95° C. The Laemmli buffer contains negatively charged SDS and β -mercaptoethanol. The SDS denatures the protein structure and binds to their positive charges. The β -mercaptoethanol reduces the possibly existing disulfide bridges, thereby support the linearization of the proteins. After unfolding the three-dimensional structure, the anionic SDS molecules attach to proteins and allow a separation in an electric field. Due to the sieving effect of the gel the small molecules migrate in the electric field faster than large molecules and protein mixture can thus be separated. Samples were loaded on a discontinuous SDS-PAGE (polyacryl amide gel electrophoresis) gels consisting of stacking gel (5%, pH6.8) followed by separating gel (10%, pH8.9). Electrophoresis was carried out in 1xRunning buffer under 25mA constant current (approx. 90V initially).

5.2.4.4 Immunological detection of proteins (Western Blotting)

Separated proteins were transferred onto nitrocellulose membrane in 1xTransfer Buffer using wet transfer chamber. The gel, sponges, nitrocellulose membrane and filter papers were equilibrated in transfer buffer. To avoid excessive heat during transfer, the blotting process was performed in the cold room for 3.5 hrs under constant current of 300 mA. Extent of transfer was verified by staining the membrane with acidic 1% Ponceau S solution.

Before detection of proteins the non-specific binding was blocked by incubation of membrane for at least one hour in 4-5% non-fat dry milk in 1xTBS/0.05% Tween. The milk proteins occupy free binding sites on the membrane and thus prevent unspecific background signal. The membrane was briefly washed with 1xTBS/0.05% Tween and subsequently incubated with indicated primary antibodies diluted in 1xTBS/0.05% Tween/5% non-fat dry milk. Membranes were incubated overnight at 4°C with moderate shaking. After washing with 1xTBS/0.05% Tween (three times 10

min at RT) the membranes were incubated with corresponding anti-rabbit or anti-mouse HRP-conjugated secondary antibodies for one hour at RT (1:10.000 dilution) and washed five to six times for 5 min each in 1xTBS/0.05% Tween.

For visualization of the desired proteins, the Super Signal West Pico chemiluminescence substrates were used. The two solutions from this system were mixed in a 1:1 ratio and added to the membrane. Following two minutes of incubation, the signal was detected with the Fusion SL (Vilbert) camera. Multiple exposures were captured.

5.2.4.5 Stripping of membranes

To detach the antibody from membranes, the membrane was incubated three times for 20 min at 50° C with stripping buffer and subsequently washed thoroughly in TBS-Tween. After blocking with milk (5% in TBS-Tween) the membranes were reprobed using another primary antibodies.

5.2.5 Working with nucleic acids

5.2.5.1 Isolation of genomic DNA from cells or mouse tail biopsies

For genotyping the tip of the mouse tail was cut using a scalpel and placed in a 1.5ml reaction tube. The biopsies (about 1-3 mm long) were incubated in 20 µl of genomic lysis buffer containing Proteinase K at 56°C overnight. The next day 480 µl of water was added to each sample and incubated for 10 min at 95°C. Following centrifugation, 3 µl of DNA sample was used for PCR reaction.

5.2.5.2 Isolation of total RNA with Trizol reagent

Total RNA was extracted using Trizol reagent (Invitrogen). At least 1- 2x10⁶ cells were harvested and washed with 1 ml of cold PBS and lysed in 1 ml of Trizol. To effectively disrupt the cells, the pellet was repeatedly passed through a blue tip, and then incubated for 5 min at RT. Per milliliter of Trizol 200 µl of chloroform was added and the sample was vigorously vortexed. After incubation for 10 min at RT, the tubes were centrifugated for 15 minutes in the cold room at 13000 rpm. This led to the separation into three phases: a lower red phenol-chloroform phase, an upper aqueous phase and a colorless intermediate interphase. The RNA was present in the aqueous /upper phase which was transferred to fresh tubes and precipitated with 500 µl of isopropanol. The RNA was pelleted at 13000 rpm for 10 min (4° C) and the supernatant carefully removed. RNA pellet was washed once with 1 ml of 75% ethanol, dried in air and dissolved in 50 µl of DEPC water and heated at 65° C for 10 minutes. All RNAs were stored at -70 ° C.

5.2.5.3 Isolation of total RNA from frozen section tissues

Total RNA from human BL specimens was extracted from frozen tissue samples preserved in Tissue-Tek using pegGOLD Blood RNA Kit (Peqlab) according to the manufacturer's protocol. The tissues were cut using a cryostat (Leica) in 10 µM slices, placed in eppendorf tubes and lysed with 600 µl of RNA lysis buffer (Peqlab), completely resuspended by pipetting followed by an addition of 600 µl of 70% ethanol before loading on PerfectBind RNA spin cartridge/Column subjected to centrifugation. The samples were washed three times with RNA wash buffer I (500 µl) and twice with RNA wash buffer II (650 µl). Finally the columns were dried by re-centrifugation and RNA was eluted with 30-50 µl of RNase free water.

5.2.5.4 Measurement of RNA

To determine the amount of total RNA in the extracts, the photometer (Pharmacia) was used. Before transferred into a quartz cuvette, RNA was diluted 1:50 in nuclease-free H₂O. This is termed as dilution factor (DL). The RNA concentration was calculated with the following formula:

$$\text{Concentration } [\mu\text{g}/\mu\text{l}] = \frac{OD_{260\text{nm}} \times DL \times \text{Factor } 40}{1000}$$

RNA was measured at absorbance (optical density/OD) 260 nm. The purity of RNA is defined by a ratio of absorbance at 260 nm and 280 nm (pure RNA theoretically is ~2.0, thus, significantly lower ratio will indicate the presence of contamination).

5.2.5.5 Reverse transcription

Complementary DNA (cDNA) synthesis was carried out on the template of total RNA using BioRad iScript cDNA Synthesis kit or Fermentas First Strand cDNA Synthesis kit according to the instructions of manufacturers. Between 300 ng –1µg of total RNA were used for cDNA synthesis with random hexamer primers (Fermentas kit) or using ready reagent mix (BioRad). Synthesized cDNA was diluted 1:2-1:12 with H₂O and directly used for RT- or Real Time PCR or stored at -20°C.

5.2.5.6 Polymerase chain reaction (PCR)

Principally, PCR is a method for the enzymatic amplification of DNA segments across three steps of cycles: denaturation of DNA template resulting in single-stranded DNA, annealing the primers to the

single-stranded DNA template and extension/elongation of primers resulting in an exponential amplification of DNA fragment.

A PCR master mix from Fermentas used in our lab consisting of 0.05U/ μ l Taq DNA Polymerase, 4 mM MgCl₂, 0.4 mM dNTPs (dATP, dCTP, dGTP, dTTP) and an optimal reaction buffer. The PCR conditions we used were: initial step (for hot start PCR: 1'-9' 95°C), 2'-3' 95°C (opening denaturation) > (20'' 95°C (denaturation) > 20'' x°C (annealing) > y' 72°C (elongation)) 37-40x > 5' 72°C (final elongation).

PCR reaction mix:	DNA	3 μ l
	2x PCR Master-Mix	10 μ l
	MgCl ₂	1 μ l
	Primer for (100 nM)	0.15 μ l
	Primer rev (100 nM)	0.15 μ l
	H ₂ O	5.7 μ l

5.2.5.7 RT-PCR

Reverse-transcription PCR (RT-PCR) is used to detect gene expression through formation of transcribed complementary DNA (cDNA) from RNA.

RT-PCR reaction mix:	cDNA	3 μ l
	2x PCR Master-Mix	10 μ l
	MgCl ₂	1 μ l
	Primer for (100 nM)	0.15 μ l
	Primer rev (100 nM)	0.15 μ l
	H ₂ O	5.7 μ l

Amplification products were separated on agarose gels and quantified using image analysis software.

5.2.5.8 Real-Time PCR

The Real-Time PCR is used to amplify and concomitantly quantify a targeted DNA molecule by using fluorescent substances, which intercalate into the DNA. We used SYBR Green as fluorescent substance that will emit light upon excitation. The number of cycles at which the fluorescence exceeds the threshold is termed as the threshold cycle (Ct).

Quantification of gene expression is using normalization procedure so called the Δ Ct-method. This method use the Ct-values to calculate the fold induction of the amplified gene in comparison to a house keeping gene as a reference, such as *L32*.

5.2.5.9 Gel electrophoresis

The agarose electrophoresis is used to separate the amplified PCR products according to their size from negative to positive in a charged electric field with constant voltage 150 V. To visualize DNA agarose gel was placed under UV-light excitation at the wavelength of 254 nm in addition of Ethidium bromide (EtBr) or Midori Green. The percentage of the agarose gels (in 1xTAE buffer) depends on the size of DNA *i.e.* $\leq 1\%$ for $\geq 1\text{kb}$ fragments and 2.5% for $\leq 500\text{bp}$ fragments. To identify the size of separated fragments the 1 kb or 100bp GeneRuler Ladders were used.

5.2.6 Imaging

5.2.6.1 Confocal fluorescence microscopy

Proteins can be visualized by immunocyto/histochemistry. Hence, fluorochrome coupled antibodies are utilized to stain proteins of interests in fixed and permeabilized cells. The stained cells can be analyzed with confocal laser scanning microscopy, which detects the emitted light of fluorochromes after excitation with laser light. The confocal laser scanning microscopy employs two pinholes to blind out diffused light and provides the possibility to scan through a whole cell thus provides significantly higher resolution and to eliminate out-of-focus light in specimens that are thicker than the focal plane. The microscope is controlled by a computer coupled with photomultiplier detection system.

5.2.6.2 Preparation of histological and immunohistochemical samples

The tissues for immunohistochemical studies were immediately preserved in fixative (4% of formaldehyde) for 24 hours at RT. To remove the water from the tissues, the samples were processed on automatic tissue processing machine (Tissue-Tek VIP-Sakura) through ascending alcohol concentrations ending with 100% xylene. The anhydrous tissues were loaded into appropriate cartridges, soaked in a hot paraffin and prepared for embedding (block paraffin). The slides were prepared with a sliding microtome (Leica) with the thickness of about 1 micron. The individual section was taken with a brush and transferred in a hot water bath. Subsequently, the sections were mounted on slides and dried. Before immunohistochemical analysis the morphology of tumors was analyzed by hematoxylin and eosin (H&E) staining which was kindly performed by the staff members of hematology and histology laboratory, Institute of Pathology or ZOM (central for operation medicine), University of Wuerzburg. To stain the tissue sections for immunohistochemistry, the antigen retrieval must be performed which was kindly provided by the staff members of immunohistochemical laboratory, Institute of Pathology.

5.2.6.3 Immunocytochemistry

Initially, 1×10^4 - 5 (depending on the cell sizes) cells in a final volume of 80-100 μ l were centrifuged at 350 rpm for 4 min onto the silanized slides. The cells were circled with a marked diamond stylus, dried in the air for 4 hrs at RT or overnight at 4°C. The cytopinned cells were fixed for 20 min in 4% FA/PBS at RT and subsequently washed (all washing steps were performed in PBS-/- in a staining jar). The slides were stained immediately or incubated at least overnight in PBS/0.1% BSA in the fridge. For permeabilization the cells were incubated for 5 min with 0.1% Triton-X100/PBS at RT. Following three washing steps the slides were transferred into a wet chamber and incubated with blocking buffer (Antibody Diluent) for 20 min at RT to block nonspecific binding. Without washing, the slides were incubated for 1hr with the primary antibody (1:100 or 1:50 depending on the antibodies) in Antibody Diluent. After three washing steps the slides were incubated with the secondary fluorescent-labeled antibody (1:400 in Antibody Diluent) in the wet chamber for 1 hr and finally washed in PBS-/- (3x5 min). A drop of mounting medium with DAPI (Fluoroshield) was added and covered with a cover slip. Finished objects were stored at 4° C in the dark.

The pictures were taken with a Leica Confocal Laser Scanning Microscope (TCS SP5 II), analyzed with the Leica Software Image Pro Plus. For further demonstration the digital images were processed using Adobe Photoshop CS3, Irfanview or Microsoft Office Power Point 2010.

Fixation solution (pH 7.4)	NaCl	137 mM
	Na ₂ HPO ₄	10 mM
	KCl	2.6 mM
	KH ₂ PO ₄	1.8 mM
	(Para-)Formaldehyd	4% (v/v)
Permeabilization solution	NaCl	137 mM
	Na ₂ HPO ₄	10 mM
	KCl	2.6 mM
	KH ₂ PO ₄	1.8 mM
	Triton X-100	0.2% (v/v)

5.2.6.4 Staining of the immunohistological sections (confocal microscope)

Following antigen retrieval the tissue sections were rinsed in PBS and subsequently incubated for 5 min with permeabilization solution 0.1% Triton-X100/PBS at RT. The slides were stained as described in section 5.2.7.3 (Immunocytochemistry).

5.2.6.5 Staining of the immunohistological sections (peroxidase based)

The tissue sections were rinsed in PBS after antigen retrieval procedure and incubated with peroxidase blocking solution for 20 min at RT. After three washing steps in PBS (5 min each) the

tissues were incubated with primary antibody (1:400-1:50 in Antibody diluent) for 1-2 hrs at RT, washed thrice and incubated with ADVANCE HRP LINK for 20 min at RT. After three more washing steps the slides were incubated with ADVANCE HRP enzyme for 20 min at RT and rinsed three times in PBS. For visualization the tissue sections were incubated with DAB for 20 min at RT followed by with Mayer's Hematoxylin for 3-5 min at RT. The slides then were rinsed in running tap water for 5 min, dehydrated through 95% ethanol for 2 min, cleared in xylene for 2x5 min at RT and finally covered with mounting medium and coverslips. Some tissue samples were stained using immunohistochemical stainer (TECAN) kindly provided by the staff members of immunohistochemical laboratory, Institute of Pathology, University of Wuerzburg.

All pictures of H&E and immunohistological stanings (peroxidase based) were captured with an Olympus Color view camera mounted on an Olympus BX41 dual-head light microscope.

5.3 Statistical Analysis

The survival analysis and student t test were employed to assess the experimental data by using GrapPad Prism version 5 (GrapPad Software Inc., California). P values ≤ 0.05 were considered statistically significant.

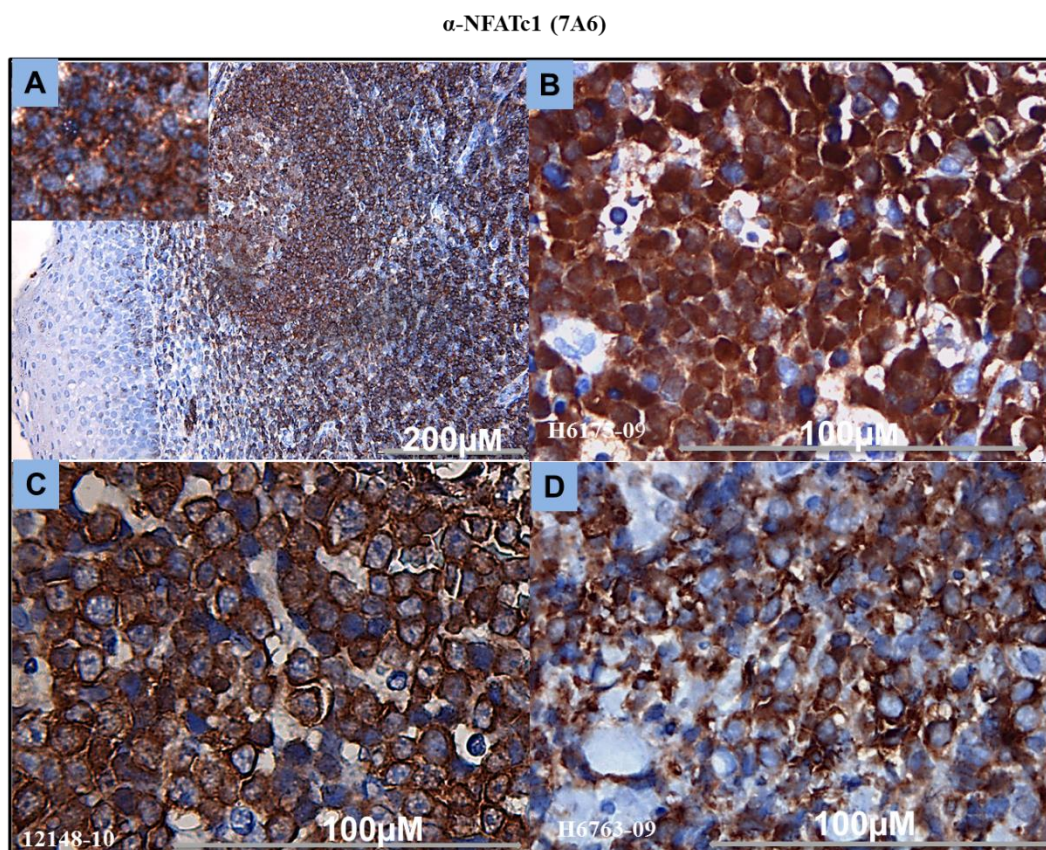
6. Results

6.1 NFATc1 in tumorigenesis

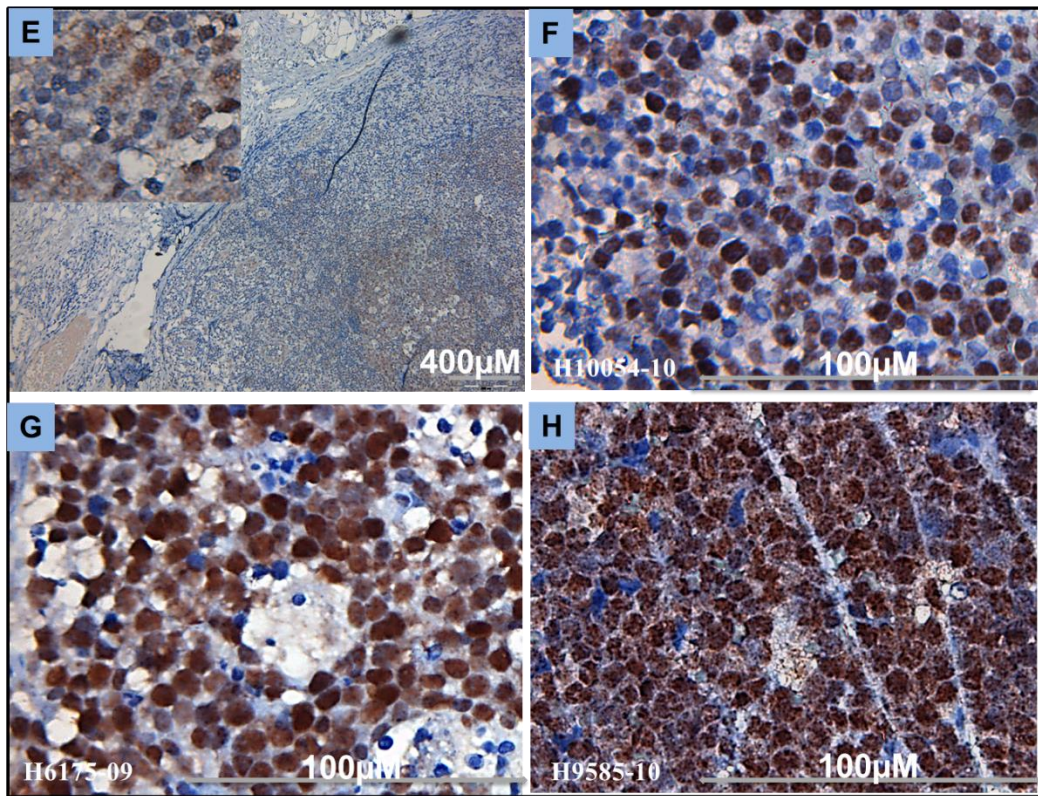
In pancreatic cancer, aberrant activation of NFATc1 upregulates *MYC* transcription resulting in cell proliferation and anchorage-independent growth (Bucholz et al., 2006). Marafioti et al. (2004) identified nuclear expression of NFATc1 proteins in more than 70% BLs they analyzed. However, the patho-physiological relevance of these findings was not addressed. In our study we focused on the role of NFATc1 expression in the survival and progression of Burkitt lymphoma

6.2 NFATc1 expression in Burkitt lymphoma

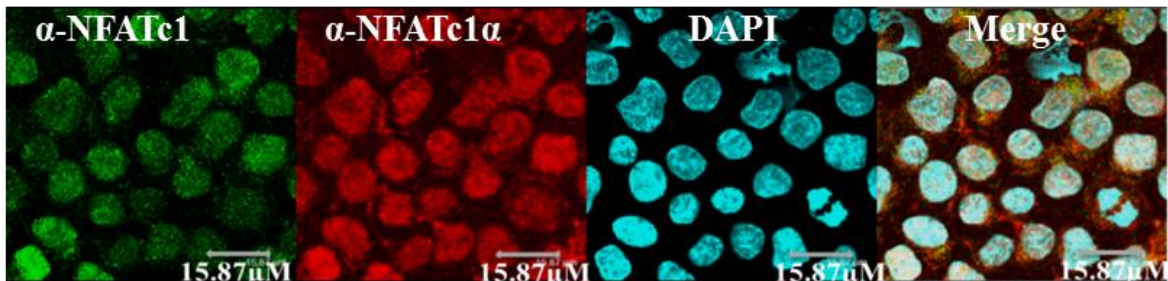
Immunohistochemical analysis using the NFATc1 antibody 7A6, which detects all NFATc1 proteins revealed two distinct patterns of NFATc1 protein expression in primary BL cases (n=20). The first pattern of staining was mixed protein expression with predominant nuclear localization (11 out of 20) (Fig. 6.1B). The second pattern was mixed protein expression with predominant cytosolic localization (9 out of 20) (Fig. 6.1C and D), Using the NFATc1- α -isoform specific antibody (IG-457), NFATc1 protein showed a predominant nuclear localization (Fig 6.1 F, G and H) in all cases (n=16). In Ramos and Namalwa cell lines NFATc1 expression was also predominantly localized in nucleus (Fig. 6.6A and B) when stained with both antibodies (7A6 and IG-457).



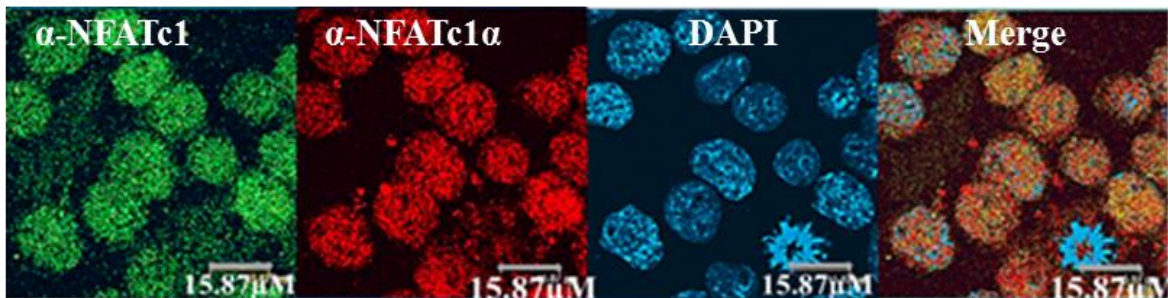
α -NFATc1 α (IG-147)



I. Ramos



J. Namalwa



In collaboration with H. Fender

Fig. 6.1 Predominantly nuclear localization of NFATc1 proteins in primary BL and BL cell lines. Immunostaining of human primary BL (B, C, D, E, F, G, and H) and BL cell lines, Ramos and Namalwa (I and J). A. Human tonsils were stained as control for B, C and D. E. Human tonsils as a control for F, G and H. Stainings were performed with the antibody directed against all NFATc1 isoforms (7A6, A, B, C, D, I and J), or NFATc1 α (IG 457) specific antibody (E, F, G, H, I and J).

6.3 Development of B cell lymphomas in *Eμ-Myc* mouse models

To investigate the functional role of NFATc1 in development and progression of BL we employed an *Eμ-Myc* transgenic mouse line (Adams et al., 1985). B cell lymphomas (BCLs) developed in this mouse model showed clinical and histological appearances similar to human BL (Fig. 6.2). Excessive growth of BCLs was detected in the BM, lymph nodes, spleen, blood and other organs, e.g. in liver, lungs, soft tissue of lumbal area and head. In all tumors a homogeneous populations of medium-sized round lymphocytes accompanied by numerous mitotic and apoptotic cells were detected.

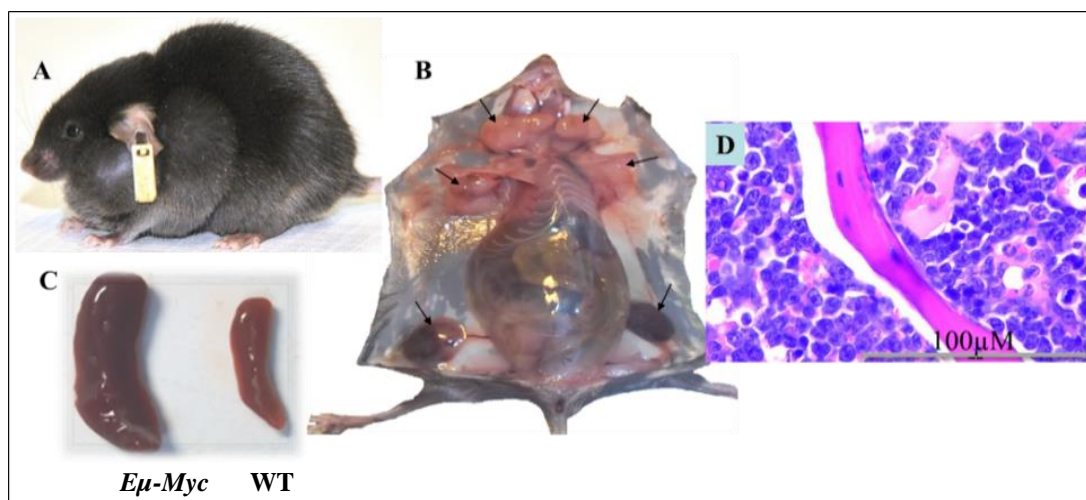


Fig. 6.2 Excessive growth of *Eμ-Myc* BCL. Similar to human BL, in the *Eμ-Myc* mice the development of tumors were detected in lymph nodes (**A and B**), spleen (**C**), BM (**D**), liver, lungs, and thymus (not shown).

Histological examination demonstrated that the tumors consisted of sheets of cells which had a “starry sky” appearance. This is a common feature among large B cell lymphomas and prominent feature of BL (Blum et al., 2004) resulting from the presence of sheets of monomorphic tumor cells interspersed with macrophages that have engulfed apoptotic cells (tingible body macrophages). Staining with a specific marker for macrophages (anti-CD68) revealed positivity in entire macrophages scattered among tumor cells (Fig. 6.3D). Both primary (Fig. 6.3B) and secondary tumors showed similar histologic features (Fig. 6.3C) in *Eμ-Myc* mouse model.

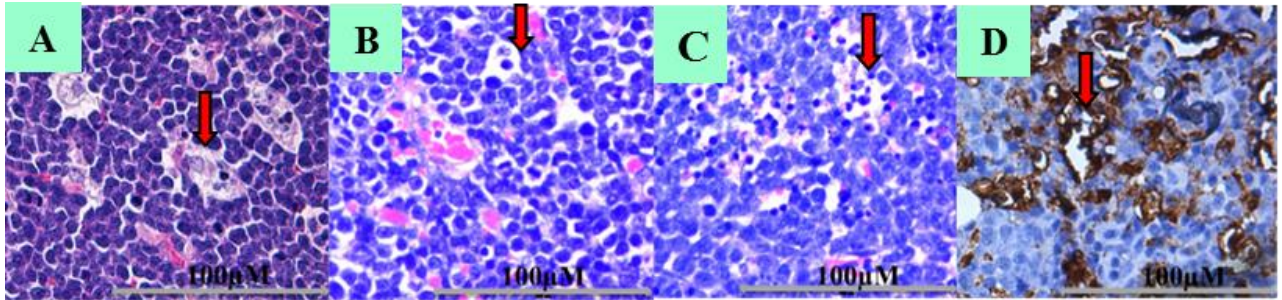


Fig.6.3 Histological analysis of *MYC*-induced tumors. Paraffin sections of human BL (#1060-04) (A), primary and secondary *Eμ-Myc* mouse tumors (B and C respectively) were stained with hematoxylin-eosin. Note the presence of homogeneous population of lymphoblast-like cells. The sheets of cells had a “starry sky” appearance, a prominent feature of BL. Red arrows indicate macrophages. D. IHC staining with antibody directed against CD68 (H13665-05).

6.4 Immunophenotype of *Eμ-Myc* induced tumors

Human BLs are originating from germinal center B cell or memory B cells (Tamaru et al., 1995; Isobe et al., 2000) and therefore express the germinal center markers IgM, CD19, CD20, CD22, CD10 and BCL6 (Blum et al., 2004). Immunocharacterization of *Eμ-Myc* tumors indicated that majority of tumors originated in BM, and corresponded to small pre-B cell (CD19⁺, B220⁺, IgM⁻, 2 tumors), or immature B-cell stages (CD19⁺, B220⁺, IgM⁺, 1 cases). In one case, phenotype of mature B cells (IgM⁺, IgD⁺, CD19⁺, B220⁺) was identified. In six cases a ‘mixed’ phenotype was observed (around half of the cells co-expressing CD19, B220 and IgM and the other half co-expressing CD19, B220, IgM and IgD [immature – mature, mixed]), suggesting the presence of several tumor clones in the same animal (Fig. 6.4B). These findings are in accord with conclusions of Adam and colleagues that tumors in *Eμ-Myc* mice originate at different stages of B cell development but not from germinal center B cells (Adam et al., 1985).

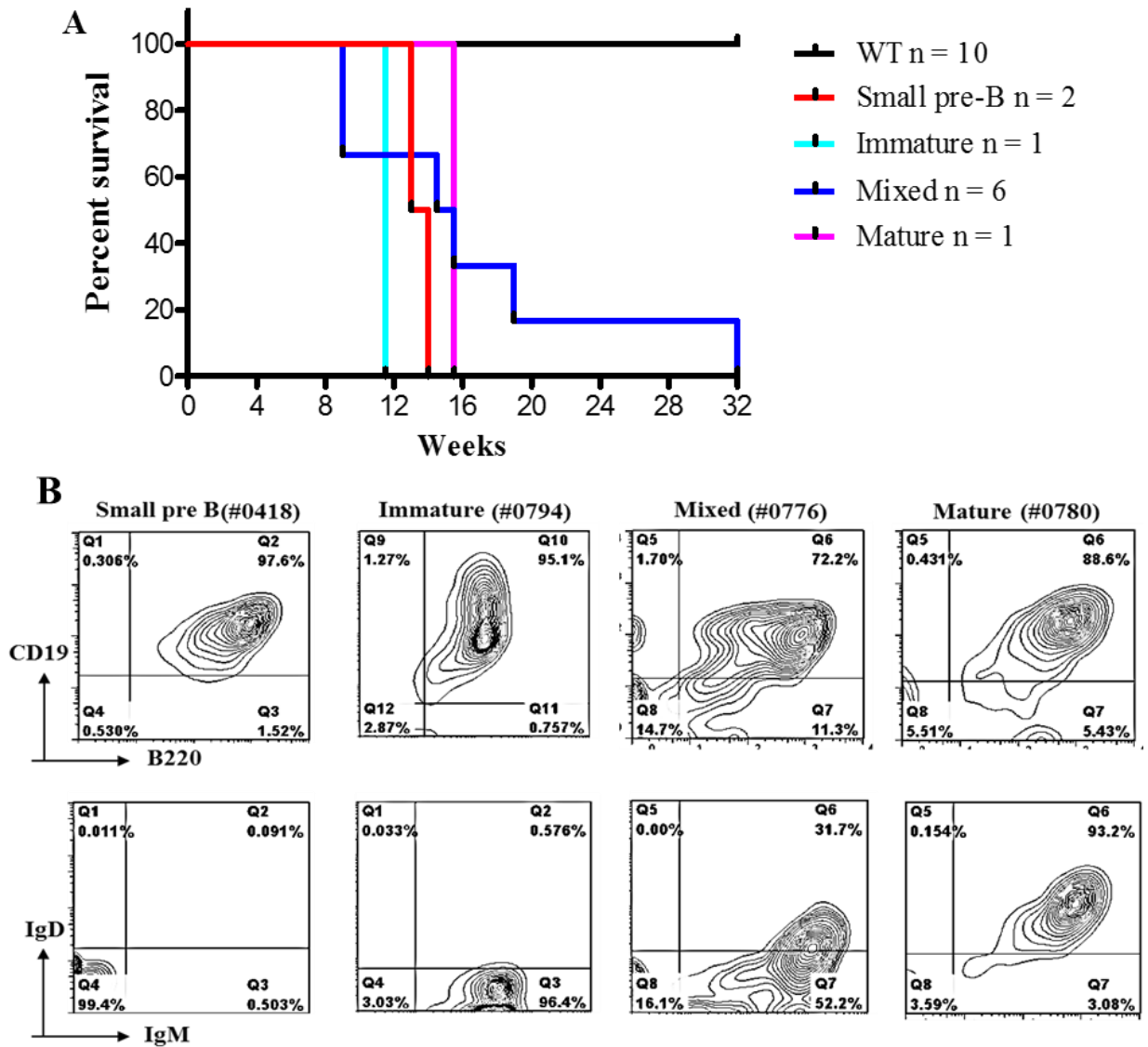
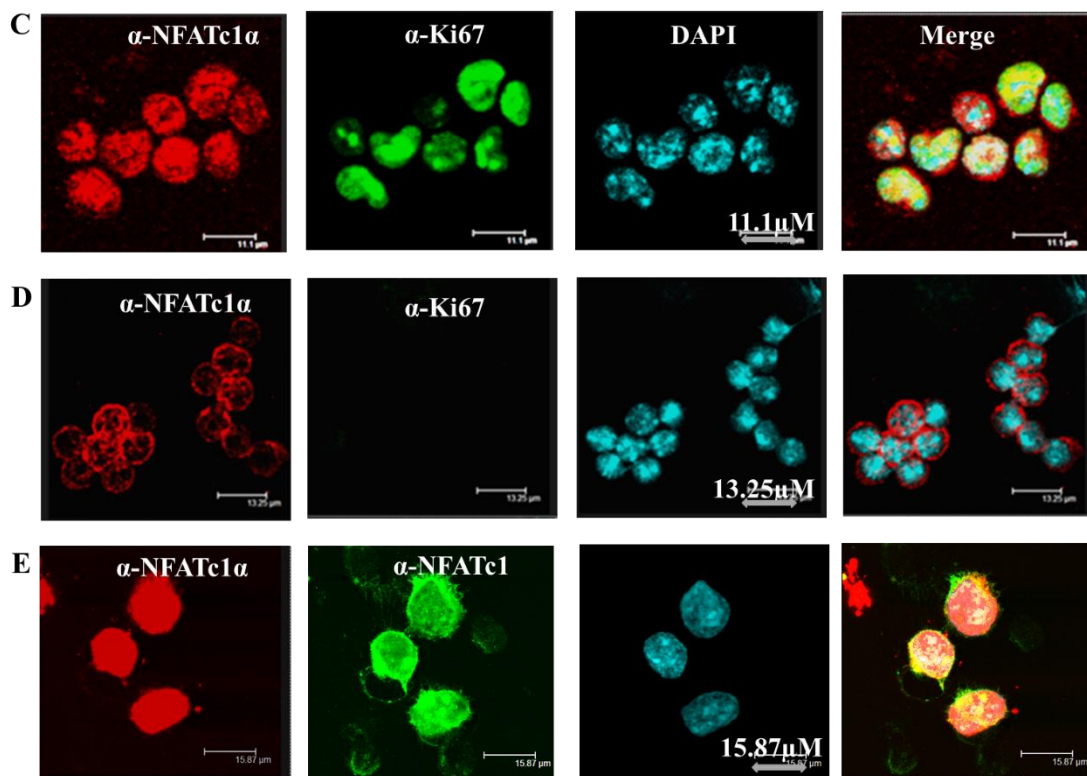
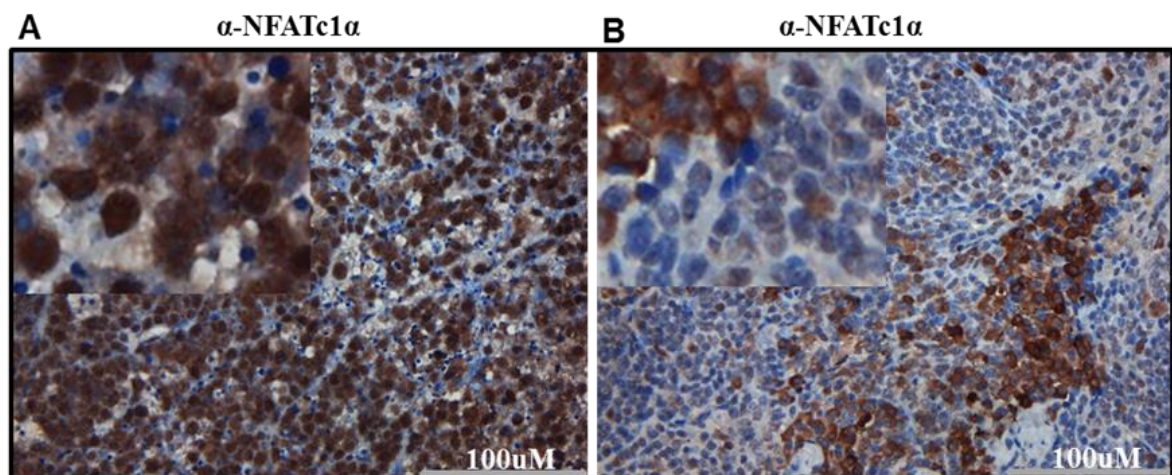


Fig. 6.4 $E\mu$ -Myc-induced tumors derive at different stages of B cell development. **A.** Survival of $E\mu$ -Myc mice (n=4 of 10). **B.** Small pre B cell tumors co-expressed CD19 and B220. Immature B-cell tumors co-expressed CD19, B220 and IgM. The ‘mixed’ phenotype was also detected. Around half of the cells co-expressing CD19, B220 and IgM and the other half co-expressing CD19, B220, IgM and IgD (immature – mature, mixed). Mature B-cell tumor type was specified by co-expression of CD19, B220, IgM and IgD.

6.5 NFATc1 expression in $E\mu$ -Myc mouse tumors

In resting B cells, NFAT are heavily phosphorylated and cytosolic localization (Rao et al., 1997). Upon activation, NFATs translocate into the nucleus and regulate the transcription of their target genes (Loh et al., 1996a; Chen et al., 1998; Garcia-Cozar et al., 1998). Immunohistochemical stainings indicated nuclear localization of NFATc1 α (Fig. 6.5A and B) in $E\mu$ -Myc tumors (Fig. 6.5C) and in BCL line which we derived from these tumors (Fig. 6.5E and 6.7A). These suggested that NFATc1 might play an important role in the survival and/or progression of MYC induced tumors.



In collaboration with H. Fender

Figure 6.5 NFATc1 localizes in the nuclei of *Eμ-Myc* induced mouse tumors. **A.** Immunostaining of an *Eμ-Myc* mouse tumor (#1913). **B.** Spleen from a wild type mouse as a control staining for **A.** Stainings were performed with an antibody directed against the α -peptide (NFATc1 α , IG 457). Confocal microscopy revealed expression and nuclear localization of NFATc1 in a primary tumor (**C**) and in BCL cell line (**E**) derived from *Eμ-Myc* tumor, in comparison with resting splenic B-cells (**D**). Stainings were performed with the antibody directed against the α -peptide (NFATc1 α , IG 457), NFATc1 (7A6) and Ki67, as indicated.

6.6 Nuclear residence of NFATc1 in BL and *Eμ-Myc* tumor cell lines is only partially dependent on calcineurine.

Nuclear localization of NFAT factors is sensitive to the commonly used CN inhibitors cyclosporine A (CsA) and FK506 (Loh et al., 1996). To determine whether CsA treatment would influence the nuclear residence of NFATc1 in BL cell lines, we treated Ramos and Namalwa cells with various concentrations of CsA (Fig. 6.6A and B). The nuclear localization of NFATc1 in normal lymphocytes was already prevented with 0.1 μg/ml of CsA. However, in Ramos and Namalwa cells this treatment relocated only around 10% of NFATc1 protein to cytosol (Fig. 6.6C and D). Importantly, increased CsA concentrations (up to 10-fold) did not increase cytosolic relocation of NFATc1 protein. These data indicated that only a part of NFATc1 nuclear pool was sensitive to CsA treatment. Decreased electrophoretic mobility of NFATc1A, -B, and -C isoforms after CsA treatment suggested that even at the lowest CsA concentration, the nuclear fraction of NFATc1 protein was completely phosphorylated (Fig. 6.6A and B). Treatment with CN inhibitors completely inhibits proliferation of stimulated normal B cells *in vitro*. Since CsA-treated Ramos and Namalwa cells were still proliferating (Fig. 6.6E and F) and the majority NFATc1 proteins remained nuclear, these data suggested that nuclear fraction of NFATc1 is still transcriptionally active.

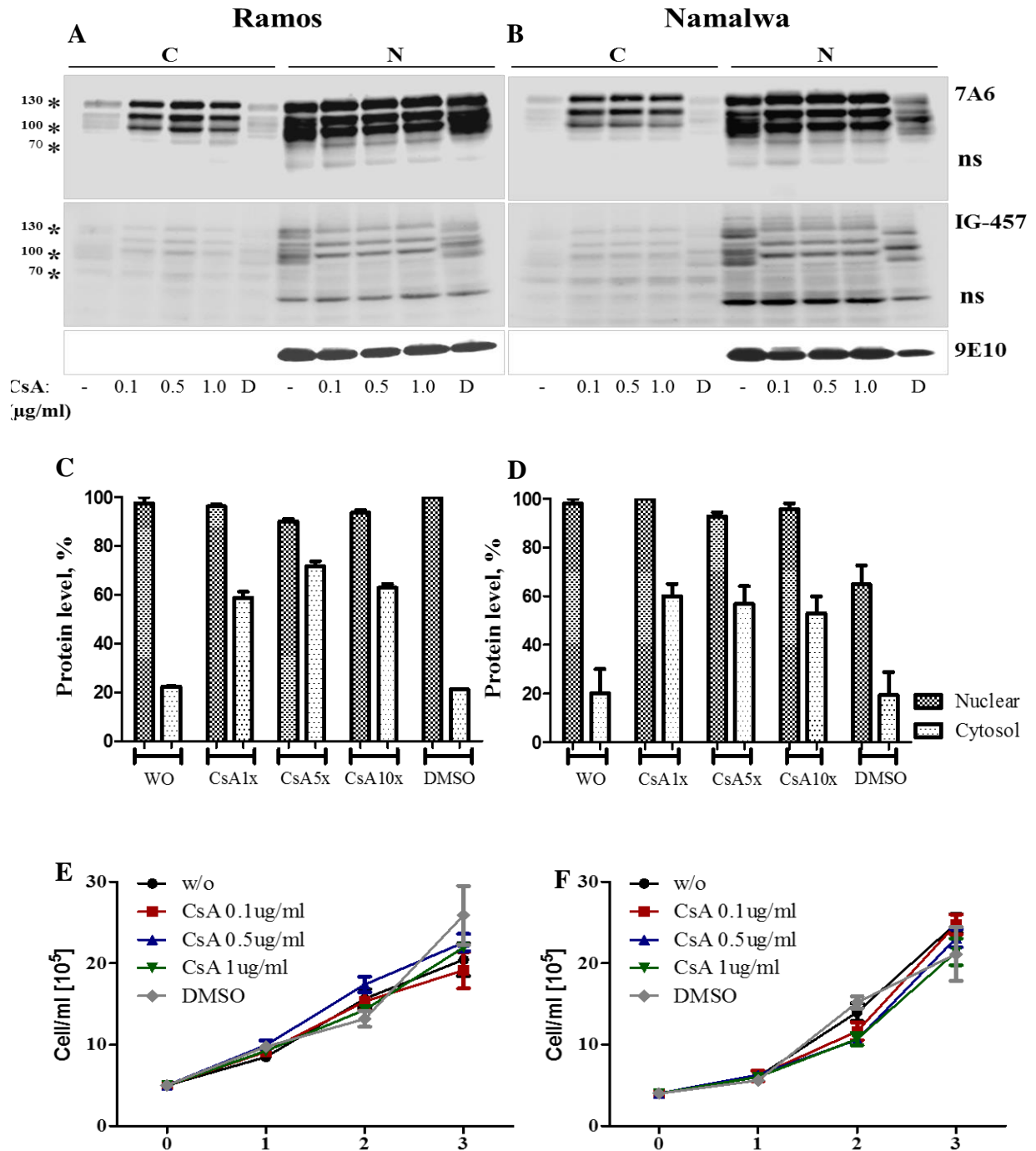


Fig. 6.6 CsA treatment relocated only a part of NFATc1 to the cytosol in BL cell lines. BL cell lines, **A**. Ramos cells and **B**. Namalwa cells were cultivated in the presence of indicated concentrations of CsA or DMSO (D, as a control) for 5 days. Western blot analyses of nuclear (N) and cytosolic (C) fractions were performed with antibodies directed against NFATc1 (7A6), NFATc1α (IG-457) and c-Myc (9E10). **C** and **D**. Quantification of NFATc1 protein expression. **E** and **F**. Proliferation of Ramos and Namalwa cells in the presence of CsA.

Likewise, CN inhibitor had also a partial effect on NFATc1 nuclear residence in *Eμ-Myc* tumor cell line, #1542B (Fig. 6.7A). Similar to human BL cell lines, mouse tumor cells were still proliferating until ca 0.5 μg/ml of CsA treatment. Very high concentrations of CsA inhibited the proliferation of 1542B cells (Fig. 6.7B), likely because of non-specific, CN-independent effect.

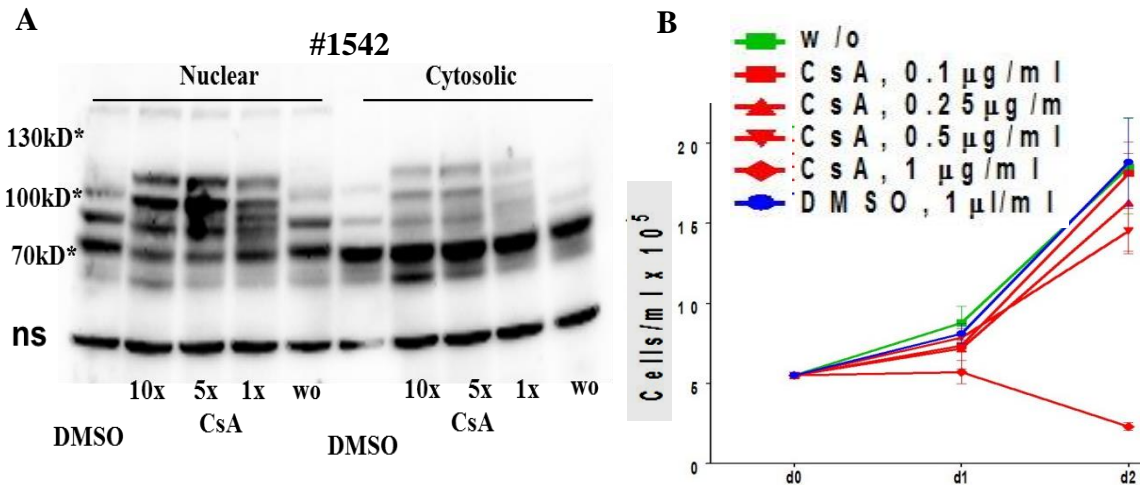
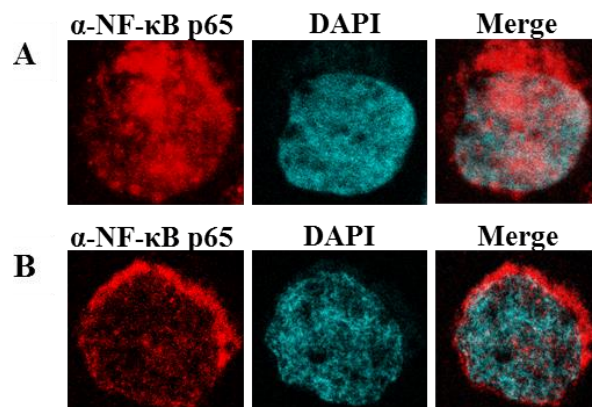


Fig. 6.7 CsA treatment resulted only in a partial cytosolic relocation of NFATc1 in *Eμ-Myc* BCL cells. **A.** Western blot analyses of nuclear (N) and cytosolic (C) protein fractions with antibodies directed against NFATc1 (7A6). **B.** Proliferation of #1542B cells in the presence of increasing concentrations of CsA.

To verify whether treatment with CsA inhibited CN activity in BL cells, we treated Ramos cells with the lowest CsA concentration (0.1 μg/ml) overnight. Quantitative relocation of RELA (NF-κB p65) protein was observed (Fig. 6.8A and B) suggesting that CsA/FK506 efficiently inhibited CN activity in BL cells. In normal lymphocytes, nuclear export of NFATc1 is also prevented with 0.1 μg/ml of CsA.



In collaboration with H. Fender

Fig. 6.8 CsA treatment completely relocates RELA protein in BL cells. Ramos cells were either left untreated (**A**) or treated with CsA (0.1 μg/ml) overnight (**B**). The next day the cells were harvested, stained with antibody directed against the RELA protein and analyzed by confocal microscopy.

6.7 Nuclear residence of NFATc1 in BL cell lines depends on intracellular Ca²⁺ level

NAFTc1 activation in lymphocytes is regulated by Ca²⁺ mobilization (Rao et al., 1997). In addition, MYC overexpression results in persistent intracellular Ca²⁺ and enhances NFAT translocation (Habib et al., 2007). Treatment of Namalwa BL cells with the cell-permeable Ca²⁺ chelator Bapta AM resulted in a concentration dependent relocation of NFATc1 in cytosol (Fig. 6.9) indicating that nuclear localization of NFATc1 protein in BL cells depends on intracellular Ca²⁺ levels.

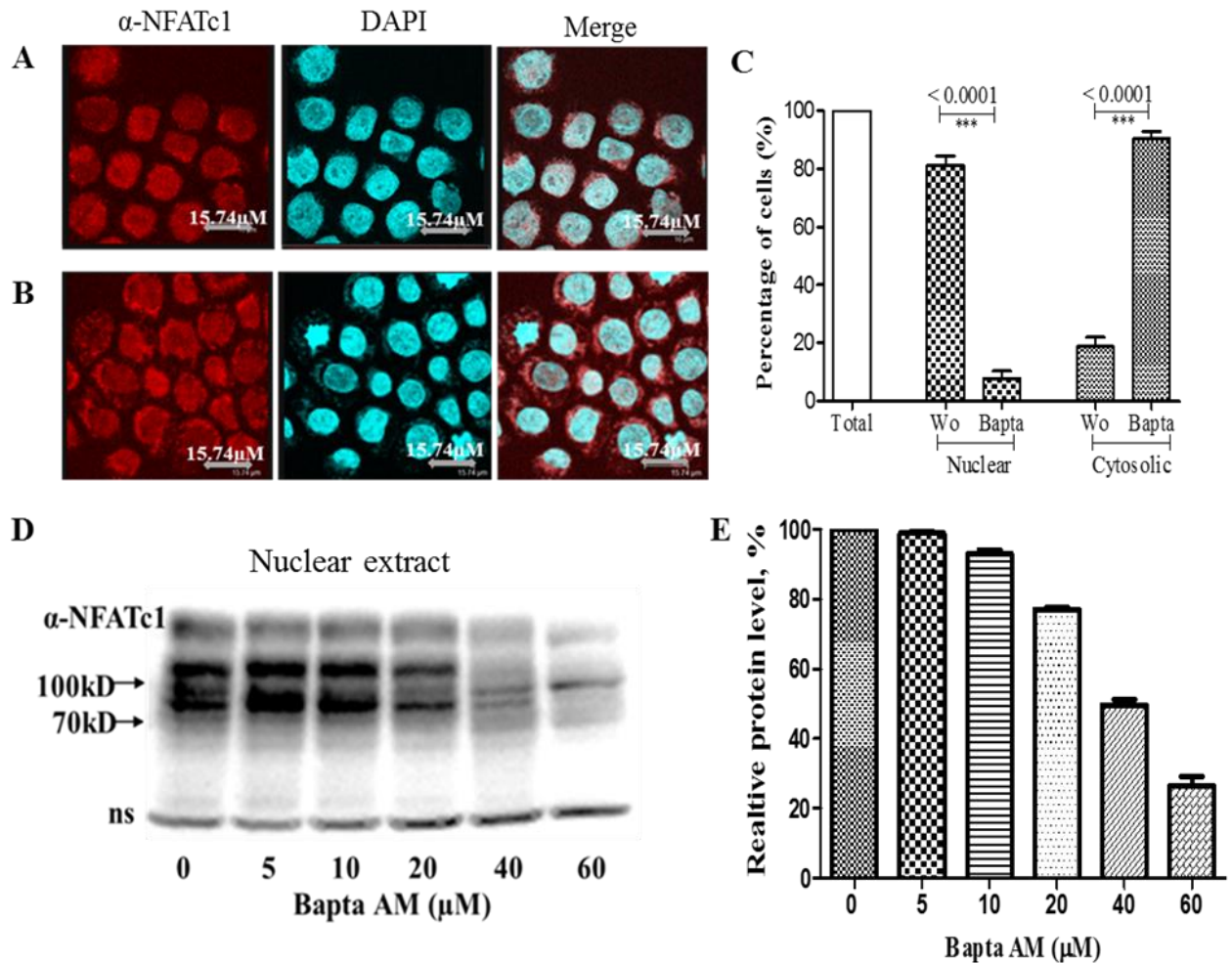


Fig. 6.9 Depletion of intracellular Ca²⁺ resulted in cytosolic relocation of NFATc1 in Namalwa cells. Namalwa cells (1×10^6) were either left without treatment (A) or treated with 20 μ M Bapta AM (B). After 3.5 hours the cells were harvested, stained with NFATc1 (7A6) antibody and analyzed by confocal microscopy. C. Statistical analysis was performed by using unpaired t-test. Total cell numbers were plotted as 100%. D. Namalwa cells (10×10^6) were either left without treatment or treated with indicated concentration of Bapta AM for 3.5 hours. Nuclear protein extracts were prepared and western blot analysis was performed with NFATc1 (7A6) antibody. Protein levels were quantified using FusionCapt Advance of Fusion Vilber Lourmat program (E).

Combined Annexin V/PI staining confirmed that depletion of intracellular Ca^{2+} levels did not significantly influence viability of Namalwa cells (Fig.6.10) within the time frame of experiment.

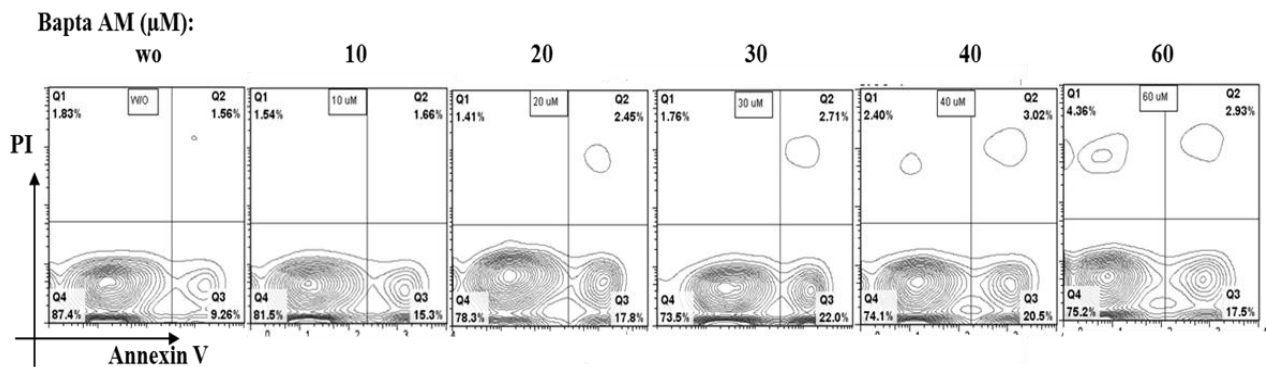


Fig. 6.10 Viability of cultures under different concentration of Bapta AM. Namalwa cells (1×10^6) were treated with Bapta AM at the indicated concentrations for 3.5 hours. The cells were stained with annexin V (for apoptotic cells) and propidium iodine (PI, for dead cells) and analyzed by flow cytometry.

To elucidate if the nuclear localization of NFATc1 in BL and d *Eμ-Myc* cell lines depends on Janus activating kinase3 (Jak3) pathways (Patra, et al., 2013), we treated BL and *Eμ-Myc* cell lines overnight with WHI-P131, a specific inhibitor of Jak3. Western blot analyses indicated that inhibition of Jak3 activity does not affect nuclear localization of NFATc1 in BL cell lines and in *Eμ-Myc* BCL line (Fig. 6.11). Interestingly, the same concentrations of WHI-P131 ($IC_{50}=50\mu M$) blocked proliferation of #1542B BCL cells indicating the presence of Jak3-dependent but NFATc1 independent proliferation pathway (H. Fender, unpublished results).

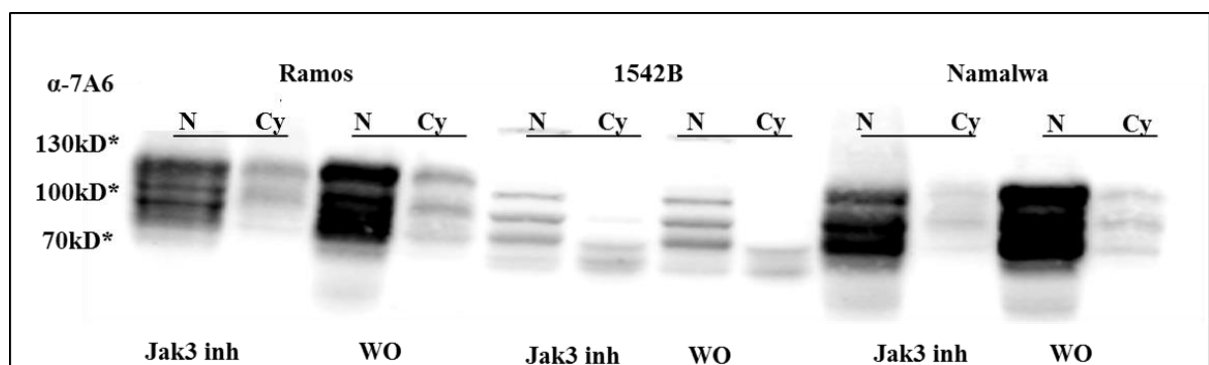


Fig. 6.11 Nuclear residence of NFATc1 in BL cell lines and *Eμ-Myc* BCL is independent on Jak3 activity. Ramos and Namalwa cells (1×10^7) were either left without treatment or treated with $100 \mu M$ Jak3 inhibitor (WHI-P131) overnight. Nuclear and cytosolic extracts were prepared, and Western blot analysis performed with NFATc1 (7A6) antibody.

6.8 Prolonged NFATc1 protein half-life mediated by MYC

The half-life of MYC protein is significantly prolonged in several BL cell lines (Gregory and Hann, 2000, Fig.6.12). To investigate stability of NFATc1 proteins we treated Ramos and Namalwa cells with the protein synthesis inhibitor cycloheximide (CHX, 100 µg/ml). Western blot analyses indicated significantly increased stability of MYC protein BL cells (Fig. 6.12A and B). The half-life of MYC in BL cells was around two hours in both cell lines, while half-life of MYC in normal proliferating cells is very short (circa 15-30 minutes, Dang, 2012; Schuhmacher and Eick, 2013). The half-life of NFATc1 protein in Ramos cells was around 6.66 hours, and even more than 6.66 hours in Namalwa cells, significantly longer than in normal B cells (4 ± 0.5 hours). To investigate if the high expression level of MYC is linked to observed increase of NFATc1 protein stability, we employed P493-6 cell line. These cells are derived from human peripheral B cells after immortalization with EBV nuclear antigen-estrogen receptor fusion protein (EBNA2-ER) and in addition contain a tetracycline-repressible *MYC* transgene (Pajic et al., 2000). Therefore, proliferation of P493-6 cells depends on high levels of MYC expression in normal medium. Addition of Doxycylin represses MYC transgene and results in reversible growth arrest. In the presence of high MYC expression levels the half-life of NFATc1 protein was significantly increased (7.14hrs against 5hrs in the absence of MYC). These data indicated that high levels of MYC expression stabilize NFATc1 protein. (Fig. 6.12C and D)

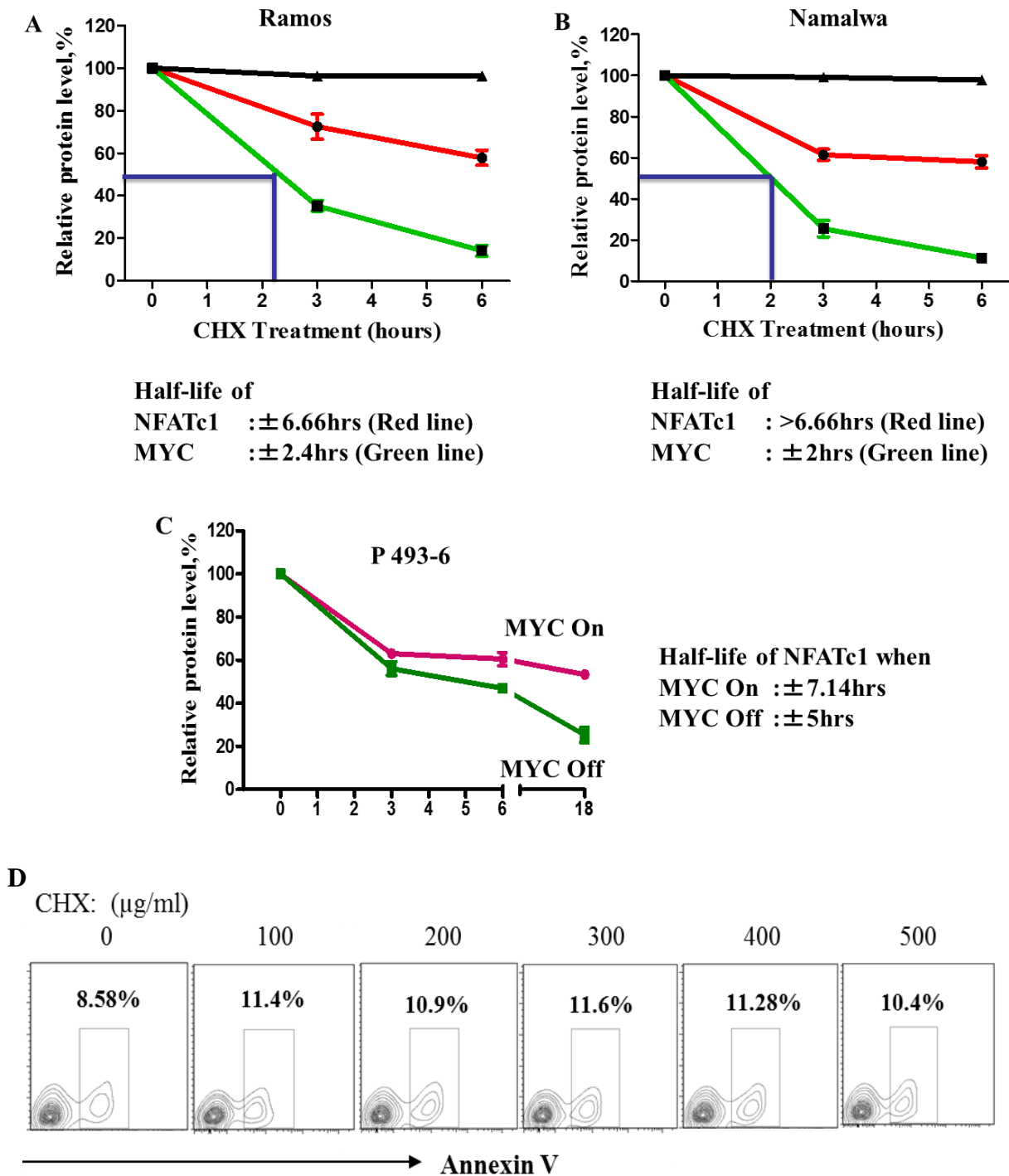


Fig 6.12 High expression levels of MYC increase stability of NFATc1 protein. A and B. BL cell lines were left untreated or treated with CHX (100 μ g/ml). Quantitation of Western blot analysis. Whole-cell protein extracts were collected at indicated time-points after CHX-treatment and analysed with antibodies directed against NFATc1 (7A6), MYC (9E10) and β -actin. C. P493-6 cells were left untreated (MYC 'ON'), and treated with doxycycline (MYC 'OFF') for three days followed by CHX (treatment 250 μ g/ml) for indicated time. Western blot analysis was performed with antibodies directed against NFATc1 (7A6). Protein expression levels were quantified using FusionCapt Advance of Fusion Vilber Lourmat program. D. CHX treatment does not significantly affect viability of P493-6 cells. The cells were treated with CHX at the indicated concentrations for 6 hours, stained with annexin V and analyzed by flow cytometry.

6.9 NFATc1 expression is regulated at the post-transcriptional level in BL and *Eμ-Myc* BCLs

Available data on BL transcriptome does not indicate that *NFATc1* expression is increased in BL in comparison with normal peripheral B cells (Dave et al., 2006). We compared the expression levels of *NFATc1* mRNA in BL patients (n=5) and BL cell lines (n=2) with those in human resting CD19⁺ B cells. The levels of *NFATc1* transcripts were not significantly upregulated in BL and BL cell lines (Fig. 6.13A). However, in *Eμ-Myc* tumor cells (n=4) and secondary tumors (n=2) the expression levels of *Nfatc1* mRNA appeared to be decreased in comparison with normal mouse resting splenic B-cells (Fig. 6.13B). These data showed that NFATc1 protein expression in human BL and in *Eμ-Myc* induced tumors does not correlate with mRNA levels. Together these findings indicated that NFATc1 expression is regulated by MYC-dependent post-transcriptional or post-translational mechanisms.

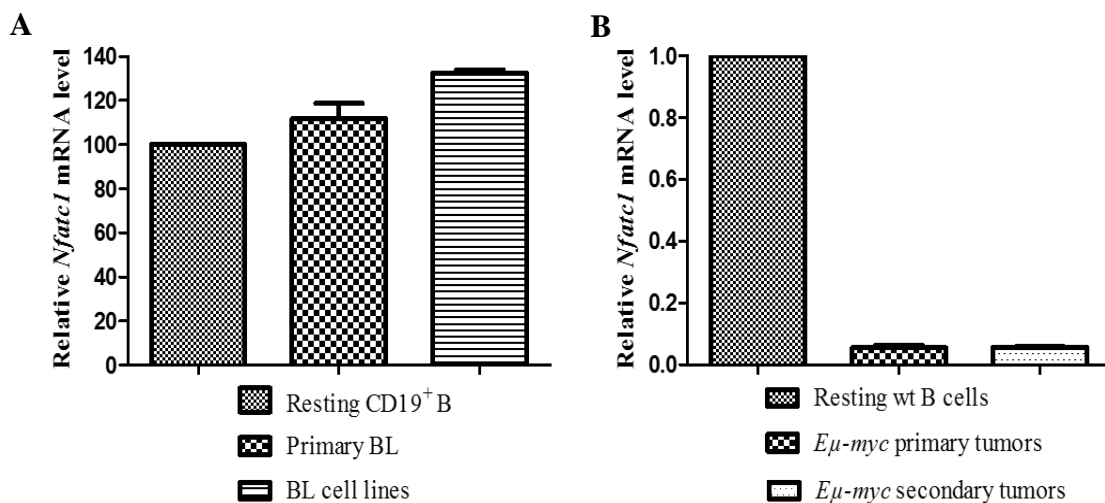


Fig. 6.13 *NFATc1* and *Nfatc1* mRNA levels in human BL cells and *Eμ-Myc* tumors. **A.** RNA was extracted from resting human B cells isolated using Ficoll gradient and CD19⁺ micro beads, frozen tissue sections of human BL and the BL cell lines Ramos and Namalwa. The total levels of *NFATc1* transcripts were analyzed using RT-PCR. **B.** RNA was isolated from resting wt B cells and from *Eμ-Myc* induced tumors. The total levels of *Nfatc1* transcripts were analyzed using Real-time PCR.

6.10 Expression of NFATc1 isoforms BL, BL cell lines and *Eμ-Myc* induced tumors

NFATc1 is transcriptionally regulated by two promoters, an inducible P1 promoter and a constitutive P2 promoter (Chuvpilo et al., 2002). Due to two polyA sites, pA1 and pA2, and alternative splicing events six prominent isoforms are generated (see Introduction Fig. 4.8). Depending on the promoter usage, the *Nfatc1* gene is transcribed into either the α or β isoforms (Park et al., 1996; Chuvpilo et al., 1999; Chuvpilo et al., 2002).

We analyzed RNAs isolated from human primary BL, BL cell lines, *Eμ-Myc* primary and secondary BCL tumors and cell lines derived from these tumors. In primary BL (n=4) we observed around 8-fold higher level of P1 transcripts in comparison to P2 transcripts (Fig. 6.14A). Similar trend was observed in BL cell lines (Ramos and Namalwa cells, Fig 6.13B). These data indicated that in human BL *NFATc1*-P1 promoter is responsible for the expression of NFATc1 α -proteins which we detected using immunohistochemistry and confocal staining (Fig. 6.1E, F, G, H, I and J).

In contrast to these data, the RT-PCR analysis of *Eμ-Myc* BCL primary tumors (Fig. 6.14D), secondary tumors (Fig. 6.14E) and cell lines (Fig. 6.14F) indicated around (8)-fold higher expression of P2-promoter transcripts compared to P1 transcripts. This suggested that in *Eμ-Myc* BCL cells, the increased relative activity of P2 promoter is responsible for predominant expression of NFATc1 β proteins, in contrast to normal activated B-lymphocytes where the anti-apoptotic NFATc1/ α A isoform is predominantly expressed under control of P1 promoter (Fig. 6.13C, Chuvpilo et al., 2002; Serfling et al., 2012; Hock et al., 2012).

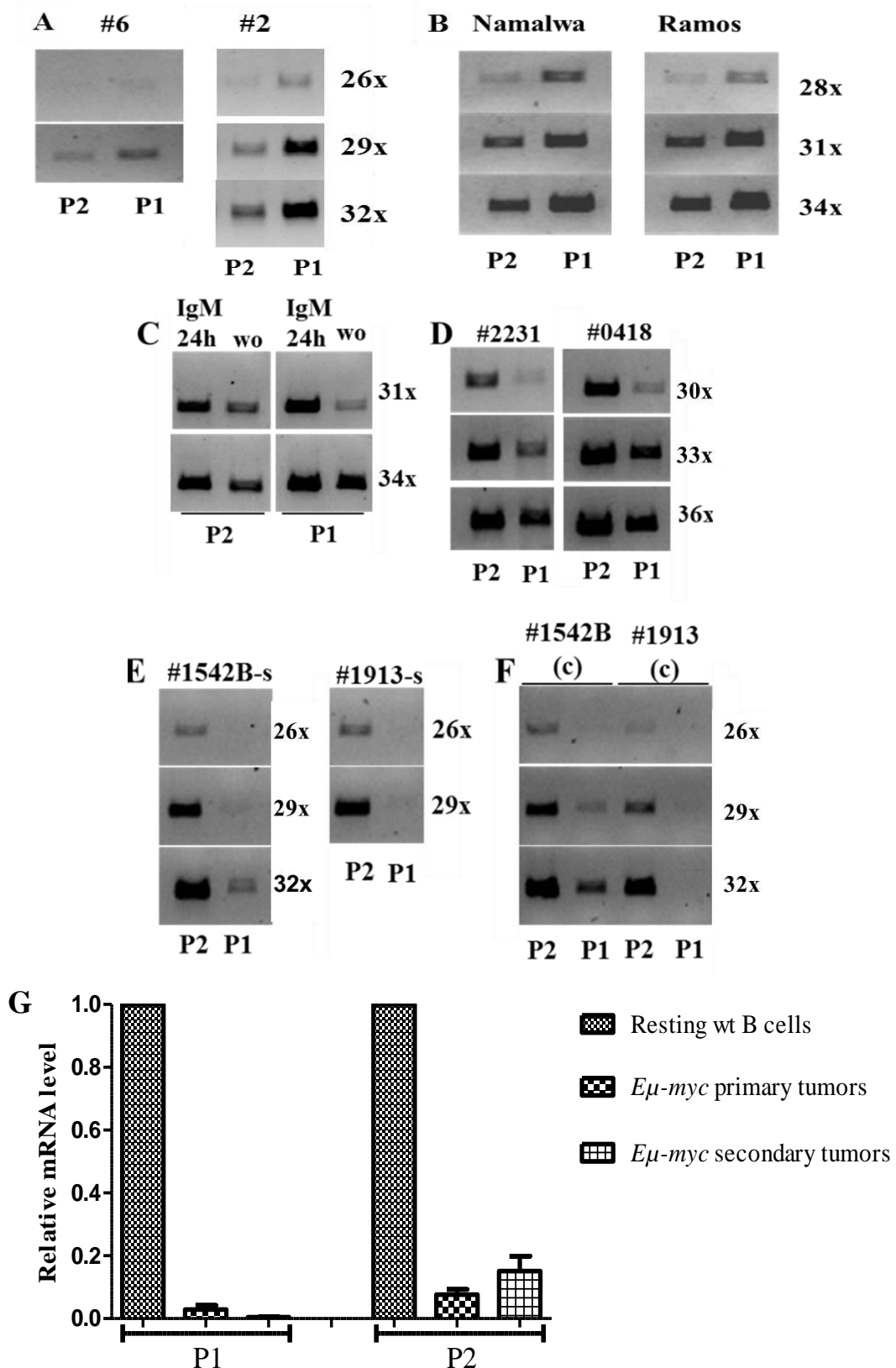


Fig. 6.14 *NFATc1a* transcripts were predominant in human BL and BL cell lines, while *Nfatc1β* transcripts were predominant in *Eμ-Myc* induced tumor cells. RT-PCR analysis of human primary BL (A), Ramos and Namalwa cells (B), normal naïve B cells without and with anti-IgM stimulation for 24 hrs (C), *Eμ-Myc*-BCL primary tumors (D), secondary tumors, #1542B-s and #1913-s (E) and BCL cell lines, #1542B and #1913 (F). Real time PCR analyses of *Eμ-Myc*-BCL primary tumors and secondary tumors (G).

To verify the correlation between the relative activities of P1/P2 promoters and expression of NFATc1 α / β isoforms we crossed *E μ -Myc* mice with a reporter mouse in which the *Nfatc1-dsRed* knock-in allele was introduced (Busch et al., 2014, manuscript, submitted). This system allowed us to detect and directly quantify expression of NFATc1 α and NFATc1 β protein. Western blot analysis of *E μ -Myc* induced tumors in these mice indicated predominant expression of NFATc1 β -isoforms in *E μ -Myc* induced tumors (Fig. 6. 15).

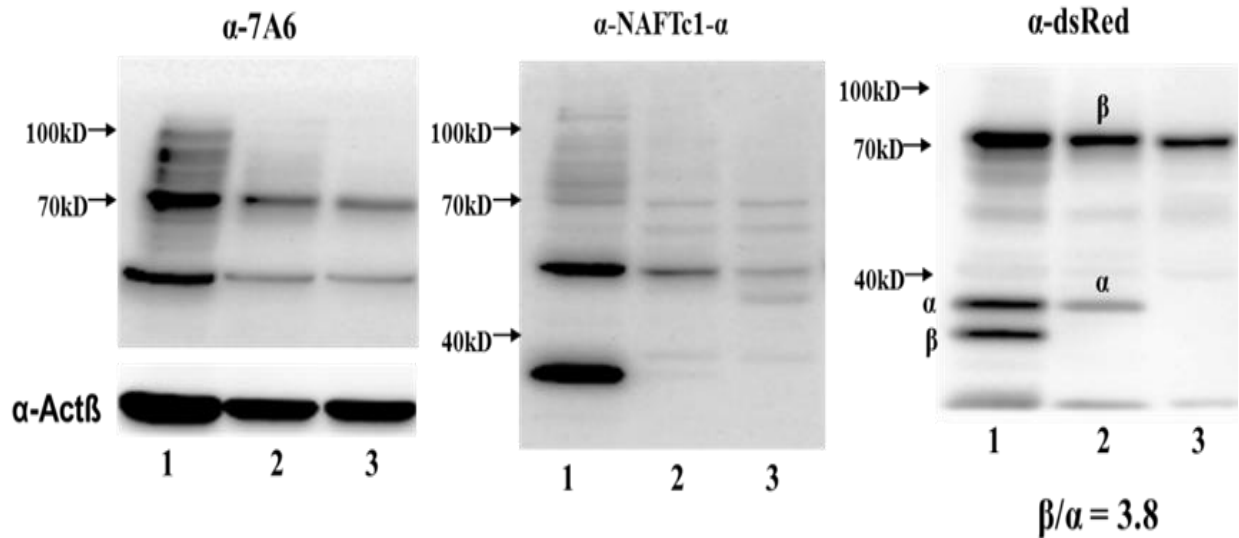


Fig. 6.15 Isoform composition of NFATc1 in *E μ -Myc/Nfatc1-dsRed* tumor cells. Resting splenic B cells from a *dsRed* mouse (1), B cell tumors from a *E μ -Myc/Nfatc1-dsRed* mouse (2) and a *E μ -Myc* mouse (3) were extracted. Whole cell extract proteins were separated on a SDS-PAGE. Western blot analysis was performed with antibodies directed against NFATc1 (7A6, A), NFATc1 α (IG-457, B) and dsRed (C). The ratio between the NFATc1 α - and NFATc1 β -isoforms can be identified with an antibody directed against dsRed (C), In resting splenocytes B cells of *dsRed* mouse (1) the ratio is almost 1, while in *E μ -Myc/Nfatc1-dsRed* tumor cells we observed predominant expression of NFATc1 β -isoform (2).

6.11 Tumorigenesis in *E μ -Myc /Nfatc1^{flx/flx}/mb1-cre* mice

To address the functional role of NFATc1 in *E μ -Myc* induced tumorigenesis we crossed *E μ -Myc* mice with *mb1-cre* and *Nfatc1^{flx/flx}* mice for the conditional inactivation of *Nfatc1* gene in B cells (*E μ -Myc/Nfatc1^{flx/flx}/mb1-cre*) starting from pre-B stage in BM. Tumors generated in these mice (n=3) were histologically indistinguishable from other *E μ -Myc* tumors, as they also showed “starry sky” pattern as shown by H&E staining (Fig. 6.16).

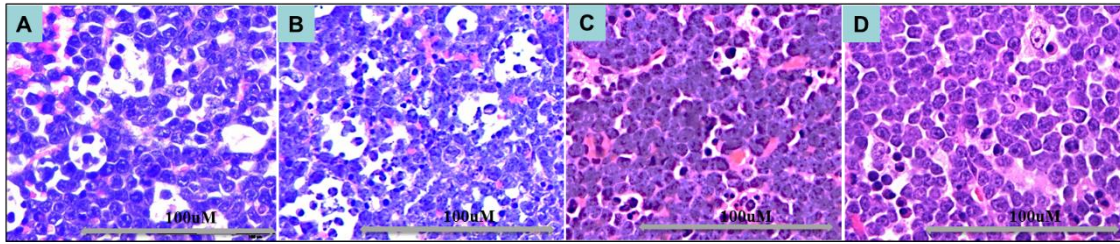


Fig. 6.16 Morphological characterization including the “starry sky” pattern were maintained in BCL cells of $E\mu$ -Myc/Nfatc1^{flx/flx} mb1-cre⁺ mice. BCL cells of four different $E\mu$ -Myc/Nfatc1^{flx/flx}/mb1-cre⁺ mice **A.** Mouse #0794, **B** #1783, **C** primary tumor of mouse #2054 (#2054P), and **D.** Secondary tumor of mouse #2054 (#2054S) were fixed in 10% formalin and embedded in paraffin. Tissues sections (2µm), stained with hematoxylin-eosin. All images were obtained with a 40X original magnification.

Tumorigenesis of NFATc1 ‘deficient’ and intact *Nfatc1* alleles reveal no differences between two groups. All mice from these two groups were kept within the same time period and under the same condition (Fig 6.17). All of mice developed tumors between 11 – 16 weeks of ages

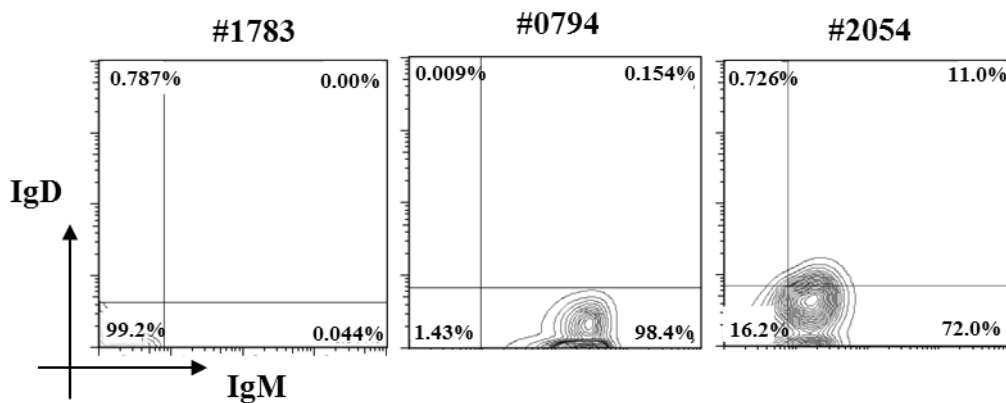
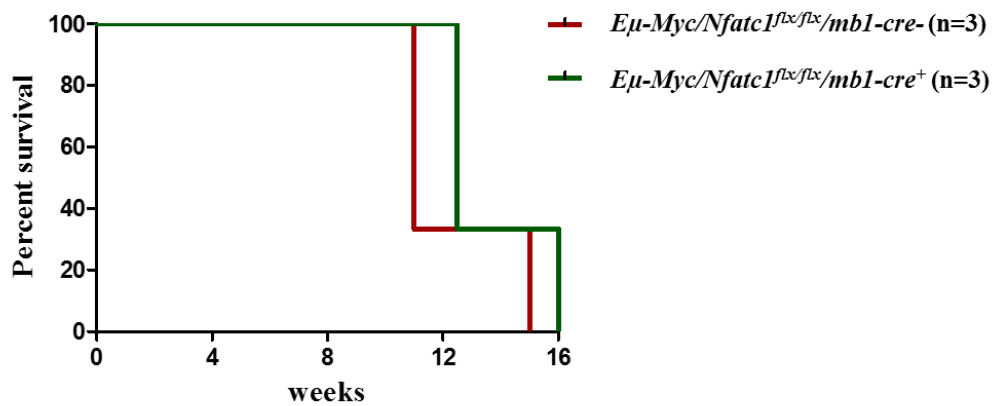


Fig. 6.17 No differences in the tumorigenesis of $E\mu$ -Myc/Nfatc1^{flx/flx}/mb1-cre and intact *Nfatc1* alleles mice. **A.** All of mice developed tumors between 11 – 16 weeks of ages. **B.** All $E\mu$ -Myc/Nfatc1^{flx/flx}/mb1-cre (#1783, #0794, and #2054) showed immature immunophenotype.

6.12 NFATc1 expression is not abolished in BCL cells of *Eμ-Myc/Nfatc1^{flx/flx}/mb1-cre* mice

Confocal microscopy analyses indicated that Ki67⁺ proliferating B-cells from *Eμ-Myc/Nfatc1^{flx/flx}/mb1-cre*⁺ mice still expressed some NFATc1 (Fig. 6.18C). These data were confirmed by Western blot analysis using protein from freshly isolated (*in vivo*) primary (#2054P) and secondary (#2054S) tumors of *Eμ-Myc/Nfatc1^{flx/flx}/mb1-cre*⁺ mice (Fig. 6.19A). Although a relatively high efficiency of mb1-cre mediated deletion of floxed sequences was reported (>90%, Hobeika et al., 2006), according to our current model, lymphomas developed only from a sub-population of B-cells in which *Nfatc1* gene remained intact. PCR analyses confirmed various incomplete deletion of *Nfatc1^{flx/flx}* allele in the tumor cells of *Eμ-Myc/Nfatc1^{flx/flx}/mb1-cre*⁺ mice (Fig. 6.18D and Fig 6.21 A).

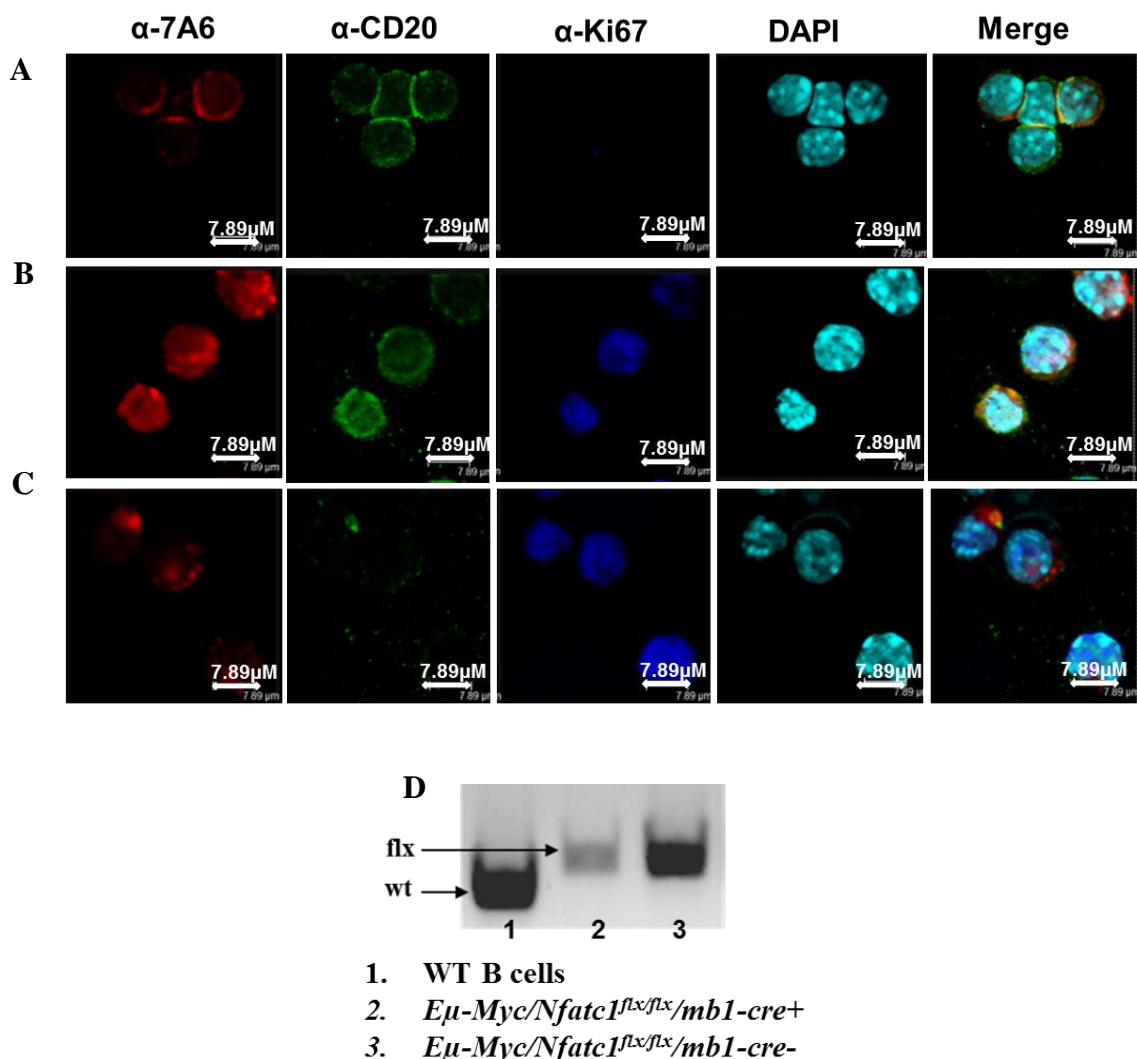


Fig. 6.18 NFATc1 protein was still expressed in BCL cells from *Eμ-Myc/Nfatc1^{flx/flx}/mb1-cre* mice. Confocal microscopy analyses of B-cells isolated from wild-type mice (A), the tumors of *Eμ-Myc* with intact *Nfatc1* allele (#1913, B), and *Eμ-Myc/Nfatc1^{flx/flx}/mb1-cre* (#0794, C) and stained with antibodies against NFATc1 (7A6), CD20 and Ki67. D. PCR analyses indicated the presence of an intact *Nfatc1* gene (line 2) in B cell tumor of *Nfatc1^{flx/flx}/mb1-cre*⁺ mouse (#0794) which showed a weaker expression in comparison to *Nfatc1^{flx/flx}/mb1-cre*⁻ (line 3).

6.13 Development of secondary *Eμ-Myc/Nfatc1^{flx/flx}/mb1-cre* tumors

We next assessed the capacity of *Eμ-Myc/Nfatc1^{flx/flx}/mb1-cre* tumor cells to promote tumor growth. The tumor cells were injected s.c. into six (6) wild type mice. During observation period (9 weeks) the secondary tumors developed in four mice and were readily detectable on day 8, week 2, 3 and 4 post injection respectively. Two of these mice were sacrificed at day 21 and day 35, respectively. In these mice, the growth of secondary tumors was not only limited to the site of injection but also spread to inguinal, axilla, mesenteric and neck lymphnodes, as well as to BM, spleen and thymus (Table 1). As control, we injected s.c. #1913 tumor cells (with intact *Nfatc1* allele) three wild type mice. In this group, the growth of secondary tumors was detected at the beginning of 2nd week in all three mice. All mice were sacrificed at day 17. In one of these mice distinct spread of tumors was evident (Table 1). We concluded that both groups exhibited similar tendency of tumor spread.

Table 1. Comparison of the secondary tumors in *Eμ-Myc/Nfatc1^{flx/flx}/mb1-cre⁺* and *Eμ-Myc/Nfatc1-dsRed* mice

Mice	#2054 <i>Eμ-Myc/Nfatc1^{flx/flx}/mb1-cre⁺</i>	#1913 <i>Eμ-Myc/Nfatc1-dsRed</i>
NFATc1 status	NAFTc1 “deficient”	<i>Nfatc1^{+/-}</i>
Tumor develop in	66.7% (4 out of 6)	100% (3 out of 3)
Sacrificed of mice	Day 21 and 35 post injection	Day 17 post injection
Tumor spread	2 out of 2 Lymphnodes, spleen, BM and thymus	1 out of 3 Lymphnodes, spleen, BM and thymus

Western blot analysis of tumor cells (*in vivo*) from primary (#2054P, Fig 6.19A, no. 1) and secondary tumors (#2054S, Fig 6.19A no. 2) showed that NFATc1 proteins were still expressed. The expression level of NFATc1 in these two tumors (#2054P and #2054S) was similar to that of control cells (resting B cells). A Western blot analysis of *ex vivo* propagated tumor cells of #2054S and #0435 showed a reduced expression of NFATc1 in #2054S tumor cells in comparison to that of #0435 (Fig. 6.19B). PCR analysis revealed incomplete deletion of *Nfatc1^{flx/flx}* allele in these tumor cells *in vivo* (Fig. 6.21A) and during limited propagation *ex vivo* (Fig. 6.21B and C). These data indicated that in both mice (#2054P and #2054S) tumorigenesis is supported in B cells in which NFATc1 protein is still expressed.

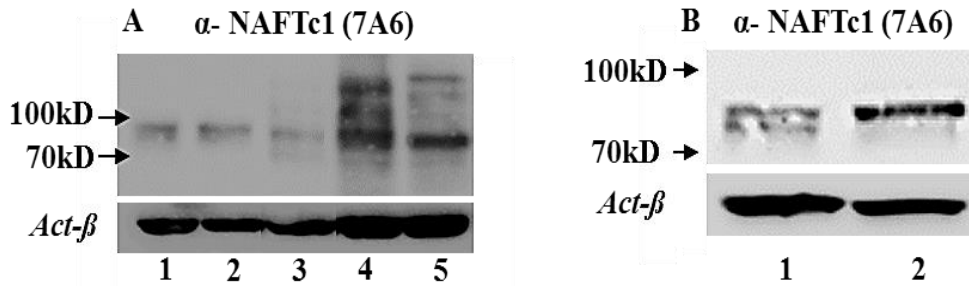


Fig. 6.19. NFATc1 is still expressed in primary and secondary tumors from NFATc1-‘deficient’ tumor cells. **A.** Western blot analyses of proteins from tumors of primary and secondary $E\mu$ -Myc/Nfatc1^{flx/flx}/mb1-cre⁺ tumors (#2054S, #2054P, lanes 1 and 2, respectively), resting and anti-IgM stimulated naïve B-cells (lanes 5 and 4, respectively). **B.** Western blot analyses of proteins from *ex vivo* propagated tumors #2054S (1) and #0435 (2). Analyses were performed with antibodies directed against NFATc1 (7A6).

6.14 NFATc1 is required for survival of $E\mu$ -Myc-induced BCL cells

Tumorigenesis in $E\mu$ -myc mice with intact *Nfatc1* allele and in $E\mu$ -Myc/Nfatc1^{flx/flx}/mb1-cre *in vivo* (Fig. 6.17) did not reveal significant differences between these two groups. It is well established that the relatively low efficiency of cre-mediated deletion *in vivo* is significantly increased after cultivation of cells *ex vivo* (Aliprantis et al., 2008). Therefore, we cultivated $E\mu$ -Myc/Nfatc1^{flx/flx}/mb1-cre⁺ BCL cells (#0794P and #1783P) and from control $E\mu$ -Myc tumor (#1913P) and other tumors with at least one intact *Nfatc1* gene allele (n=10). All BCL tumors from the control group (n=10) started to grow vigorously *ex vivo* after a short lag phase, while all BCL cells from NFATc1-deficient mice (#0794P and #1783P) died within 3 days (see Fig. 6.20A as an example).

Both primary and secondary tumors of $E\mu$ -Myc/Nfatc1^{flx/flx}/mb1-cre mice (#2054P-#2054S) showed different trend *ex vivo*. These cells proliferated *in vitro*, albeit at a significantly lower rate. Initial PCR analysis of these cells indicated an incomplete deletion of *Nfatc1* gene (Fig. 6.21A). However, around day 8 complete absence of *Nfatc1* allele was detected, culture seized to proliferate and started to die (Fig. 6.20B and C). Cytological examination and FACS analysis of these cells confirmed an increased apoptosis and cell death compared to those with one intact *Nfatc1* allele (Fig. 6.20D and E). Together these data indicated that inactivation of the *Nfatc1* gene results in decreased survival of BCL cells, at least *ex vivo*.

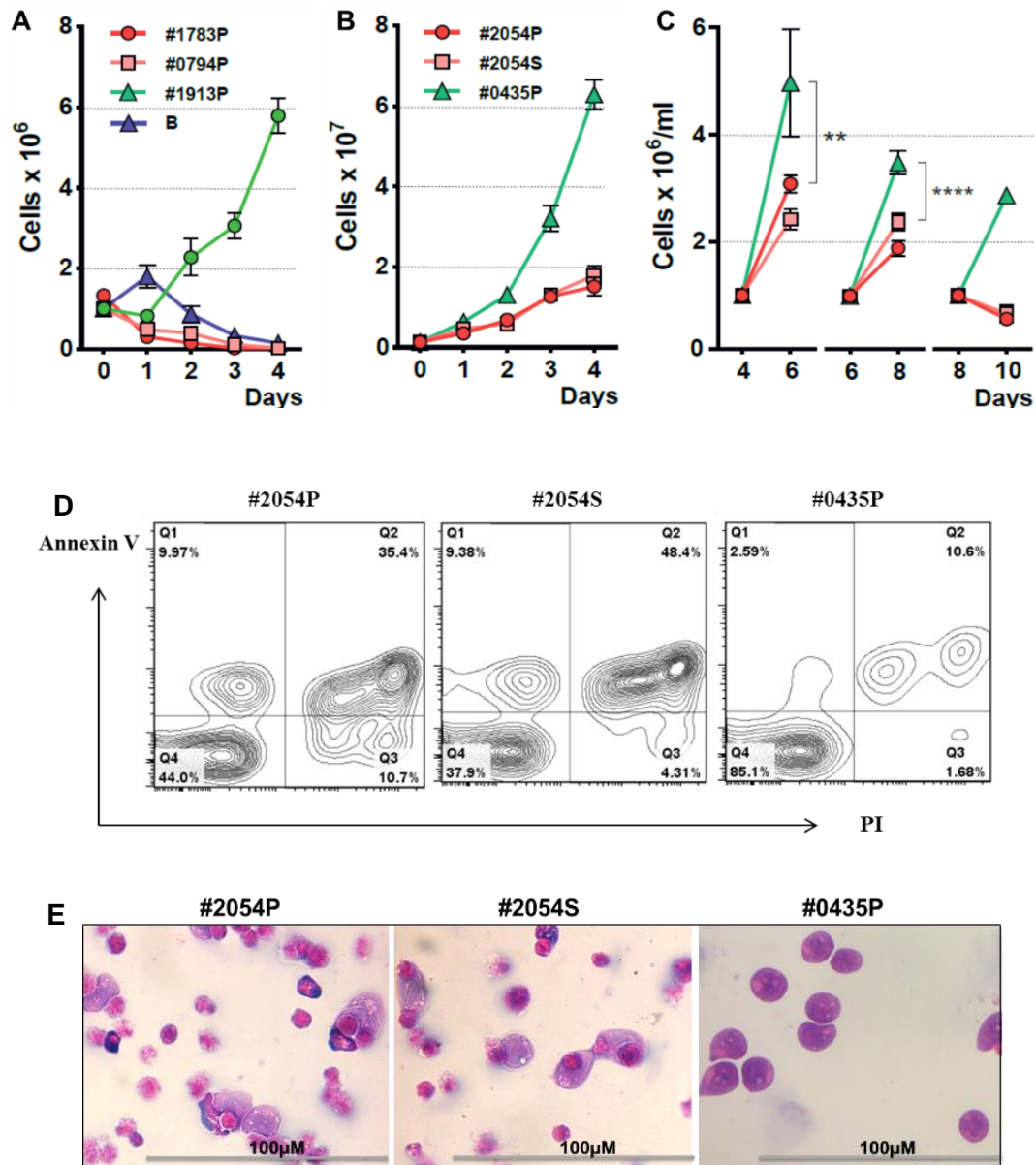


Fig. 6.20 Reduced expansion and survival of NFATc1-deficient tumor cells upon prolonged culture *ex vivo*. **A**. Primary tumor cells from *Nfatc1^{flx/flx}/mb1-cre⁺* (#1783 and #0794), *Eµ-Myc/Nfatc1-dsRed* (#1913) and resting splenic wild type B cells (B). **B.** and **C.** Primary and secondary tumors of #2054 (#2054P and #2054S) and primary tumor from a mouse with intact *Nfatc1* alleles (#0435P). The all tumor cells and resting splenic wild type B cells were cultured and enumerated daily at indicated time. **D.** Primary and secondary tumors of NFATc1-deficient at day 6 of culture (on panel C above) showed decreased proliferation and increased cell death compared to tumor cells with intact *Nfatc1* allele (#0435P). **E.** Haematoxylin-eosin staining of #2054P, #2054S and #0435P cultures at day 6 of cultivation.

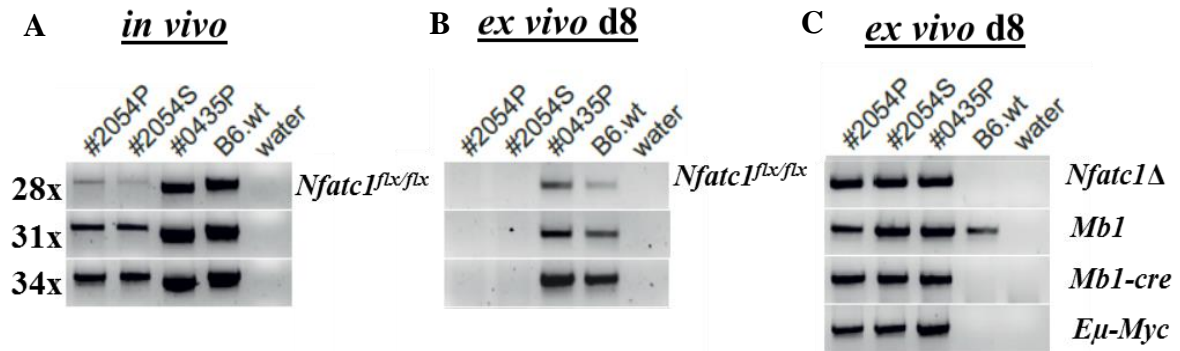


Fig. 6.21 *Nfatc1* is completely inactivated during prolonged cultivation *ex vivo*. PCR analysis confirmed incomplete inactivation of *Nfatc1^{flx/flx}* allele in the cells of #2054P and #2054S tumors *in vivo* (A) and complete inactivation *ex vivo* (B and C).

6.15 Caspase-3 and -7 are activated in *Eμ-Myc/Nfatc1^{flx/flx}/mb1-cre* tumor cells

We asked whether apoptosis is induced in tumor cells from *Eμ-Myc/Nfatc1^{flx/flx}/mb1-cre* mice via the caspase pathways, in particular by inducing caspase-3 and caspase-7. Western blot analysis indicated that in NFATc1-deficient tumor cells (from *Eμ-Myc/Nfatc1^{flx/flx}/mb1-cre*, #2054P and #2054S) both caspases were activated as shown by their cleavage products which are not observed in tumor cells from mice with intact *Nfatc1* alleles (#0435, Fig. 6.22A and B).

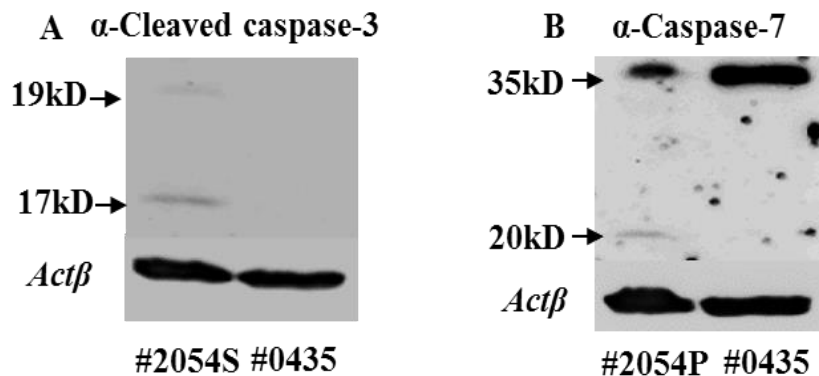


Fig. 6.22 Caspase-3 and -7 are activated in *Eμ-Myc/Nfatc1^{flx/flx}/mb1-cre* tumor cells. Tumors cells of *Eμ-Myc/Nfatc1^{flx/flx}/mb1-cre* (#2054P and #2054S) mice and *Eμ-Myc/Nfatc1^{flx/wt}/mb1-cre* (#0435P) were isolated. Whole cell protein extract were separated by SDS-PAGE. Western blot analysis was performed with antibodies directed against Cleaved caspase-3 (A) and Caspase-7 antibodies (B).

6.16 Interaction of CD40-CD40L induced apoptosis of *Eμ-Myc* induced BCL cells

Activation of NF- κ B signals was postulated to be incompatible with the survival of BL cells with high MYC expression levels (Keller et al., 2005; Schmitz et al., 2012). To verify if the interaction between CD40 and CD40-ligand (CD40L) can induce apoptosis in *Eμ-Myc* tumor cells we co-cultured #0435 tumor cells with 40LB feeder cells which expresses the CD40-ligand (and BAFF, Nojima et al., 2011), in the presence and absence of IL-4. In co-cultures *Eμ-Myc* BCL cells started to die after day 2. The controls, tumor cells of #0435 alone *i.e.* without feeder cells did not die and at day 4 they accumulated almost 50 times (Fig. 6.23A). FACS analysis at day 3 confirmed that under co-culture conditions more than 90% of *Eμ-Myc* induced tumor cells underwent apoptosis (Fig.6.23B). These data suggested that interaction between CD40 and CD40L induces apoptosis in *Eμ-Myc* BCL cells after more than 2 days co-culture.

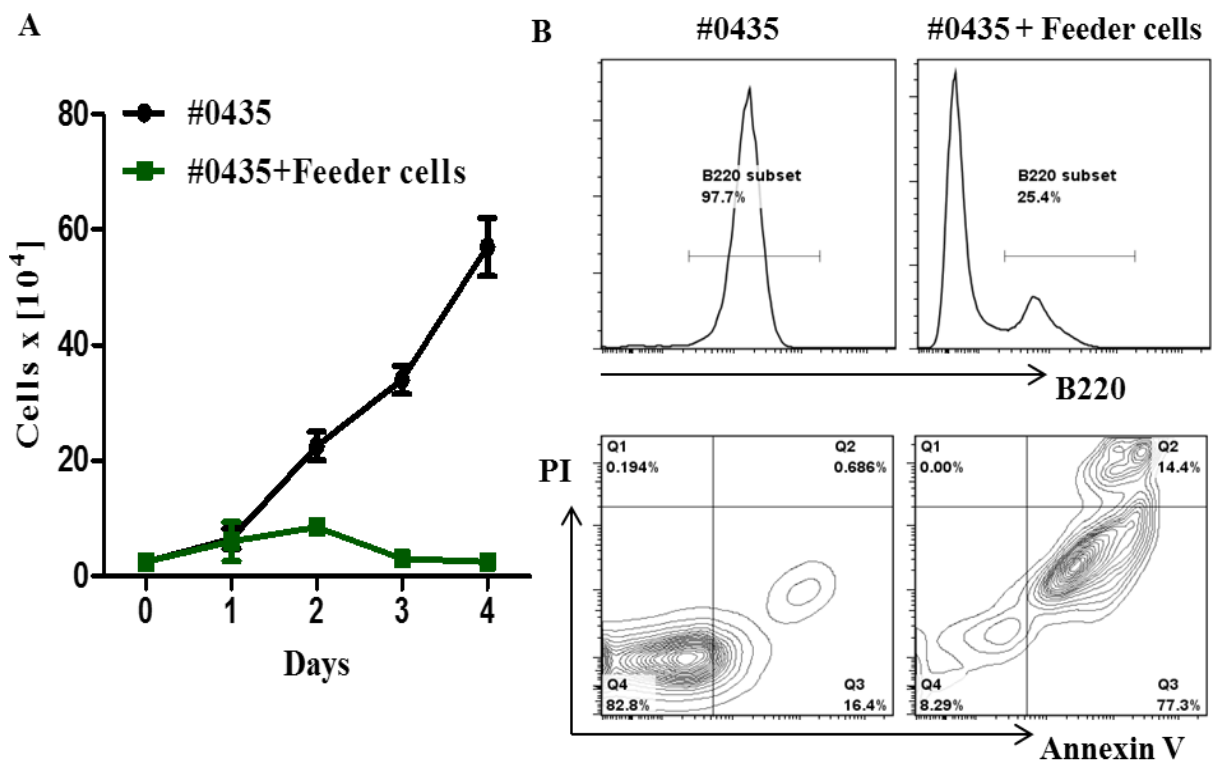


Fig. 6.23 CD40-CD40L interaction induced apoptosis in *Eμ-Myc* tumor cells. **A.** *Eμ-Myc* tumor cells (#0435) were cultivated with or without irradiated 40LB feeder cells. **B.** Co-cultured and control cells were stained with antibodies against B220, Annexin V and PI. FACS analyses were gated on B220⁺ cell populations (below).

6.17 Interaction between NFATc1 and BCL6 in maintenance of BL

We were interested to elucidate which factors might influence the sustained residence of NFATc1 in the nucleus of BL cells. NFATc1 and BCL6 are co-expressed in nucleus of GC-B cells and GC derived-lymphomas including BL (Saito et al., 2007; Kim et al., 2012, and G. Ott, personal

communication). Indeed, NFATc1 and BCL6 were co-expressed in BL cell lines, Ramos, Namalwa (Fig. 6.24A and B, Fig. 6.25D).

BCL6 is degraded by the ubiquitin/proteasome pathway following its phosphorylation via mitogen-activated protein kinases (MAPKs) or via p300 mediated acetylation (Niu et al., 1998; Bereshchenko et al., 2002). CsA treatment of Ramos cells did not affect nuclear levels of BCL6 protein (Fig. 6.24A and B). However, treatment of Namalwa cells with increasing concentrations of Ca²⁺ chelator, Bapta AM, led to concentration dependent decrease of nuclear BCL6 protein, concomitant with cytosolic relocation of NFATc1 protein (Fig. 6.24B) suggesting that interaction with BCL6 might be at least partially contributing to sustained CN-independent nuclear residence of NFATc1 in BL cells.

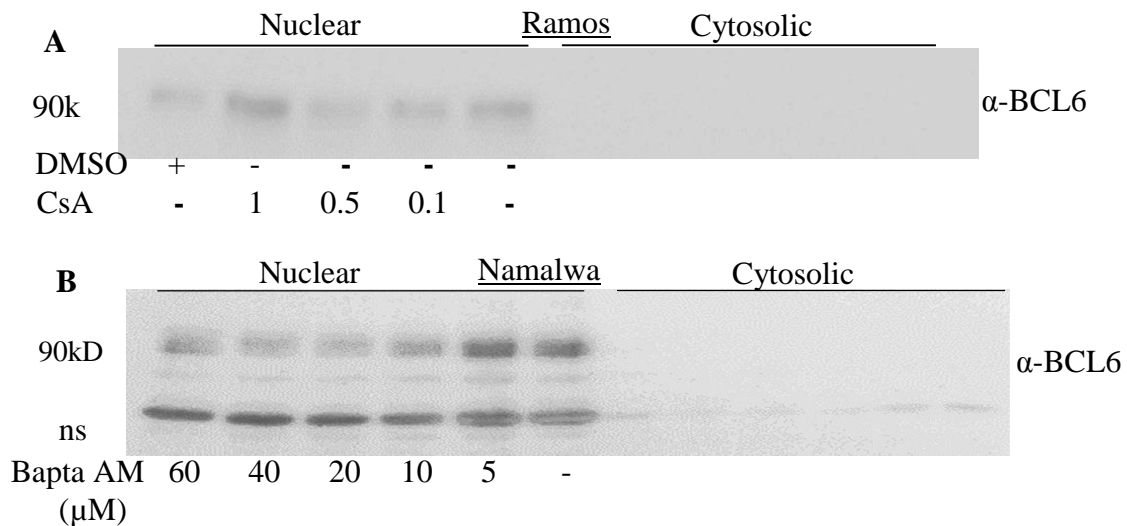


Fig. 6.24 Nuclear expression of BCL6 is affected by the intracellular Ca²⁺ levels. **A.** Ramos cells were treated with CsA at the indicated concentrations. **B.** Namalwa cells were treated with BAPTA AM for 3.5 hours at indicated concentrations. Cytoplasmic and nuclear protein extracts were analysed by Western blotting using antibodies directed against BCL6.

To determine putative interactions among MYC, NFATc1 and BCL6 we employed P493-6 cells. Upon treatment with doxycycline, the expression of MYC is abolished (Table 2) resulting in reversible G1 arrest (Fig. 6.25D). RT-PCR analysis indicated that MYC expression level in P493-6 cells did not affect neither total level of *NFATc1* transcripts nor modulated activities of P1 or P2 promoters (Fig. 6.25A). The expression levels of *NFATc2* transcripts also remained unaffected by *MYC*.

Table 2. P493-6 cells, indicated treatments and effects

P493-6	Treatment	Effects	Cell condition
#1	(-)	MYC-ON	Proliferation
#2	Doxycycline	MYC-OFF	G1-arrest
#3	Estrogen	MYC-ON EBNA-ON	Proliferation
#4	Estrogen and Doxycycline	MYC-OFF EBNA-ON	Proliferation

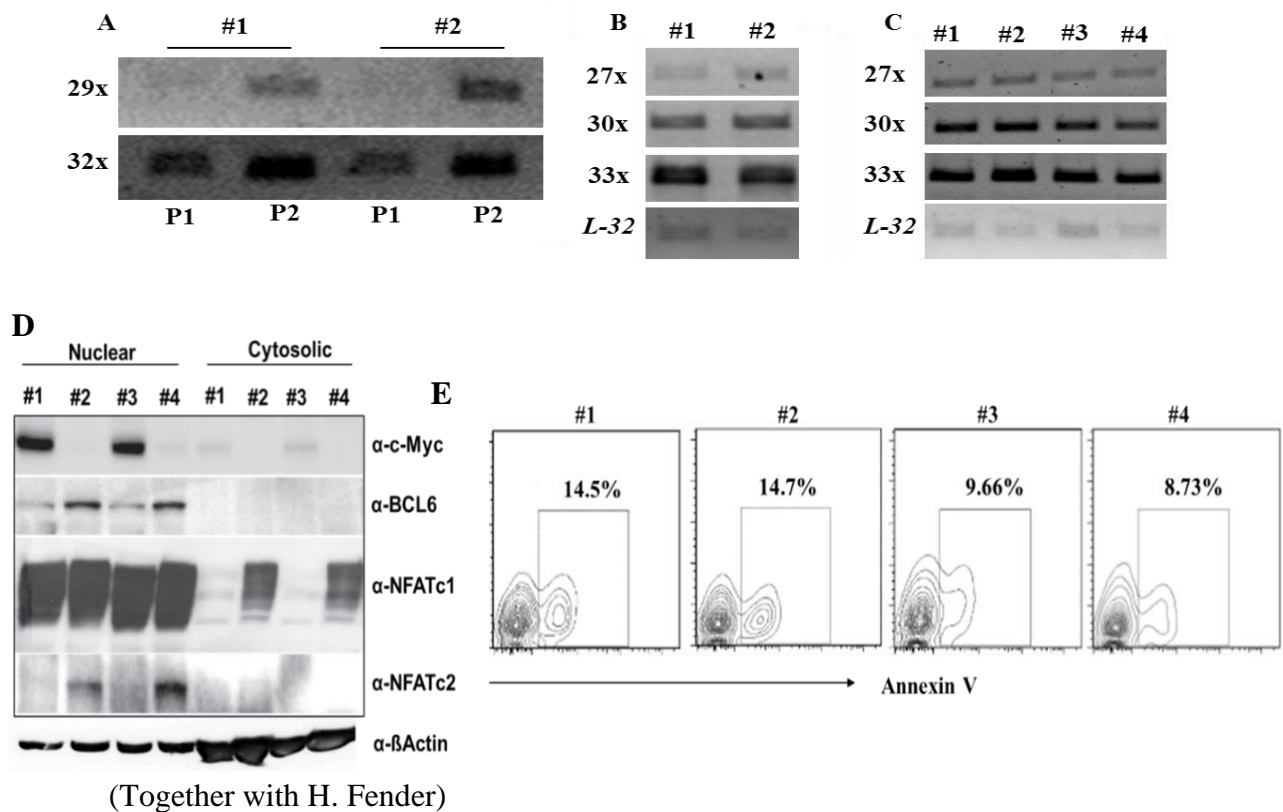


Fig 6.25 Putative interaction between NFATc1 and BCL6. **A. B. and C.** The activities of NFATc1 P1 and P2 promoters (A), the total levels of *NFATc1* (B) and *NFATc2* (C) transcripts were analyzed by RT-PCR. **D.** P493-6 cells were left untreated (#1), and treated with doxycycline (#2), estrogen (#3), or doxycycline and estrogen (#4) for three days. Nuclear and cytoplasmic protein extracts were analysed. Western blot analysis with indicated antibodies directed against NFATc1 (7A6), BCL6 (D65C10) and c-Myc (9E10). **E.** FACS analysis of Annexin V stained P493-6 cells after 4 days of indicated treatments.

MYC regulates intracellular level of Ca^{2+} . Therefore, a high expression level of MYC sustained Ca^{2+} influx (Habib et al., 2007) in BL. Both BCL6 and NFATc1 are regulated by the Ca^{2+} signaling pathway (Fig. 6.6A and B, Fig. 6.24A and B, Kim et al., 2012). Downregulation of MYC protein expression results in increased nuclear expression of BCL6 and NFATc2 in growth arrested

as well as proliferating of P493-6 cells (Fig. 6.24C). Concomitantly, a partial cytosolic translocation of NFATc1 is evident.

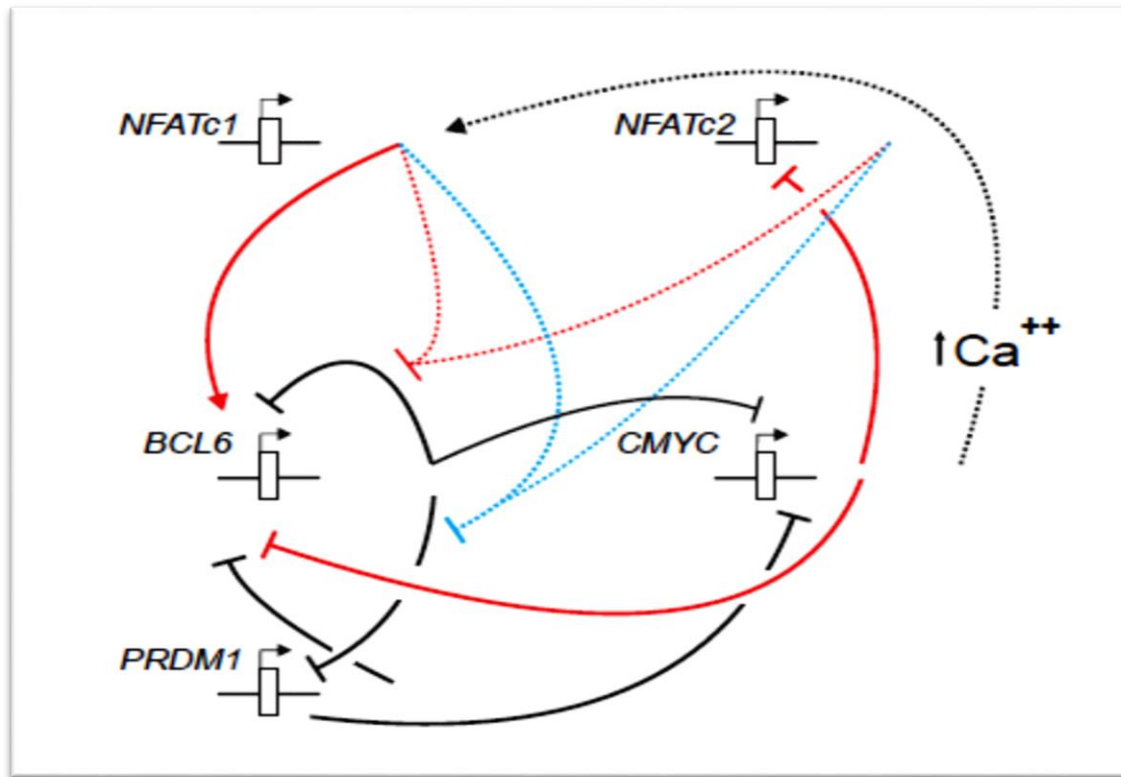


Fig. 6.26 Model of NFATc1-MYC-BCL6-PRDM1 regulatory network. Increased MYC expression increases intracellular of Ca^{2+} levels leading to sustained exclusively nuclear localization of NFATc1. NFATc1 might be recruited to DNA-bound BCL6 and affect autoregulatory loop of BCL6 expression and, in turn, BCL6-mediated repression of *PRDM1* gene. Thus, NFAT proteins are important modulators of well-established MYC-BCL6-PRDM1 regulatory network. Established connections are shown in black. Our proposed pathways are shown in red and blue. Solid lines specify protein/DNA interactions, interrupted lines represent protein/protein interactions.

Evidence from our group revealed that the regulatory domain of NFATs directly interacted with the DNA binding domain of BCL6 (Busch et al., 2014, manuscript, submission), and that such interaction might be responsible for the partial cytosolic retention of BCL6 and NFAT proteins and/or recruitment of NFATs to BCL6 DNA binding sites. Therefore, we speculate that this interaction might affect a negative autoregulatory loop of BCL6 expression and BCL6 mediated repression of *PRDM1* gene. Therefore, our data suggest that NFAT proteins are important modulators of well-established MYC-BCL6-PRDM1 regulatory network (Fig. 6.26).

7. Discussion

7.1 NFATc1 expression in Burkitt lymphoma

The expression of *NFATc1* in lymphomagenesis/leukemogenesis has been addressed (Marafioti et al, 2004; Pham et al., 2010; Akimzhanov et al., 2008; Le Roy et al., 2012). Interestingly, although most aggressive BCLs including Burkitt lymphoma express NFATc1 (Marafioti et al, 2004; Pham et al., 2010), the role of these observations in generation and/or maintenance of tumors was never addressed before.

We identified several NFATc1 localization patterns in BL cases assessed by immunohistochemistry using an antibody which detects all NFATc1 protein isoforms (7A6) and an NFATc1- α -isoform specific antibody (IG-457) (Fig. 6.1A-H). The major expression pattern was predominantly nuclear localization, also found by Marafioti et al. (2004). Additional expression patterns were characterized by near equal staining of nuclear and cytosolic compartments or preferentially cytosolic staining. Therefore, in all cases at least part of NFATc1 was localized in nucleus suggesting transcriptional activity of NFATc1. Preferentially nuclear expression pattern was observed in all BL cell lines analysed (H. Fender, unpublished). As example, in Ramos and Namalwa cells NFATc1 was exclusively nuclear (Fig. 6.1I-J). Western blot analysis confirmed specificity of immunohistochemical and immunofluorescence stainings (Fig. 6.6A and B).

Increased expression of NFATc1 was linked with MYC protein overexpression (Pham et al., 2010), however, there is no direct correlation between patterns of NFATc1 immunostaining and *MYC* translocation (Marafioti et al., 2004). It might be interesting to correlate different NFATc1 immunostaining patterns to clinical aspects of BL, *i.e.* patient survival or management options. Unfortunately, for BL cases analyzed in a current study the data of patient survival and therapeutic management are not available. Stainings of BL cases with NFATc1 antibody might be considered as a prognostic tool in the future.

In line with transcriptome analysis of BL (Dave et al., 2006), our data revealed lack of significant upregulation of *NFATc1* transcripts in primary BL and BL cell lines (Fig. 6.13A) suggesting that in tumor cells NFATc1 protein expression is mainly affected by post transcriptional or post-translational mechanisms.

7.2 B cell lymphomas in *E μ -Myc* mice

To verify the role of NFATc1 in BCL survival and progression, we utilized *E μ -Myc* mouse (Adam et al., 1985). B cell lymphomas (BCLs) which developed in *E μ -Myc* mice are similar to human BL in respect to clinical and histologic appearances (Adam et al., 1985). BLs in human are derived from GC B or memory B cells (Tamaru et al., 1995; Klein et al., 1995; Isobe et al., 2000). Hence, BL

tumor cells basically express surface markers of their origin *i.e.* CD20, CD10, BCL6, (Blum et al., 2004). Tumors from *Eμ-Myc* mice derive from different B cell stages *i.e.* small pre-B, immature, and mature B cells but not from GC B cells (Fig.6.4B). These results are in agreement with Adam and colleagues (Adam et al., 1985). Therefore, in respect to tumor origin *Eμ-Myc* model does not reflect human BL. In 70% cases (n=10) of our *Eμ-Myc* mice tumors develop from mature stages of B cell development, as evident from the presence of tumors with mixed (IgD⁻ and IgD⁺, n=6) and mature (IgD⁺, n=1) immunophenotypes.

7.3 NFATc1 expression in *Eμ-Myc* mouse tumors

In peripheral lymphocytes, upon activation NFATc1 translocates into the nucleus and controls the transcription of target genes (Loh et al, 1996a; Chen et al, 1998; Garcia-Cozar et al, 1998). Similar to BL, in *Eμ-Myc* induced primary and secondary tumors and in all BCL lines which we have derived from these tumors (Fig. 6.5E and 6.7A) NFATc1 was predominantly expressed in nuclei (Fig. 6.5A and C). This suggested that NFATc1 plays an important role in the survival and progression of *Eμ-Myc* induced tumors. Interestingly, we found that the expression levels of *Nfatc1* mRNA in *Eμ-Myc* tumor cells was rather decreased in comparison with normal resting splenic B-cells (Fig. 6.13B) indicating that NFATc1 protein expression in *Eμ-Myc* induced tumors is significantly affected by post transcriptional and/or post-translational mechanisms.

7.4 Comparative analysis of NFATc1 isoform expression in BL, BL cell lines and *Eμ-Myc* induced tumor

Different properties and functions of NFATc1 α and NFATc1 β proteins in lymphocytes and macrophages are well established (Chuvpilo et al., 2002; Serfling et al., 2012; Busch et al., 2014 manuscript, submitted). To differentiate between expression of NFATc1/ α and β isoforms in BL and *Eμ-Myc* BCL tumors we analyzed the relative amounts of P1- and P2-promoter directed transcripts. In human BL, P1-directed *NFATc1* transcripts were expressed at around 8-fold higher levels than P2-directed transcripts (Fig. 6.14A and B). In MYC-overexpressing human P493-6 cells (Fig. 6.24A) about 8-fold higher level of P2-directed transcripts compared to P1-directed *NFATc1* transcripts was observed. Neither total amount of *Nfatc1* transcripts nor relative activities of promoters were affected by the MYC expression levels in these cells. In *Eμ-Myc* BCL tumors we observed around 8-fold higher expression of P2-directed *Nfatc1* transcripts in comparison to P1-directed *Nfatc1* transcripts (Fig. 6.14D-G). We confirmed these findings with analysis of the *Eμ-Myc/Nfatc1-dsRed* tumor where NFATc1/ β isoforms were expressed at around 4-fold higher levels than NFATc1 α suggested NFATc1 β isoform was predominant in *Eμ-Myc* tumor (Fig. 6.15). Therefore our data revealed lack

of strict correlation between the expression of six NFATc1 isoforms in different BL-related entities suggesting that both NFATc1/ α A and $-\beta$ A isoforms provide survival functions and that NFATc1/ α / β B and $-\alpha$ / β C isoforms either do not possess pro-apoptotic properties in BL cells or these properties are counterbalanced.

7.5 Stability NFATc1 protein in MYC induced tumors

MYC protein is degraded through the ubiquitin-proteasome pathway (Wierstra and Alves, 2008). In BL cell lines (Ramos and Namalwa) the half-life of MYC protein is prolonged (till around 2 hrs, Fig. 6.12A and B), compared to 15-30 minutes in normal proliferating cells (Dang, 2012; Schumacher and Eick, 2013). We observed that stability of NFATc1 protein is also increased in Ramos and Namalwa cells. To investigate expected link between high expression of MYC and stabilization of NFATc1 protein we employed P493-6 cell line. In the presence of high MYC expression levels the half-life of both NFATc1 α and $-\beta$ isoforms was significantly increased (7.14hrs against 5hrs in the absence of MYC). These data indicated that high levels of MYC expression stabilize NFATc1 protein independently from N-terminal α / β -peptides, which themselves have different protein half-lives (Hock et al., 2013).

7.6 Nuclear residence of NFATc1 in MYC induced tumors is largely insensitive to calcineurin inhibitors.

Increased intracellular Ca^{2+} in peripheral lymphocytes elicits the activation of CN which dephosphorylates NFATc1, exposing a nuclear localization sequence which then leads to NFATc1 translocation into the nucleus. Nuclear localization of NFAT factors is sensitive to the CN inhibitors cyclosporine A (CsA) and FK506 (Loh et al., 1996a). We demonstrated that upon treatment with various concentration of CsA (0.1-11 $\mu\text{g}/\text{ml}$) there was only about 10% of NFATc1 protein were exported to cytosol in Ramos and Namalwa cells (Fig. 6.6A and C). Nuclear localization of NFATc1 in normal lymphocytes is completely prevented with 0.1 $\mu\text{g}/\text{ml}$ of CsA. Importantly, increased CsA concentrations (up to 10-fold) did not result in an increased cytosolic relocation of NFATc1. Even the lowest concentrations of CsA resulted in a complete relocation of nuclear RELA (p65) protein in Ramos cells indicating that in BL cells the major part of NFATc1 nuclear pool is independent from CN activity.

In addition, our data indicated that nuclear residence of NFATc1 is not affected by inhibition of Jak3 activity, which is responsible for NFATc1 nuclear translocation in double-negative thymocytes (Patra et al., 2013). Interestingly, even moderate (IC_{50}) concentrations of Jak3 inhibitor

blocked proliferation of Ramos and BCL (#1542B) cells indicating the presence of Jak3-dependent/NFATc1-independent proliferation pathway in BL cells.

Decreased electrophoretic mobility of NFATc1A, -B, and -C isoforms after CsA treatment suggested that even at the lowest CsA concentration the nuclear fraction of NFATc1 protein is becoming highly phosphorylated (Fig. 6.6A-D). NFATc1 nuclear export is regulated via the phosphorylation of its serine residues by certain kinases *i.e.* Glycogen synthase kinase-3 (GSK), protein kinase A (PKA), Casein kinase 1 (CK1), p38 MAPK and c-Jun N-terminal kinase 1 (JNK1) (Beals et al., 1997; Sheridan et al., 2002; Okamura et al., 2004; Gomez del arco et al., 2000; Liang et al., 2003). Our results does not exclude the possibility that phosphorylation pattern of NFATc1 under CsA treatment of BL cells is different from that required for nuclear export. Because portion (10%) of nuclear NFATc1 is relocated to cytosol after CsA treatment we believe that regulation/requirements for nuclear export are similar in BL and normal B-lymphocytes.

The closest explanation for the constitutive NFATc1 nuclear residence is MYC-dependent reduction of Ca^{2+} efflux due to decreased expression of plasma membrane Ca^{2+} -adenosine triphosphatase (PMCA) efflux pump (Habib et al., 2007). This leads to a sustained increase in intracellular Ca^{2+} level and results in constitutive nuclear localization of NFATc1 (Habib et al., 2007). Therefore, MYC activation together with constitutive NFATc1 signals promotes B cell activation, proliferation and ultimately tumorigenesis. Once they become malignant, the survival of lymphoma cells is maintained via Ca^{2+} /NFATc1 pathways.

Functional characterization of phosphorylated nuclear NFATc1 (under CsA regimen) requires further analysis. Phosphorylated NFATc1 might bind (albeit with lower affinity) to regulatory elements of NFAT target genes. Some fraction of nuclear phosphorylated NFATc1 might be dephosphorylated by intranuclear phosphatases and retained in the nucleus with full transcriptional activity. Indeed, CsA treatment does not affect proliferation of Ramos, Namalwa or BCL cells (Fig. 6.6E and F and 6.7B).

7.7 Tumorigenesis in *Eμ-myc/Nfatc1^{flx/flx}/mb1-cre* mice

Our experiments revealed that BCL tumors develop in *Eμ-Myc/Nfatc1^{flx/flx}/mb1-cre⁺* (n=3) mice with conditional NFATc1 deficiency. However, none of these mice showed the presence of tumor clones with mature B-cell immunophenotype, which was predominant (70%) in mice with intact *Nfatc1* alleles. This indicates that NFATc1 expression is required for generation/survival of BCL.

We observed different behavior of the tumor cells from *Eμ-Myc/Nfatc1^{flx/flx}/mb1-cre⁺* mice during cultivation *ex vivo* compared to cells with intact *Nfatc1* alleles. The tumor cells of two mice (#0794 and #1783) did not proliferate upon cultivation, after 2 days of lag-phase they died (Fig.

6.20A). While the tumor cells from other *Eμ-Myc/Nfatc1^{flx/flx}/mb1-cre⁺* mice (#2054 primary and secondary) still survive during cultivation. The reason for this might be related to lower initial levels of 'residual' *Nfatc1* gene in tumors cells of these two mice (#0794 and #1783) compared to that of #2054 primary and secondary tumors. Therefore, complete inactivation of *Nfatc1* gene *in vitro* was achieved in a few days. While in the tumor cells of mouse #2054 primary and secondary, complete inactivation of *Nfatc1* gene was achieved after more than four weeks of cultivation. These indicated in our mouse model BCL developed only from a sub-population of B-cells in which *Nfatc1* gene remained intact, and this was confirmed by PCR analyses showed incomplete inactivation of *Nfatc1^{flx/flx}* allele in these cells (Fig. 6.18E and 6.21A). Together these observations indicated the variability of cutting efficiency of cre-mediated deletion, although high efficiency of mb-1 cre mediated deletion in non-tumor cells (Hobeika *et al.*, 2006). The mb1-cre mediated deletion might be of limited value to study the conditional alleles in certain tumor types, including in *Eμ-Myc* mouse models.

BL cells typically show low activity of the pro-survival factor NF-κB (Dave *et al.*, 2006) and activation of NF-κB signals is not compatible with survival of BL cells with high MYC expression level (Keller *et al.*, 2005; Schmitz *et al.*, 2014). CD40 is expressed at all stages of B cell development (van Kooten and Banchereau, 2000) and in human and murine *MYC*-induced lymphoma cell lines (Klapproth *et al.*, 2009). Cross-linking of CD40 leading to activation of NF-κB (van Kooten and Banchereau, 2000). In BL cell lines, increased cell death related to NF-κB, caspase-8 dependent and Fas expression were observed (Klapproth *et al.*, 2009; Klapproth and Wirth, 2010), thus, activation of NF-κB induced cell death in certain BL cell lines (Klapproth *et al.*, 2009). We showed induction of apoptosis in *Eμ-Myc* tumor cells upon co-cultured after day 2 with 40LB feeder cells expressing CD40L (and BAFF, Fig. 6.23A and B). These data suggested interaction of CD40-CD40-ligand might activate NF-κB signaling leading to the induction of apoptosis of *Eμ-Myc* tumor cells after day 2 co-cultured.

7.8 Interaction of NFATc1 and BCL6 in maintenance of BL survival

In BL, high expression of MYC leads to sustains Ca²⁺ influx (Habib *et al.*, 2007) and to constitutive nuclear residence of NFATc1 (Fig. 6.6A-B and 6.7A) and most likely affects BCL6 expression (Fig. 6.24A and B, Kim *et al.*, 2012). Indeed, BCL6 is expressed in nuclei of BL cells and is one of key features in BL diagnosis (G. Ott, personal communication). In GC environment, NF-κB activation related to up-regulation of IRF4 is followed by down regulation of BCL6 (Saito *et al.*, 2007). This is not the case in BL, where suppression of BCL6 is blocked. One reason for this might be affected

negative autoregulatory loop of BCL6 expression due to direct interaction of regulatory domain of NFATs with the DNA binding domain of BCL6 (Busch et al., 2014, manuscript, submitted).

In BL tumors high rate of apoptosis of some cells is competed by increased proliferation of other tumor cells (Bellan et al., 2003; Blum et al., 2004; Ferry 2006; Shankland et al., 2012). We believe that fluctuations of NFATc1 expression levels and/or nuclear localization might be one of the reason(s) for these observations. The cells, which undergo apoptosis might have reduced or missing NFATc1 expression, the cells which proliferate might still have adequate levels of NFATc1. In BL cells NFATc1 protein is stabilized, hence, BL cells are basically more prone to proliferation. This is in line with our observations that in human BL and in P493-6 cells MYC stabilizes NFATc1 protein therefore NFATc1 is constitutively nuclear and ensures survival of tumor cells.

Our studies revealed an important role of NFATc1 in survival of BCL cells, suggesting that components of the CN-independent Ca^{2+} /NFAT signalling pathway are promising targets for cancer therapy of B cell lymphomas, in particular BLs. Further studies with large cohort might be needed to validate the predictive significance of levels and patterns of NFATc1 protein expression in BL assessed by immunohistochemistry, probably in a combination with other markers such as BCL6.

To summarize, we show that NFATc1 is constitutively expressed in nuclei of BL, BL cell lines and in *E μ -Myc* induced BCL cells (1). Nuclear residence of NFATc1 is independent from CN, but depends on intracellular Ca^{2+} (2). NFATc1 is important for survival of tumor cells, thus NFATc1 ablation has strongly correlates to increased apoptosis of tumor cells (3). In *MYC* induced tumors, NFATc1 protein expression is regulated at post transcriptional and post translational levels (4). NFATc1 α/β isoforms play redundant functions in survival of BL and MYC-induced tumor cells (5). Pro-apoptotic activity of NFATc1/B and -C isoforms is counterbalanced in BL cells.

8. References

- Abbott, K.L., Friday, B.B., Thaloor, D., Murphy, T.J., and Pavlath, G.K. (1998). Activation and cellular localization of the cyclosporine A-sensitive transcription factor NF-AT in skeletal muscle cells. *Mol. Biol. Cell* 9, 2905-2916.
- Adams, J.M., Harris, A.W., Pinkert, C.A., Corcoran, L.M., Alexander, W.S., Cory, S., Palmiter, R.D., and Brinster, R.L. (1985). The c-myc oncogene driven by immunoglobulin enhancers induces lymphoid malignancy in transgenic mice. *Nature* 318, 533-538.
- Akimzhanov, A., Krenacs, L., Schlegel, T., Klein-Hessling, S., Bagdi, E., Stelkovic, E., Kondo, E., Chuvpilo, S., Wilke, P., Avots, A., et al. (2008). Epigenetic changes and suppression of the nuclear factor of activated T cell 1 (NFATC1) promoter in human lymphomas with defects in immunoreceptor signaling. *Am. J. Pathol.* 172, 215-224.
- Al-Daraji, W.I., Malak, T.T., Prescott, R.J., Abdellaoui, A., Ali, M.M., Dabash, T., Zelger, B.G., and Zelger, B. (2009). Expression, localisation and functional activation of NFAT-2 in normal human skin, psoriasis, and cultured keratocytes. *Int. J. Clin. Exp. Med.* 2, 176-192.
- Aliprantis, A. O., Ueki, Y., Sulyanto, R., Park, A., Sigrist, K.S., Sharma, S.M., Ostrowski, M.C., Olsen, B.R., and Glimcher, L.H. (2008). NFATc1 in mice represses osteoprotegerin during osteoclastogenesis and dissociates systemic osteopenia from inflammation in cherubism. *J. Clin. Invest.* 118, 3775–3789.
- Aramburu, J., Yaffe, M.B., Lo'pez-Rodri'guez, C., Cantley, L.C., Hogan, P.G., and Rao, A. (1999). Affinity-driven peptide selection of an NFAT inhibitor more selective than cyclosporin A. *Science* 285, 2129-2133.
- Arvanitis, C., and Felsher, D.W. (2006). Conditional transgenic models define how MYC initiates and maintains tumorigenesis. *Semin. Cancer Biol.* 16, 313–317.
- Avots, A., Buttmann, M., Chuvpilo, S., Escher, C., Smola, U., Bannister, A.J., Rapp, U.R., Kouzarides, T., and Serfling, E. (1999). CBP/p300 integrates Raf/Rac-signaling pathways in the transcriptional induction of NF-ATc during T cell activation. *Immunity* 10, 515-524.
- Basso, K., and Dalla-Favera, R. (2012). Roles of BCL6 in normal and transformed germinal center B cells. *Immunol. Rev.* 247, 172–183.
- Basso, K., Saito, M., Sumazin, P., Margolin, A.A., Wang, K., Lim, W-K., Kitagawa, Y., Schneider, C., Alvarez, M.J., Califano, A., et al. (2010). Integrated biochemical and computational approach identifies target genes controlling multiple pathways in normal germinal center B cells. *Blood* 115, 975-984.
- Beals, C.R., Sheridan, C.M., Turck, C.W., Gardner, P., and Crabtree, G.R. (1997). Nuclear export of NFATc enhanced by glycogen synthase kinase-3. *Science* 275, 1930-1933.
- Bellan, C., Lazzi, S., De Falco, G., Nyongo, A., Giordano, A., and Leoncini, L. (2003). Burkitt's lymphoma: new insights into molecular pathogenesis. *J. Clin. Pathol.* 56, 188–193.

- Beral, V., Peterman, T., Berkelman, R., and Jaffe, H. (1991). AIDS-associated non-Hodgkin lymphoma. *Lancet* 337, 805–809.
- Bereshchenko, O.R., Gu, W., and Dalla-Favera, R. (2002). Acetylation inactivates the transcriptional repressor BCL6. *Nat. Genet.* 32, 606-613.
- Bernheim, A., Berger, R., and Lenoir, G. (1981). Cytogenetic studies on African Burkitt's lymphoma cell lines: t(8;14), t(2;8) and t(8;22) translocations. *Cancer Genet. Cytogenet.* 3, 307-315.
- Bhattacharyya, S., Deb, J., Patra, A.K., Pham, D.A.T., Chen, W., Vaeth, M., Berberich-Siebelt, F., Klein-Hessling, S., Lamperti, E.D., Reifenberg, K., et al. (2011). NFATc1 affects mouse splenic B cell function by controlling the calcineurin-NFAT signaling network. *J. Exp. Med.* 208, 823-839.
- Blum, K.A., Lozanski, G., and Byrd, J.C. (2004). Adult Burkitt leukemia and lymphoma. *Blood* 104, 3009-3020.
- Bonavida, B., and Vega, M.I. (2005). Rituximab-mediated chemosensitization of AIDS and non-AIDS non-Hodgkin's Lymphoma. *Drug. Resist. Updat.* 8, 27–41.
- Bross, L., Fukita, Y., McBlane, F., Demolliere, C., Rajewsky, K., and Jacobs, H., (2000). DNA double-strand breaks in immunoglobulin genes undergoing somatic hypermutation. *Immunity* 13, 589–597.
- Brugge, J., Hung, M.C., and Mills, G.B. (2007). A new mutational activation in the PI3K pathway. *Cancer Cell* 12, 104-107.
- Buchholz, M., Schatz, A., Wagner, M., Michl, P., Linhart, T., Adler, G., Gress, T.M., and Ellenrieder, V. (2006). Overexpression of c-myc in pancreatic cancer caused by ectopic activation of NFATc1 and the Ca²⁺/calcineurin signaling pathway. *EMBO J.* 25, 3714–3724.
- Bunting, K.L., and Melnick, A.M. (2013). New effector functions and regulatory mechanisms of BCL6 in normal and malignant lymphocytes *Curr. Opin. Immunol.* 25, 339–346.
- Burkitt, D. (1958). A sarcoma involving jaws in African children. *Br. J. Surg.* 46, 218–223.
- Burkitt, D.P. (1983). The discovery of Burkitt's lymphoma. *Cancer* 51, 1777-1786.
- Calado, D.P., Sasaki, Y., Godinho, S.A. Pellerin, A., Köchert, K., Sleckman, B.P., de Alborán, I.M., Janz, M., Rodig, S., and K Rajewsky, K. (2012). The cell-cycle regulator c-Myc is essential for the formation and maintenance of germinal centers. *Nat. Immunol.* 13, 1092-1101.
- Cain, D., Kondo, M., Chen, H., and Kelsoe, G. (2009). Effects of acute and chronic inflammation on B-cell development and differentiation. *J. Invest. Dermatol.* 129, 266-277.
- Carey, J.B., Moffatt-Blue, C.S., Watson, L.C., Gavin, A.L., and Feeney, A.J. (2008). Repertoire-based selection into the marginal zone compartment during B cell development. *J. Exp. Med.* 205, 2043-2052.
- Casola, S. (2007). Control of peripheral B-cell development. *Curr. Opin. Immunol.* 19, 143–149.

- Castillo, J.J., Winer, E.S., and Olszewski, A.J. (2013). Population-based prognostic factors for survival in patients with Burkitt lymphoma an analysis from the surveillance, epidemiology, and end results database. *Cancer* *119*, 3672-3679.
- Chen, L., Glover, J.N., Hogan, P.G., Rao, A., and Harrison, S.C. (1998). Structure of the DNA-binding domains from NFAT, Fos and Jun bound specifically to DNA. *Nature* *392*, 42-48
- Chuvpilo, S., Avots, A., Berberich-Siebelt, F., Glöckner, J., Fischer, C., Kerstan, A., Escher, C., Inashkina, I., Hlubek, F., Jankevics, E. et al. (1999). Multiple NF-ATc isoforms with individual transcriptional properties are synthesized in T lymphocytes. *J. Immunol.* *162*, 7294-7301.
- Chuvpilo, S., Jankevics, E., Tyrsin, E., Akimzhanov, Moroz, D., Jha, M.K., Santner-Nanan, B., König, T., Avots, A., Berberich-Siebelt, F. et al. (2002). Autoregulation of NFATc1/A expression facilitates effector T cells to escape from rapid apoptosis. *Immunity* *16*, 881-895.
- Cobaleda, C., Schebesta, A., Delogu, A., and Busslinger, M. (2007). Pax5: the guardian of B cell identity and function. *Nat. Immunol.* *8*, 463-470.
- Corcoran, L.M., Cory, S., and Adams, J.M. (1985). Transposition of the immunoglobulin heavy chain enhancer to the myc oncogene in a murine plasmacytoma. *Cell* *40*, 71 -79.
- Dang, C.V. (2012). MYC on the path to cancer. *Cell* *149*, 22-35.
- Dave, S.S., Fu, K., Wright, G.W., Lam, L.T., Kluin, P., Boerma, E.J., Greiner, T.C., Weisenburger, D.D., Rosenwald, A., Ott, G., et al. (2006). Molecular diagnosis of Burkitt's lymphoma. *N. Engl. J. Med.* *354*, 2431-2442.
- de la Pompa, J.L., Timmerman, L.A., Takimoto, H., Yoshida, H., Elia, A.J., Samper, E., Potter, J., Wakeham, A., Marengere, L., Langille, B.L., et al. (1998). Role of the NF-ATc transcription factor in morphogenesis of cardiac valves and septum. *Nature* *392*, 182-186.
- Dominguez-Sola, D., Victora, G.D., Ying, C.Y., Phan, R.T., Saito, M., Nussenzweig, M.C., and Dalla-Favera, R. (2012). The proto-oncogene MYC is required for selection in the germinal center and cyclic reentry. *Nat. Immunol.* *13*, 1083-1092.
- Duan, S., L.Cermak, L., Pagan, J.k., Rossi, M., Martinengo, C., di Celle, P.F., Chapuy, B., Shipp, M., Chiarle, R., and Pagano, M. (2012). FBXO11 targets BCL6 for degradation and is inactivated in diffuse large B-cell lymphomas. *Nature* *481*, 90-94.
- Dunleavy, K., Pittaluga, S., Shovlin, R.N.M., Steinberg, S.M., Cole, D., Grant, C., Widemann, B., Staudt, L.M., Jaffe, E.S., Little, R.F., et al. (2013). Low-intensity therapy in adults with Burkitt's lymphoma. *N. Eng. J. Med.* *369*, 1915-1925.
- Duque, J., Fresno, M., and Iniguez, M.A. (2005). Expression and function of the nuclear factor of activated T cells in colon carcinoma cells involvement in the regulation of cyclooxygenase-2. *J. Biol. Chem.* *280*, 8686-8693.
- Duy, C., Yu, J.J., Nahar, R., Swaminathan, S., Kweon, S.M. Polo, J.M., Valls, E., Klemm, L., Shojaee, S., Cerchiatti, L., et al. (2010). BCL6 is critical for the development of a diverse primary B cell repertoire. *J. Exp. Med.* *207*, 1209-1221.

- Evan, G.I., Christophorou, M., Lawlor, E.A., Ringshausen, I., Prescott, J., Dansen, T., Finch, A., Martins, C., and Murphy, D. (2005). Oncogene-dependent tumor suppression: using the dark side of the force for cancer therapy. *Cold Spring Harb. Symp. Quant. Biol.* *70*, 263-273.
- Evans, L.S., and Hancock, B.W. (2003). Non-Hodgkin lymphoma. *Lancet* *362*, 139–146.
- Felsher, D.W., and Bishop, J. (1999). Reversible tumorigenesis by MYC in hematopoietic lineages. *Mol. Cell* *4*, 199-207.
- Ferry, J.A. (2006). Burkitt's lymphoma: clinicopathologic features and differential diagnosis. *Oncologist* *11*, 375–383.
- Fric, J., Lim, C.X.F., Koh, E.G.L., Hofmann, B., Chen, J., Tay, H.S., Mohammad Isa, S.A., Mortellaro, A., Ruedl, C., and Ricciardi-Castagnoli, P. (2012). Calcineurin/NFAT signalling inhibits myeloid haematopoiesis. *EMBO Mol. Med.* *4*, 269–282.
- Furman, J.L., Sama, D.M., Gant, J.C., Beckett, T.L., Murphy, M.P., Bachstetter, A.D., Van Eldik, L.J., and Norris, C.M. (2012). Targeting astrocytes ameliorates neurologic changes in a mouse model of Alzheimer's disease. *J. Neurosci.* *32*, 16129–16140.
- Garcia-Cozar, F.J., Okamura, H., Aramburu, J.F., Shaw, K.T., Pelletier, L., Showalter, R., Villafranca, E., and Rao, A. (1998) Two-site interaction of nuclear factor of activated T cells with activated calcineurin. *J. Biol. Chem.* *273*, 23877-23883.
- Gomez del Arco, P., Martinez-Martinez, S., Maldonado, J.L., and Redondo, J.M. (2000). A role for the p38 MAP Kinase pathway in the nuclear shuttling of NFATp. *J. Biol. Chem.* *275*, 13872–13878.
- Gong, J.Z., Stenzel, T.T., Bennett, E.R., Lagoo, A.S., Dunphy, C.H., Moore, J.O., Rizzieri, D.A., Tepperberg, J.H., Papenhausen, P., and Buckley, P.J. (2003). Burkitt lymphoma arising in organ transplant recipients: a clinicopathologic study of five cases. *Am. J. Surg. Pathol.* *27*, 818–827.
- Graef, I.A., Chen, F., and Crabtree, G.R. (2001). NFAT signaling in vertebrate development. *Curr. Opin. Gen. Dev.* *11*, 505–512.
- Grandori, C., Cowley, S.M., James, L.P., and Eisenman, R.N. (2000). The Myc/Max/Mad network and the transcriptional control of cell behavior. *Annu. Rev. Cell Dev. Biol.* *16*, 653–699.
- Gregory, M.A., and Hann, S.R. (2000). c-Myc proteolysis by the ubiquitin-proteasome pathway: stabilization of c-Myc in Burkitt's lymphoma cells. *Mol. Cell. Biol.* *20*, 2423-2435.
- Greiner, A., Müller, K.B., Hess, J., Pfeffer, K., Muller-Hermelink, H.K., and Wirth, T. (2000). Up-regulation of BOB.1/OBF.1 expression in normal germinal center B cells and germinal center derived lymphomas. *Am. J. Pathol.* *2000*, 501-507.
- Gwack, Y., Feske, S., Srikanth, S., Hogan, P.G., and Rao, A. (2007). Signalling to transcription: store-operated Ca²⁺ entry and NFAT activation in lymphocytes. *Cell Calcium* *42*, 145-156.
- Habib, T., Park, H., Tsang, M., de Alborán, I.M., Nicks, A., Wilson, L., Knoepfler, P.S., Andrews, S., Rawlings, D.J., Eisenman, R.N., et al. (2007). Myc stimulates B lymphocyte differentiation and amplifies calcium signaling. *J. Cell Biol.* *179*, 717-731.

- Hanahan, D., and Weinberg, R.A. (2000). The hallmarks of cancer. *Cell* *100*, 57–70.
- Hardy, R. R., Carmack, C. E., Shinton, S. A., Kemp, J. D., Hayakawa, K. (1991). Resolution and characterization of pro-B and pre-pro-B cell stages in normal mouse bone marrow. *J. Exp. Med.* *173*, 1213-1225.
- Hardy, R.R., and Hayakawa, K. (2001). B cell development pathways. *Annu. Rev. Immunol.* *19*, 595–621.
- Harris, A.W., Pinkert, C.A., Crawford, M., Langdon, W.Y., Brinster, R.L., and Adams, J.M. (1988). The E μ -Myc Transgenic Mouse a model for high-incidence spontaneous lymphoma and leukemia of early B cells. *J. Exp. Med.* *167*, 353-371.
- Hecht, J.L., and Aster, J.C. (2000). Molecular biology of Burkitt's lymphoma. *J. Clin. Oncol.* *18*, 3707-3721.
- Hess, J., Nielsen, P.J., Fischer, K.D., Bujard, H., and Wirth, T. (2001). The B lymphocyte-specific coactivator BOB.1/OBF.1 is required at multiple stages of B-cell development. *Mol. Cell. Biol.* *21*, 1531–1539.
- Hobeika, E., Thiemann, S., Storch, B., Jumaa, H., Nielsen, P.J., Pelanda, R., and Reth, M. (2006). Testing gene function early in the B cell lineage in mb-1 cre mice. *Proc. Natl. Acad. Sci. USA* *103*, 13789-13794.
- Hock, M., Vaeth, M., Rudolf, R., Patra, A.K., Pham, D.A., Muhammad, K., Pusch, T., Bopp, T., Schmitt, E., Rost R, et al. (2013). NFATc1 induction in peripheral T and B lymphocytes. *J. Immunol.* *190*, 2345-2353.
- Hogan, P.G., Chen, L., Nardone, J., and Rao, A. (2003). Transcriptional regulation by calcium, calcineurin, and NFAT. *Genes Dev.* *17*, 2205–2232.
- Horsley, V., Polak, A.O.A.L., Glimcher, L.H., and Fuchs, E. (2008). NFATc1 balances quiescent and proliferation of skin stem cells. *Cell* *321*, 299-310.
- Hummel, M., Bentink, S., Berger, H., Klapper, W., Wessendorf, S., Barth, T.F.E., Bernd, H-W., Cogliatti, S.B., Dierlamm, J., Feller, A.C., et al. (2006). A biologic definition of Burkitt's lymphoma from transcriptional and genomic profiling. *N. Engl. J. Med.* *354*, 2419-2430.
- Isobe, K., Tamaru, J-I., Nakamura, S., Harigaya, K., Mikata, A., and Ito, H. (2002). VH gene analysis in sporadic Burkitt's lymphoma: somatic mutation and intraclonal diversity with special reference to the tumor cells involving germinal center. *Leuk. Lymphoma* *43*, 159–164.
- Jaffe, E.S., Harris, N.L., Stein, H., Campo, E., Pileri, S.A., and Swerdlow, S.H. (2008). Introduction and overview of the classification of the neoplasms. In WHO Classification of Tumours of Hematopoietic and Lymphoid Tissue, S.H. Swerdlow, E. Campo, N.L. Harris, E.S. Jaffe, S.A. Pileri, H. Stein, J. Thiele, J.W. Vardiman, eds. (Lyon, France: International Agency for Research on Cancer), pp 158-166.
- Jaffe, E.S., and Pittaluga, S. (2011). Aggressive B-cell lymphomas: a review of new and old entities in the WHO Classification. *Hematology Am. Soc. Hematol. Educ. Program* *2011*, 506–514.

- Janz, S., Potter, M., and Rabkin, C.S. (2003). Lymphoma and leukemia associated chromosomal translocations in healthy individuals. *Genes Chromosomes Cancer* 36, 211-223.
- Jauliac, S., Lopez-Rodriguez, C., Shaw, L.M., Brown, L.F., Rao, A., and Toker, A. (2002). The role of NFAT transcription factors in integrin-mediated carcinoma invasion. *Nat. Cell Biol.* 4, 540-544.
- Jazirehi, A.R., Vega, M.I., and Bonavida, B. (2007). Development of rituximab-resistant lymphoma clones with altered cell signaling and cross-resistance to chemotherapy. *Cancer Res.* 67, 1270-1281.
- Kalungi, S., Wabinga, H., and Bostad, L. (2012). Expression of apoptosis associated proteins Survivin, Livin and Thrombospondin-1 in Burkitt lymphoma. *APMIS* 121, 239-245.
- Keller, U., Nilsson, J.A., Maclean, K.H., Old, J.B., and Cleveland, J.L. (2005). *Nfkb1* is dispensable for Myc-induced lymphomagenesis. *Oncogene* 24, 6231-6240.
- Kempkes, B., Spitkovsky, D., Jansen-Durr, P., Ellwart, J.W., Kremmer, E., Delecluse, H.J., Rottenberger, C., Bornkamm, G.W., and Hammerschmidt, W. (1995). B-cell proliferation and induction of early G1-regulating proteins by Epstein-Barr virus mutants conditional for EBNA2. *EMBO J.* 14, 88-96.
- Kim, J., Kim, D.W., Chang, W., Choe, J., Kim, J., Park, C-S., Song, K., and Lee, I. (2012). Wnt5a is secreted by follicular dendritic cells to protect germinal center B cells via Wnt/Ca²⁺/NFAT/NF-κB-B cell lymphoma 6 signaling. *J. Immunol.* 188, 182-189.
- Kitamura, D., Kudo, A., Schaal, S., Müller, W., Melchers, F., and Rajewsky, K. (1992). A critical role of λ5 protein in B cell development. *Cell* 69, 823-831.
- Klapproth, K., and Wirth, T. (2010). Advances in the understanding of MYC-induced lymphomagenesis. *Br. J. Haematol.* 149, 484-497.
- Klapproth, K., Sander, S., Marinkovic, D., Baumann, B., and Wirth, T. (2009). The IKK2/NF-κB pathway suppresses MYC-induced lymphomagenesis. *Blood.* 114, 2448-2458.
- Klein, U., Klein, G., Ehlin-Henriksson, B., Rajewsky, K., and Kuppers, R. (1995). Burkitt's lymphoma is a malignancy of mature B cells expressing somatically mutated V region genes. *Mol. Med.* 1, 495-505.
- Klein, U., and Dalla-Favera, R. (2008). Germinal centres: role in B-cell physiology and malignancy. *Nat. Rev. Immunol.* 8, 22-33.
- Kondo, M., Wagers, A.J., Manz, M.G., Prohaska, S.S., Scherer, D.C., Beilhack, G.F., Shizuru, J.A., and Weissman, I.L. (2003). Biology of hematopoietic stem cells and progenitors: implications for clinical application. *Annu Rev Immunol.* 21, 759-806.
- Küppers, R., Klein, U., Leohansmann, M., and Rajewsky, K. (1999). Cellular origin of human B-cell lymphomas. *N. Engl. J. Med.* 341, 1520-1529.
- Küppers, R. (2005). Mechanisms of B-cell lymphoma pathogenesis. *Nat. Rev. Cancer* 5, 251-262.
- Kurosaki, T., Shinohara, H. and Baba, Y. (2010). B cell signaling and fate decision. *Annu. Rev. Immunol.* 28, 21-55.

- Lemercier C, Brocard MP, Puvion-Dutilleul F, Kao HY, Albagli O, and Khochbin S. (2002). Class II histone deacetylases are directly recruited by BCL6 transcriptional repressor. *J. Biol. Chem.* 277, 22045-22052.
- Lenze, D., Leoncini, L., Hummel, M., Volinia, Liu, C.G., Amato, T., De Falco, G., Githanga, J., Horn, H., Nyagol, J. et al. (2011). The different epidemiologic subtypes of Burkitt lymphoma share a homogenous micro RNA profile distinct from diffuse large B-cell lymphoma. *Leukemia* 25, 1869-1876.
- Leoncini, L., Raphael, M., Stein, H., Harris, N.L., Jaffe, E.S., and Kluin, P.M. (2008). Burkitt lymphoma. In *WHO Classification of Tumours of Hematopoietic and Lymphoid Tissue*, S.H. Swerdlow, E. Campo, N.L. Harris, E.S. Jaffe, S.A. Pileri, H. Stein, J. Thiele, J.W. Vardiman, eds. (Lyon, France: International Agency for Research on Cancer), pp 262-264.
- Le Roy, C., Deglesne, P.A., Chevallier, N., Beitar, T., Eclache, V., Quettier, M., Boubaya, M., Letestu, R., Lévy, V., Ajchenbaum-Cymbalista, F., et al. (2012). The degree of BCR commitment and differential NFAT activation are responsible for chronic lymphocytic leukemia evolutivity. *Blood* 120, 356-365.
- Levens, D. (2008). How the c-myc promoter works and why it sometimes does not. *J. Natl. Cancer. Inst. Monogr.* 39, 41-43.
- Liang, Q., Bueno, O.F., Wilkins, B.J., Kuan, C.Y., Xia, Y., and Molkentin, J.D. (2003). c-Jun N-terminal kinases (JNK) antagonize cardiac growth through cross-talk with calcineurin-NFAT signaling. *EMBO J.* 22, 5079-5089.
- Loh, C., Shaw, K.T., Carew, J., Viola, J.P., Luo, C., Perrino, B.A., and Rao, A. (1996a) Calcineurin binds the transcription factor NFAT1 and reversibly regulates its activity. *J. Biol. Chem.* 271, 10884–10891.
- Loh, C., Carew, J.A., Kim, J., Hogan, P.G., and Rao, A. (1996). T-cell receptor stimulation elicits an early phase of activation and a later phase of deactivation of the transcription factor NFAT1. *Mol. Cell. Biol.* 16, 3945-3954.
- Lopez-Rodriguez, C., Aramburu, J., Rakeman, A.S., and Rao, A. (1999). NFAT5, a constitutively nuclear NFAT protein that does not cooperate with Fos and Jun. *Proc. Natl. Acad. Sci. USA* 96, 7214-7219.
- Luo, C., Shaw, K.T., Raghavan, A., Aramburu, J., Garcia-Cozar, F., Perrino, B.A., Hogan, P.G., and Rao, A. (1996). Interaction of calcineurin with a domain of the transcription factor NFAT1 that controls nuclear import. *Proc. Natl. Acad. Sci. USA* 93, 8907–8912.
- Macian, F. (2005). NFAT proteins: key regulators of T-cell development and function. *Nat. Rev. Immunol.* 5, 472-484.
- MacLennan, I. C. (1994). Germinal centers. *Annu. Rev. Immunol.* 12, 117-139.
- Mancini, M., and Toker, A. (2009). NFAT proteins: emerging roles in cancer progression. *Nat. Rev. Cancer* 9, 810–820.

- Marafioti, T., Pozzobon, M., Hansmann, M-L., Ventura, R., Pileri, S.A., Robertson, H., Gesk, S., Gaulard, P., Barth, T.F.E., Du, M.Q., et al. (2004). The NFATc1 transcription factor is widely expressed in white cells and translocates from the cytoplasm to the nucleus in a subset of human lymphomas. *Br. J. Haematol.* *128*, 333–342.
- Masclé, X., Albagli, O., and Lemerrier, C. (2003). Point mutation in BCL6 DNA-binding domain reveal distinct roles for the six zinc fingers. *Biochem. Biophys. Res. Commun.* *300*, 391-396.
- Medyouf, H., Alcalde, H., Berthier, C., Guillemin, M.C., dos Santos, N.R., Janin, A. Decaudin, D., de Thé, H., and Ghysdael, J. (2007). Targeting calcineurin activation as a therapeutic strategy for T-cell acute lymphoblastic leukemia. *Nat. Med.* *13*, 736–741.
- Mognol, G.P., de Araujo-Souza, P.S., Robbs, B.K., Teixeira, L.K., and Viola, J.P.B. (2012). Transcriptional regulation of the c-Myc promoter by NFAT1 involves negative and positive NFAT-responsive elements. *Cell Cycle* *11*, 1014-1028.
- Molyneux, E.M., Rochford, R., Griffin, B., Newton, R., Jackson, G., Menon, G., Harrison, C.J., Israels, T., and Bailey, S. (2012). Burkitt's lymphoma. *Lancet* *379*, 1234–1244.
- Monroe, J.G. (2006). ITAM-mediated tonic signalling through pre-BCR and BCR complexes. *Nat. Rev. Immunol.* *6*, 284-294.
- Müller, M.R., and Rao, A. (2010). NFAT, immunity and cancer: a transcription factor comes of age. *Nat. Rev. Immunol.* *10*, 645-656.
- Muramatsu, M., Kinoshita, .K., Fagarasan, S., Yamada, S., Shinkai, Y., and Honjo, T. (2000). Class switch recombination and hypermutation require activation-induced cytidine deaminase (AID), a potential RNA editing enzyme. *Cell* *102*, 553–563.
- Nagasawa, T. (2006). Microenvironmental niches in the bone marrow required for B-cell development. *Nat. Rev. Immunol.* *6*, 107-115.
- Nahar, R., Ramezani-Rad, P., Mossner, M., Duy, C., Cerchietti, L., Geng, H., Dovat, S., Jumaa, H., Ye, B.H., Melnick, A., et al. (2011). Pre-B cell receptor-mediated activation of BCL6 induces pre-B cell quiescence through transcriptional repression of MYC. *Blood* *118*, 4174-4178.
- Neal, J.W., and Clipstone, N.A. (2003). A constitutively active NFATc1 mutant induces a transformed phenotype in 3T3-Li fibroblast. *J. Biol. Chem.* *278*, 17246-17254.
- Nieuwenhuis, P., and Opstelten, D. (1984). Functional anatomy of germinal centers. *Am. J. Anat.* *170*, 421-435.
- Niu, H., Ye, B. H., and Dalla-Favera, R. (1998). Antigen receptor signaling induces MAP kinase-mediated phosphorylation and degradation of the BCL-6 transcription factor. *Genes Dev.* *12*, 1953-1961.
- Nojima, T., Haniuda, K., Moutai, T., Matsudaira, M., Mizokawa, S., Shiratori, I., Azuma, T., and Kitamura, D. (2011). In-vitro derived germinal centre B cells differentially generate memory B or plasma cells in vivo. *Nat. Commun.* *2*, 465.

- Nussenzweig, A.N., and Nussenzweig, M.C. (2010). Origin of chromosomal translocations in lymphoid cancer. *Cell* *141*, 27–38.
- O’Conor, G.T. (1961). Malignant lymphoma in African children. II. A pathological entity. *Cancer* *14*, 270–283.
- Oettinger M.A., Schatz, D.G., Gorka, C., and Baltimore, D. (1990). RAG-1 and RAG-2, adjacent genes that synergistically activate V(D)J recombination. *Science* *248*, 1517-1523.
- Oikawa, T., Nakamura, A., Onishi, N., Yamada, T., Matsuo, K., and Saya, H. (2013). Acquired expression of NFATc1 downregulates E-cadherin and promotes cancer cell invasion. *Cancer Res.* *73*, 5100-5109.
- Okamura, H., Garcia-Rodriguez, C., Martinson, H., Qin, J., Virshup, D.M., and Rao, A. (2004). A conserved docking motif for CK1 binding controls the nuclear localization of NFAT1. *Mol. Cell. Biol.* *24*, 4184-4195.
- Ott, G., Rosenwald, A., and Campo, E. (2013). Understanding-driven aggressive B-cell lymphomas: pathogenesis and classification. *Blood* *122*, 575-583.
- Pajic, A., Spitkovsky, D., Christoph, B., Kempkes, B., Schuhmacher, M., Staeger, M.S., Brielmeier, M., Ellwart, J., Kohlhuber, F., Bornkamm, G.W., et al. (2000). Cell cycle activation by c-myc in a Burkitt lymphoma model cell line. *Int. J. Cancer* *87*, 787-793.
- Park, J., Takeuchi, A., and Sharma, S. (1996). Characterization of a new isoform of the NFAT (Nuclear Factor of Activated T cell) gene family member NFATc. *J. Biol. Chem.* *271*, 20914-20921.
- Pasqualucci, L., Migliazza, A., Basso, K., Houldsworth, J., Chaganti, R.S.K., and Dalla-Favera, R. (2003). Mutations of the BCL6 proto-oncogene disrupt its negative autoregulation in diffuse large B-cell lymphoma. *Blood* *101*, 2914-2923.
- Patra, A.K., Avots, A., Zahedi, R.P., Schüler, T., Sickmann, A., Bommhardt, U., and Serfling, E. (2013). An alternative NFAT-activation pathway mediated by IL-7 is critical for early thymocyte development. *Nat. Immunol.* *14*, 127-135.
- Pham, L.V., Tamayo, A.T., Li, C., Bueso-Ramos, C., and Ford, R.J. (2010). An epigenetic chromatin remodeling role for NFATc1 in transcriptional regulation of growth and survival genes in diffuse large B-cell lymphomas. *Blood*, *116*, 3899–3906.
- Pieper, K., Grimbacher, B., and Eibel, H. (2013). B cell biology and development. *J. Allergy Clin. Immunol.* *131*, 959-971.
- Qiao, Q., Jiang, Y., and Li, G. (2013). Inhibition of the PI3K/AKT-NF-κB pathway with curcumin enhanced radiation-induced apoptosis in human Burkitt’s lymphoma. *J. Pharmacol. Sci.* *121*, 247 – 256.
- Ranger, A.M., Hodge, M.R., Gravalles, E.M., Oukka, M., Davidson, L., Alt, F.W., de la Brousse, F.C., Hoey, T., Grusby, M., and L.H. Glimcher. (1998). Delayed lymphoid repopulation with defects in IL-4-driven responses produced by inactivation of NFATc. *Immunity* *8*, 125-134.

- Rao, A., Luo, C., and Hogan, P.G. (1997). Transcription factors of the NFAT family: regulation and function. *Annu. Rev. Immunol.* *15*, 707–747.
- Refaeli, Y., Young, R.M., Turner, B.C., Duda, J., Field, K.A., and Bishop, J.M. (2008). The B cell antigen receptor and overexpression of MYC can cooperate in the genesis of B cell lymphomas. *PLoS Biol.* *6*, 1208-1225.
- Ryan, K.M., and Birnie, G.D. (1996). Myc oncogenes: the enigmatic family. *Biochem. J.* *314*, 713-721.
- Saito, M., Gao, J., Basso, K., Kitagawa, Y., Smith, P.M., Bhagat, G., Pernis, A., Pasqualucci, L., and Dalla-Favera, R. (2007). A signaling pathway mediating downregulation of BCL6 in germinal center B cells is blocked by BCL6 gene alterations in B cell lymphoma. *Cancer Cell* *12*, 280–292.
- Sánchez-Beato, M., Sánchez-Aguilera, A., and Piris, M.A. (2003). Cell cycle deregulation in B-cell lymphomas. *Blood* *101*, 1220-1235.
- Sander, S., Calado, D.P., Srinivasan, L., Köchert, K., Zhang, B., Rosolowski, M., Rodig, S.J., Holzmann, K., Stilgenbauer, S., Siebert, R., et al. (2012). Synergy between PI3K signaling and MYC in Burkitt lymphomagenesis. *Cancer Cell* *22*, 167-179.
- Schmitz, R., Ceribelli, M., Pittaluga, S., Wright, G., and Staudt, L.M. (2014). Oncogenic mechanisms in Burkitt lymphoma. *Cold Spring Harb. Perspect. Med.* *4*.
- Schmitz, R., Young, R.M., Ceribelli, M., Jhavar, S., Xiao, W., Zhang, M., Wright, G., Shaffer, A.L., Hodson, D.J., Buras, E., et al. (2012). Burkitt lymphoma pathogenesis and therapeutic targets from structural and functional genomics. *Nature* *490*, 116-120.
- Schuhmacher, M., and Eick, D. (2013). Dose-dependent regulation of target gene expression and cell proliferation by c-Myc levels. *Transcription* *4*.
- Schulz, T.F., Boshoff, C.H., and Weiss, R.A. (1996). HIV infection and neoplasia. *Lancet* *348*, 587–591.
- Sears, R., Nuckolls, F., Haura, E., Taya, Y., Tamai, K., and Nevins, J.R. (2000). Multiple Ras-dependent phosphorylation pathways regulate Myc protein stability. *Genes Dev.* *14*, 2501–2514.
- Serfling, E., Avots, A., Klein-Hessling, S., Rudolf, R., Vaeth, M., and Berberich-Siebelt, F. (2012). NFATc1/ α A: the other face of NFAT factors in lymphocytes. *Cell Commun. Signal* *10*, 16.
- Serfling, E., Barthelmäs, R., Pfeuffer, I., Schenk, B., Zarius, S., Swoboda, R., Mercurio, F., and Karin, M. (1989). Ubiquitous and lymphocyte-specific factors are involved in the induction of the mouse interleukin 2 gene in T lymphocytes. *EMBO J.* *8*, 465-473.
- Serfling, E., Berberich-Siebelt, F., Avots, A., Chuvpilo, S., Klein-Hessling, S., Jha, M. K., Kondo, E., Pagel, P., Schulze-Luehrmann, J., and Palmethofer, A. (2004). NFAT and NF-kappaB factors—the distant relatives. *Int. J. Biochem. Cell. Biol.* *36*, 1166-1170.
- Serfling, E., Chuvpilo, S., Liu, J., Thomas Höfer, T., and Palmethofer, A. (2006). NFATc1 autoregulation: a crucial step for cell-fate determination. *Trends Immunol.* *27*, 461-469.

- Serfling, E., Klein-Hessling, S., Palmethofer, A., Bopp, T., Stassen, M., and Schmitt, E. (2006a). NFAT transcription factors in control of peripheral T cell tolerance. *Eur. J. Immunol.* *36*, 2837–2843.
- Shaffer, A.L., Rosenwald, A., and Staudt, L. M. (2002). Lymphoid malignancies: the dark side of B-cell differentiation. *Nat. Rev. Immunol.* *2*, 920-932.
- Shankland, K.R., Armitage, J.O., and Hancock, B.W. (2012). Non-Hodgkin lymphoma. *Lancet* *380*, 848–857.
- Shapira, J., and Peylan-Ramu, N. (1998). Burkitt's lymphoma. *Oral Oncol.* *34*, 15-23.
- Shaw, J.P., Utz, P.J., Durand, D.B., Toole, J.J., Emmel, E.A., and Crabtree, G.R. (1988). Identification of a putative regulator of early T cell activation genes. *Science* *241*, 202-205.
- Sheridan, C.M., Heist, E.K., Beals, C.R., Crabtree, G.R., and Gardner, P. (2002). Protein kinase A negatively modulates the nuclear accumulation of NF-ATc1 by priming for subsequent phosphorylation by glycogen synthase kinase-3. *J. Biol. Chem.* *277*, 48664–48676.
- Shibasaki, F., Price, E.R., Milan, D., and McKeon, F. (1996). Role of kinases and the phosphatase calcineurin in the nuclear shuttling of transcription factor NF-AT4. *Nature* *382*, 370–373.
- Slack, G.W., and Gascoyne, R.D. (2011). MYC and aggressive B-cell lymphomas. *Adv. Anat. Pathol.* *18*, 219–228.
- Smith, S.M., Anastasi, J., Cohen, K.S., and Godley, L.A. (2010). The impact of MYC expression in lymphoma biology: beyond Burkitt lymphoma. *Blood Cells Mol. Dis.* *45*, 317–323.
- Swerdlow, S.H., Campo, E., Harris, N.L., Jaffe, E.S., Pileri, S.A., Stein, H., Thiele, J., and Vardiman, J.W. (2008). WHO Classification of Tumours Haematopoietic and Lymphoid Tissues (Lyon: International Agency for Research on Cancer).
- Tamaru, J., Hummel, M., Marafioti, T., Kalvelage, B., Leoncini, L., Minacci, C., Tosi, P., Wright, D., and Stein, H. (1995). Burkitt's lymphomas express VH genes with a moderate number of antigen-selected somatic mutations. *Am. J. Pathol.* *147*, 1398-1407.
- Tao, Q., Robertson, K.D., Manns, A., Hildesheim, A., and Ambinder, R.F. (1998). Epstein-Barr virus (EBV) in endemic Burkitt's lymphoma: molecular analysis of primary tumor tissue. *Blood* *91*, 1373-1381.
- Tarlinton, D. (2006). B-cell memory: are subsets necessary? *Nat. Rev. Immunol.* *6*, 785-790.
- The Non-Hodgkin's Lymphoma Classification Project. (1997). A clinical evaluation of the International Lymphoma Study Group Classification of Non-Hodgkin's Lymphoma. *Blood* *89*, 3909-3918.
- Thomas, M.D., Srivastava, B., and Allman, D. (2006). Regulation of peripheral B cell maturation. *Cell. Immunol.* *239*, 92–102.
- Tripathi, P., Wang, Y., Coussens, M., Manda, K.R., Casey, A.M., Lin, C., Poyo, E., Pfeifer, J.D., Basappa, N., Bates, M., et al. (2014). Activation of NFAT signaling establishes a tumorigenic microenvironment through cell autonomous and non-cell autonomous mechanisms. *Oncogene* *33*, 1840-1849.

- van den Bosch, C.A. (2004). Is endemic Burkitt's lymphoma an alliance between three infections and a tumour promoter? *Lancet Oncol* 5, 738–746.
- van Kooten, C., and Banchereau, J. (2000). CD40-CD40 ligand. *J. Leukoc. Biol.* 67, 2-17.
- Victora, G.D., and Nussenzweig, M.C. (2012). Germinal Centers. *Annu. Rev. Immunol.* 30, 429–457.
- Vita, M., and Henriksson, M. (2006). The Myc oncoprotein as a therapeutic target for human cancer. *Semin. Cancer Biol.* 16, 318-330.
- Walusansa, V., and Okuku, F. (2012). Burkitt lymphoma in Uganda, the legacy of Denis Burkitt and an update on the disease status. *Br. J. Haematol.* 156, 757–760.
- Wierstra, I., and Alves, J. (2008). The c-myc promoter: still mystery and challenge. *Adv. Cancer Res.* 99, 113-333.
- Willis, T.G., and Dyer, M.J.S. (2000). The role of immunoglobulin translocations in the pathogenesis of B-cell malignancies. *Blood* 96, 808-822.
- Winslow, M.M., Pan, M., Starbuck, M., Gallo, E.M., Deng, L., Karsenty, G., and Crabtree, G.R. (2006). Calcineurin/NFAT signaling in osteoblasts regulates bone mass. *Dev. Cell* 10, 771-782.
- Yoshida, H., Nishina, H., Takimoto, H., Marengere, L.E., Wakeham, A.C., Bouchard, D., Kong, Y.Y., Ohteki, T., Shahinian, A., Bachmann, A., et al. (1998). The transcription factor NF-ATc1 regulates lymphocyte proliferation and Th2 cytokine production. *Immunity* 8, 115-124.
- Zech, L., Haglund, U., Nilsson, K., and Klein, G. (1976). Characteristic chromosomal abnormalities in biopsies and lymphoid-cell lines from patients with Burkitt and non-Burkitt lymphomas. *Int. J. Cancer* 17, 47-56.
- Zhang, M., Srivastava, G., and Lu, L. (2004). The pre-B cell receptor and its function during B cell development. *Cell. Mol. Immunol.* 1, 89-94.

9. Appendix

9.1. Attended Conferences

1. 17th Joint meeting of the Signal Transduction Society (STS) ‘Signal transduction receptors, mediators and genes’ (6th November 2013) in Weimar, Germany
2. 8th Network Meeting of DFG research training groups GK1660, GK520 and SFB685 (21th – 23rd July 2013) in Obertrubach, Germany
3. 16th Joint meeting of the Signal Transduction Society (STS) ‘Signal transduction receptors, mediators and genes’ (5th – 7th November 2012) in Weimar, Germany
4. 7th International symposium the graduate school of life sciences (16th – 17th October 2012) in Wuerzburg, Germany
5. 6th International symposium the graduate school of life sciences (19th - 20th October 2011) in Wuerzburg, Germany
6. 6th Network Meeting of the DFG graduate programs from Würzburg, Tübingen, and Erlangen (6th – 8th June 2011) in Neresheim, Germany
7. 7th Annual Meeting of Immunology Training Network of Tübingen, Erlangen and Würzburg (15th – 17th July 2012) in Schöntal, Germany.
8. International Workshop of the DFG-Transregional Research Center TR52: Transcriptional Programming in the Immune System in Würzburg, Germany. (17th -20th November 2010)
9. 5th Network Meeting of DFG graduate schools GK1160, GK520 and GK794 (7th – 9th November 2010) Schöntal, Germany
10. 5th International Symposium (Chiasma-GSLS student symposium), Würzburg, (13th - 14th October 2010) in Wuerzburg, Germany.

9.2 Poster and oral presentations at conferences and symposia

1. Krisna Murti, Hendrik Fender, Rhoda Busch, Vannesa Wild, Martin Winterberg, Edgar Serfling and Andris Avots (2013). The role of NFATc1 isoforms in development and progression of c-Myc induced B cell lymphomas. 8th Network Meeting of DFG research training groups GK1660, GK520 and SFB685 (21th – 23rd July 2013) in Obertrubach, Germany.
2. Krisna Murti, Hendrik Fender, Rhoda Busch, Vannesa Wild, Martin Winterberg, Edgar Serfling and Andris Avots (2012). Nuclear NFATc1 α is a hallmark of Burkitt lymphoma and c-Myc induced B-cell tumors in mice. 16th Joint meeting of Signal Transduction Society (STS) ‘Signal transduction receptors, mediators and genes’ (5th – 7th November 2012) in Weimar, Germany.
3. Krisna Murti, Hendrik Fender, Rhoda Busch, Edgar Serfling and Andris Avots (2012). Nuclear NFATc1 α is a hallmark of Burkitt lymphoma and c-Myc induced B-cell tumors in mice. 7th International symposium the graduate school of life sciences (16th – 17th October 2012) in Würzburg, Germany.

4. Krisna Murti (2012). The role of NFATc1 isoforms in development and progression of c-myc induced B cell lymphomas. 7th Annual Meeting: Immunology Training Network of Tübingen, Erlangen and Würzburg (15th – 17th July 2012) in Kloster Schöntal, Germany (oral presentation).

5. Krisna Murti and Andris Avots (2011). Rotenone and CAPE as inhibitors of inducible NFATc1/ α A isoform expression in lymphoid cells. 6th International Symposium (BioBang-GSLS students symposium) (19th - 20th October 2011) in Wuerzburg, Germany.

6. Krisna Murti and Andris Avots (2011). Rotenone and CAPE as inhibitors of inducible NFATc1/ α A isoform expression in lymphoid cells (2011). 6th Network Meeting of DFG graduate schools GK1160, GK520 and GK794 (6th – 8th June 2011) in Kloster Neresheim, Germany.

9.3 Attended Workshops

1. Statistic course part I (16th – 18th June 2011) in Würzburg, Germany
2. Statistic course part II (11th – 13th July 2011) in Würzburg, Germany
3. Grundkurs Tierschutz und Versuchstierkunde (10th – 14th October 2011) in Würzburg, Germany
4. Poster design and presentation workshop, Würzburg (8th October 2012) in Würzburg, Germany

10. List of scientific publications

1. Rhoda Busch, **Krisna Murti**, Jiming Liu, Amiya Patra, Klaus-Peter Knobloch, Monika Lichtinger, Constanze Bonifer, Simone Woertge, Kurth Reifenberg, Ari Waisman, Volker Ellenrieder, Edgar Serfling and Andris Avots. NFATc1/ β is required for a timely release of BCL6-mediated repression of chemokine gene expression in peritoneal resident macrophages. 2014. Manuscript, submission and revision.
2. **Krisna Murti**, Hendrik Fender, Rhoda Busch, Edgar Serfling, Andris Avots. NFATc1 is required for survival of *E μ -Myc*-induced tumor. 2014. In preparation.
3. Johannes Baur, Ulli Steger, Tobias Pusch, **Krisna Murti**, Rhoda Busch, C.T. Germer, Edgar Serfling, Christoph Otto and Andris Avots. NFATc1 deficiency in recipient T-cells is sufficient to prevent acute rejection of allogeneic heart transplant. 2014. In preparation.
4. Khalid Muhammad, Hani Alrefai, Ralf Marienfeld, **Krisna Murti**, Amiya K. Patra, Andris Avots, Eisaku Kondo, Stefan Klein-Hessling and Edgar Serfling. NF- κ B Factors Support the Induction of NFATc1 in B Lymphocytes. 2014. Manuscript, submission and revision.
5. Karen Chiam, Natalie K. Ryan, Carmela Ricciardelli, Tanya K. Day, Grant Buchanan, Aleksandra M. Ochnik, **Krisna Murti**, Luke A. Selth, Australian Prostate Cancer Bio Resource, Lisa M. Butler, Wayne D. Tilley and Tina Bianco-Miotto. Characterization of the prostate cancer susceptibility gene KLF6 in human and mouse prostate cancers. *Prostate*. 2013;73 (2):182-93.
6. Luke A. Selth, Scott Townley, Joanna L. Gillis, Aleksandra M. Ochnik, **Krisna Murti**, Robyn J. Macfarlane, Kim N. Chi, Villis R. Marshall, Wayne D. Tilley and Lisa M. Butler. Discovery of circulating microRNAs associated with human prostate cancer using a mouse model of disease. *Int J Cancer*. 2012 1;131 (3):652-61.
7. **Krisna Murti**, Lisa M. Butler, Andrew Sakko, Carmela Ricciardelli, Tina B. Mitto, Alexandra Ochnik, Jurgen Stahl and Wayne D. Tilley. Androgen Receptor Levels during Progression of Prostate Cancer in the TRAMP Model. *Medical Journal of Indonesia* 2010; 19 (1):5-13.

11. Abbreviation

α	Anti, Alpha
A	Ampère
BL/6	Black six, standardized mouse strain
°C	Grade Celcius
CD	Cluster of differentiation
Cre	Causes/circular recombination
d	Day
DMEM	Dulbeco's modified eagle medium
DMSO	Dimethyl sulfoxide
DNA	Desoxyribonucleid acid
et al.	Et aliter
EtOH	Ethanol
FITC	Fluorescence Isothiocyanat
g	Gramm
h (hrs)	Hours
HRP	Horseradish peroxidase
IL	Interleukin
k	Kilo (10^3)
kD	Kilo Dalton
L	Liter
M	Molar (mol per liter)
min	Minutes
mol	12g carbon particles (Isotop ^{12}C)
m	Milli (10^{-3})
μ	Micro (10^{-6})
n	Nano (10^{-9})
NF- κ B	Nuclear Factor kappaB
OD	Optical Density
o.n	Over night
PAGE	Polyacrylamid-Gel electrophorese
PI	Propidium iodide
PBS	Phosphate-buffered saline
PE	Phycoerythrin
PFA	Paraformaldehyde
RPMI	Roswell Park Memorial Institute, a cell culture medium
rpm	Rotations per minutes
RT	Room temperature ($\sim 20^\circ\text{C}$)
TBS	Tris-buffered saline
Tris	THAM (hydroxymethyl)aminomethan
U	Enzyme unit (unit)
V	Vol
wt	<i>Wild type</i>

12. Curriculum Vitae

Personal profile

Name : Krisna Murti
Date of Birth : 10th December 1963
Nationality : Indonesian
Gender : Female
Marital : Married
Address : Komplek PLN no. 16, Boom Baru, 3 Ilir, Palembang 30116
South Sumatera, Indonesia

Academic profile

2010-2014 Julius Maximilians University of Wuerzburg, Institute of Pathology, Department of Molecular Pathology, Doctoral student in the group of Serfling

2000-2005 Medicine Specialist Program in Anatomical Pathology, Faculty of Medicine, Sriwijaya University

2003-2005 Master Degree: M. Biotech., Stud. in Biotechnology Studies Department of Medical Biotechnology, Health Science, Flinders University of South Australia

1983-1990 Graduate Program in Medicine, Faculty of Medicine, Sriwijaya University

Krisna Murti, Wuerzburg, June 17th, 2014

